

**Assessment of Community Metabolism
and Associated Kinetic Parameters
in the Klamath River**

Prepared by:

George H. Ward
Consultant in Water Resources
Austin, Texas

Neal E. Armstrong
Consulting Engineer
Austin, Texas

Prepared for:

U.S. Fish and Wildlife Service
Arcata Fish and Wildlife Office
1655 Heindon Rd.
Arcata, CA 95521

Project Officer Paul Zedonis

6 August 2010

TABLE OF CONTENTS

1. Data sources and processing	1
2. Example analyses and sources of error	8
3. Behavior of DO and its kinetics in the Klamath	23
4. Interpretation: Associations and Correlations	41
5. Concluding remarks	59
References	64
Appendix	67

LIST OF FIGURES

1	Decision tree for assignment of “grade” to deployment period DO data	3
2	Sonde records of DO and water temperature, Station OR, July 2005	8
3	Sonde records of DO and saturation, Station OR 22 July 2005, and least-squares fit to estimated photosynthesis, equation (3)	9
4	Regression of dC/dt versus deficit, from nighttime sonde data, Station OR, nighttime period 22-23 July 2005	10
5	Sonde records of DO and saturation, Station OR 21-25 July 2005, with least-squares fits to estimated photosynthesis	11
6	Sonde records of DO and saturation, Station OR 11-15 July 2005, with least-squares fits to estimated photosynthesis	12
7	Reaeration coefficients, Station OR July 2005	13
8	Amplitude S of photosynthesis, Station OR July 2005	14
9	Sonde records of DO and saturation, Station OR 6-10 June 2005, with least-squares fits to estimated photosynthesis	15
10	Regression of dC/dt versus deficit, from nighttime sonde data, Station OR 2005, nighttime periods 8-9 June and 9-10 June	16
11	Regression of dC/dt versus deficit, from nighttime sonde data, Station SH 2005, nighttime periods 27-28 July and 28-29 July	17
12	Sonde records of DO and saturation, Station HC 1-5 July 2005, with least-squares fits to estimated photosynthesis	18
13	Schematic of application of data screen	20
14	Stem diagram of Klamath and major tributaries showing relative locations of sonde stations	23
15	Measured DO time series (corrected) at Station IG, 2005, with streamflow, relative insolation and computed kinetic variable	25
16	Measured DO time series (corrected) at Station WE, 2005, with streamflow, relative insolation and computed kinetic variable	27
17	Station WE, Klamath at Weitchpec, 8 September 2005	28
18	Longitudinal variation of means of 2001-05 annual averages of K_a from sonde data	30
19	Comparison of annual averages of K_a from sonde data and from O’Connor-Dobbins formula (4)	32

(continued)

LIST OF FIGURES

(continued)

20	Computed gross production (daily) and daily-mean community respiration rates, 2001	37
21	Computed gross production (daily) and daily-mean community respiration rates, 2002	37
22	Computed gross production (daily) and daily-mean community respiration rates, 2003	38
23	Computed gross production (daily) and daily-mean community respiration rates, 2004	38
24	Computed gross production (daily) and daily-mean community respiration rates, 2005	39
25	Gauged flows in mainstem of Klamath, 2001	41
26	Gauged flows in mainstem of Klamath, 2002	42
27	Gauged flows in mainstem of Klamath, 2003	42
28	Gauged flows in mainstem of Klamath, 2004	43
29	Gauged flows in mainstem of Klamath, 2005	43
30	Travel times from Iron Gate in mainstem of Klamath, 2001-05	44
31	One-day replacement distances in mainstem of Klamath, 2001-05	45
32	Gross production, relative autotrophy, and water chemistry, Jun-Sep 2001 means in Klamath	46
33	Gross production, relative autotrophy, and water chemistry, Jun-Sep 2002 means in Klamath	47
34	Gross production, relative autotrophy, and water chemistry, Jun-Sep 2003 means in Klamath	47
35	Gross production, relative autotrophy, and water chemistry, Jun-Sep 2004 means in Klamath	48
36	Gross production, relative autotrophy, and water chemistry, Jun-Sep 2005 means in Klamath	48
37	Annual profiles of June-September mean chlorophyll-a in Klamath	55
38	Association of sonde-derived average main-stem production and decay rates from model fits to nutrient data	57
39	Mainstem Klamath profiles of 2001-2005 average summer (June-September) metabolic parameters	61

LIST OF TABLES

1a	Number of records of complete diurnal cycle measured by sondes	6
1b	Number of records of complete diurnal cycle measured by sondes, after correction process	7
1c	Number of records of complete diurnal cycle measured by sondes, after correction process, June – September	7
2	Screening thresholds in order of application	20
3a	Number of records of complete diurnal cycle measured by sondes, after correction process, screened by thresholds of Table 2	22
3b	Number of records of complete diurnal cycle measured by sondes, after correction, June – September, screened by thresholds of Table 2	22
4	Reaeration coefficient (K_a) from kinetic analysis and from O-Connor-Dobbins formula, all data	31
5	June – September averaged values of kinetic parameters from <i>screened</i> sonde data	33-35
6	Correlations of screened data for June – September period	51-53
A-1	Attributes of sonde station locations in Klamath and tributaries	67
A-2	Longitudinal positions of sonde stations in Klamath and tributaries	67
A-3	Monthly averaged values of kinetic parameters from <i>screened</i> sonde data, 2001	68-69
A-4	Monthly averaged values of kinetic parameters from <i>screened</i> sonde data, 2002	69-70
A-5	Monthly averaged values of kinetic parameters from <i>screened</i> sonde data, 2003	71-72
A-6	Monthly averaged values of kinetic parameters from <i>screened</i> sonde data, 2004	72-73
A-7	Monthly averaged values of kinetic parameters from <i>screened</i> sonde data, 2005	74-75
A-8	Correlation arrays of monthly means, all months, screened data, 2001	76-77
A-9	Correlation arrays of monthly means, all months, screened data, 2002	78-79
A-10	Correlation arrays of monthly means, all months, screened data, 2003	80-81
A-11	Correlation arrays of monthly means, all months, screened data, 2004	82-84
A-12	Correlation arrays of monthly means, all months, screened data, 2005	84-86

1. Data sources and processing

For the past several years, the Arcata Office of the U.S. Fish & Wildlife Service (AFWO) has maintained a network of moored sondes in the Klamath River (Turner and Zedonis, 2004a). These are battery-powered automatic data loggers whose multiprobe sensors measure water temperature, pH, conductivity and dissolved oxygen. This activity is part of a larger program of monitoring and analysis of the Klamath conducted by AFWO, including hydrology, water quality, and riverine ecology. (Other companion reports in this program are cited in the text, where relevant.) The principal sonde stations are summarized in Appendix A, see also Armstrong and Ward (2005). In this report, we present a detailed analysis of sonde data collected from the five-year period 2001-2005. The data resource amassed over this period is formidable, approaching half-a-million independent sets of measurements of the four-parameter suite (i.e., nearly 2 million independent data points), distributed among thirteen principal sampling stations on the Klamath and its tributaries.

Emphasis in the present analysis is upon the variation of dissolved oxygen, from which can be inferred several key parameters characterizing the kinetics and ecology of the Klamath. Application of the sonde records for this purpose first requires that the data be corrected for several anomalies, which attend the deployment and automatic operation of such “robot” systems, including electronic aging, calibration shifts, and biofouling. With increasing use of sonde technology, several approaches to the data-correction problem have been promulgated in recent years (e.g., Ward, 2003; WEI, 2003; Wagner et al., 2006). A data-correction protocol was devised specific to the AFWO Klamath program, taking advantage of the full data resources available and addressing the operational behavior of the instruments employed (Ward and Armstrong, 2006b, 2006c, 2006d). The approach is to produce two archival data products:

- the uncorrected sonde data files, exactly as downloaded from the sonde units, together with ancillary measurements (e.g., Post-Cal data, Quanta measurements, etc.)

- a corrected sonde data file, embodying the use of all information and judgment by AFWO, accompanied by a brief document summarizing the corrections applied.

A user would then have the option to accept the AFWO corrected sonde data or work with the uncorrected data applying whatever corrections or adjustments that user deems appropriate. The AFWO correction procedure is a step-by-step protocol that is based upon first processing the sonde dissolved oxygen (DO) data record as a 24-hr running mean and associated root-mean-square (*rms*), designed to separate the diurnal variation (presumably dominated by temperature effects on solubility and by insolation-driven photosynthesis) from the longer term variation of measured DO. If the *rms* is found to be consistent over a deployment period (typically about two weeks), or, if variable, to be correlated with known hydrographic variations (notably measured insolation, streamflow, and meteorology), then it is assumed that any anomalies in probe operation can be detected in the variation of the 24-hr running mean. These are subjected to a series of diagnostics to identify such effects, for which various correction strategies are available, ranging from shifts in magnitude, or (more generally) application of an empirical linear trend, to expunging of some or all of a deployment record. The correction procedure involves both quantitative assessment and judgment, and is implemented in a complex workbook for each station/year of the program, which also serves as an archival documentation of the corrected data as well as the basis for correction. Finally, each corrected deployment is assigned a “grade”, based upon the nature and extent of the corrections employed and the quality of the information upon which that correction is based, an example decision process for which is diagrammed in Figure 1.

The analysis of production and kinetics reported here is based upon the corrected time series of sonde-measured DO. Typically, these are time series of measurements of DO concentration C and water temperature T at 30 minute intervals over a time period from late spring to early fall. The temperature data has already been determined to be quite accurate and therefore require no additional correction procedures (Turner and Zedonis, 2004b). (The AFWO sonde program also logs pH and conductivity, which are also corrected for anomalies in the same process as the DO, but these data are not employed in the present analyses.) From water temperature, solubility of

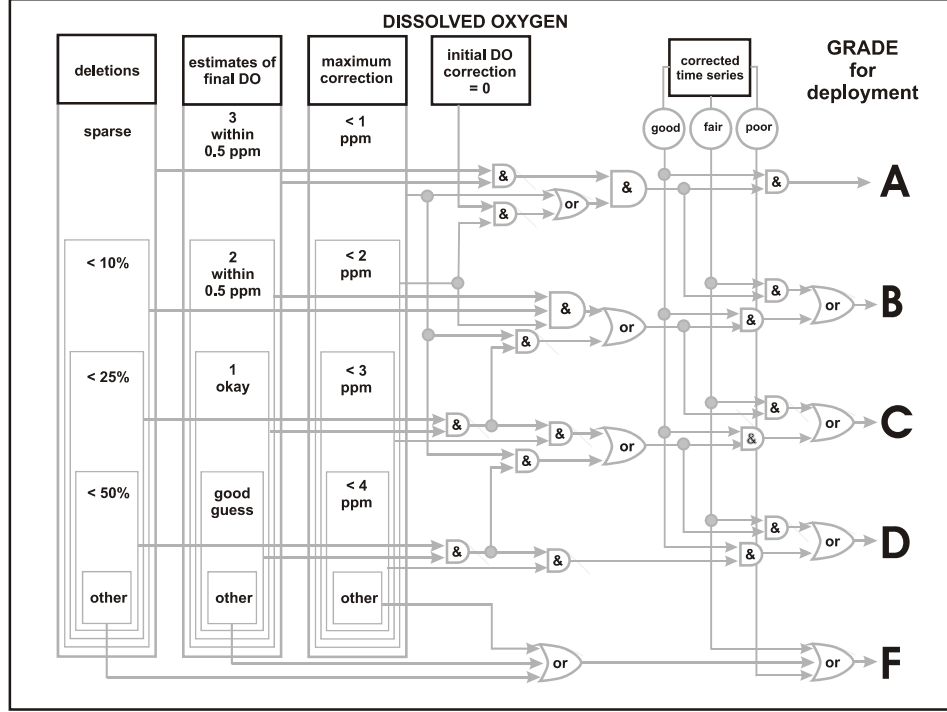


Figure 1 - Decision tree for assignment of “grade” to deployment period DO data (Ward and Armstrong, 2006d)

DO, as saturation concentration C_s , can be calculated rather precisely using the Weiss (1970) equation, together with a correction for elevation (given in Ward and Armstrong, 2006f). The calculation of primary production and related kinetic parameters is detailed in Ward and Armstrong (2006e), summarized as follows. The concentration of section-mean DO in a stream may be written:

$$\frac{dC}{dt} = (K_a D + C_r) + P \quad (1)$$

where dC/dt is the (material) time derivative of C . The influx of oxygen into the stream by mechanical reaeration at the surface is $K_a D$, where $(C_s - C) \equiv D$ is the DO deficit, and K_a is the reaeration coefficient. The coefficient K_a is a standard parameter in the analysis of stream water quality (e.g., Chapra, 1997), for which many engineering formulae exist, of which the most widely used quasi-theoretical relation is that of O'Connor and Dobbins (1958), and a commonly employed empirical equation appropriate for the Klamath is the CEB equation (Churchill et al.,

1962). Both of these formulae require the depth and velocity of the watercourse. For the USGS stations on the Klamath, field observations of cross-sectional area and width (whose ratio is section-mean depth), and current velocity are given on the USGS website, from which power-law regressions on streamflow were developed. Community respiration C_r is the sum of sediment oxygen demand, bacterial respiration (the product of BOD and an oxygen deoxygenation coefficient), plant respiration (mainly phytoplankton and periphyton), and respiration of zooplankton and macroheterotrophs (Odum, 1956). Finally, P is the influx of oxygen due to gross production by phytoplankton and periphyton.

Several assumptions are invoked to apply equation (1) to the sonde measurements of DO, as follows:

- (i) The stream is sufficiently well-mixed that DO is substantially constant over the cross section, and the longitudinal gradient in DO is small enough that $u \partial C / \partial x$ is negligible compared to $\partial C / \partial t$.
- (ii) The community respiration terms proceed at constant rates during the diurnal period.
- (iii) The rate coefficient for reaeration K_a is constant throughout the diurnal period.

Assumption (i) implies that the sonde measurement is a reliable approximation to the section-mean value of DO used in equation (1), and that the time variation in DO measured by the sonde is due to local variation in DO only, and not to the streamflow moving water of different DO into the sonde location. Assumption (ii) posits that the respiring organisms, notably the microorganisms responsible for sediment oxygen demand and for bacterial stabilization of organics, as well as the phytoplankton and periphyton, are stable and vary on time scales longer than a day. Assumption (iii) in effect dictates that the same physical processes controlling mechanical aeration are maintained throughout the day and night. In a river, the turbulence that mixes saturated water from the surface film down into the water column is considered to derive from the velocity of flow (in contrast to wind and waves, which are important in large, deep, relatively stagnant watercourses, such as lakes). If the river flow varies on time scales longer than a day, this assumption should be valid.

We impose one further assumption, that

- (iv) Primary production $P(t)$ proceeds at a rate proportional to incident light.

Under conditions of homogeneous transparency (of which a clear sky is a special case), this implies that $P(t) = S \cos\{\pi(t-t_n)/t_d\}$, where t_n is time of local noon and $t_d \equiv t_s - t_r$ is the daylight period, t_r and t_s denote times of sunrise and sunset, resp., and S , the cosine amplitude, is a constant (dimensions [DO]/[T]). Here times are measured in any convenient (but consistent) unit and convention, e.g., Universal Coordinated, prevailing civil, or local solar (for which $t_n = 12$ hrs = 0.5 d exactly). This assumption thereby neglects any superposed nonlinearities between photosynthetic oxygen evolution and light intensity, including photosaturation and photoinhibition (see, e.g., Kirk, 1994, Falkowski and Raven, 1997).

Assumptions (ii) and (iii) together imply that any inferences drawn from analysis of nighttime measurements are applicable as well to the associated daytime period. In particular, in absence of daylight, the production term $P(t) = 0$ in (1), and the equation reduces to $dC/dt =$ linear function of deficit D , whose slope is K_a and y-intercept C_r . Every pair of measurements in time from the sonde allows calculation of $\Delta C/\Delta t$ and the associated deficit ($C_s - C$) over the sampling interval Δt , so a linear regression of the nighttime values of $\Delta C/\Delta t$ versus deficit provides an estimate of K_a and C_r . Equation (1) can be rewritten:

$$\begin{aligned} C(t) - C(t_r) - K_a \int_{t_r}^t D(t) dt - C_r (t - t_r) &= \int_{t_r}^t P(t) dt \\ &= S t_d (\sin\{\pi(t-t_n)/t_d\} + 1) / \pi \end{aligned} \quad (2)$$

and with the values of K_a and C_r established, every term on the left-hand side can be calculated from the sonde data. Indeed, every time t_i that a sonde measurement is logged during the daylight period corresponds to a sample value for the left side of equation (2), viz.:

$$z_i = C(t_i) - C(t_r) - [K_a \Delta t \sum_{t_r}^{t_i} D(t) + C_r(t_i - t_r)] \quad (3)$$

so that by fitting the values z_i by least-squares to a function of the form $\sin\{\pi(t - t_n)/t_d\} + 1$, the amplitude S , and therefore daily gross primary production $\int_{t_r}^{t_s} P(t)dt$, can be computed (Ward and Armstrong, 2006e).

The numbers of complete diurnal cycles captured in the sonde data are summarized in Table 1a. There are over 7,100 such cycles, spread over the sampling network of thirteen stations and over the five years of monitoring. The correction processes involve some rejection of data, which amounts to about 16% of the data set. Even at this, there remain some 5,960 complete (corrected) diurnal cycles of DO available to support analyses of primary production and associated kinetic parameters, as summarized in Table 1b. These are summed over the period March – November. The vast majority of these data fall in the period May – October, and in the present analysis, we focus on the June – September period, because this is the period generally

Table 1a
Number of records of complete diurnal cycle measured by sondes

<i>Station</i>	<i>2001</i>	<i>2002</i>	<i>2003</i>	<i>2004</i>	<i>2005</i>
IG	151	143	181	118	109
K1				175	131
SH	151	144	68	130	117
K2			73	90	108
SC	150	145		170	106
SV	145	146	55	85	130
HC	118	111	77	91	144
SA	118	103	45	160	141
OR	141	129	101	88	137
WE	125	122	150	107	132
TR	101	85	146	117	136
MF/TC/KBW	115	94	140	135	125
TG/KAT	109	142	49	150	132
Total	1424	1364	1085	1616	1648

Table 1b
Number of records of complete diurnal cycle measured by sondes, after correction process

<i>Station</i>	<i>2001</i>	<i>2002</i>	<i>2003</i>	<i>2004</i>	<i>2005</i>
IG	126	126	92	104	100
K1				157	121
SH	128	140	62	113	108
K2			48	72	99
SC	119	126		144	98
SV	123	114	43	62	106
HC	98	92	65	71	110
SA	107	85	38	147	111
OR	119	107	80	76	113
WE	101	82	129	100	118
TR	82	49	118	107	125
MF/TC/KBW	92	60	116	126	67
TG/KAT	109	131	42	132	124
Total	1204	1112	833	1411	1400

Table 1c
Number of records of complete diurnal cycle measured by sondes, after correction process, June - September

<i>Station</i>	<i>2001</i>	<i>2002</i>	<i>2003</i>	<i>2004</i>	<i>2005</i>
IG	87	93	86	51	85
K1				104	106
SH	88	95	26	101	106
K2			42	56	86
SC	87	98		96	84
SV	83	81	43	62	90
HC	71	79	60	66	81
SA	86	72	20	95	84
OR	88	84	70	76	86
WE	78	67	90	81	104
TR	66	31	81	88	105
MF/TC/KBW	74	47	88	107	64
TG/KAT	81	97	16	98	109
Total	889	844	622	1081	1190

subject to more stable river flow and the main period for phytoproduction. Table 1c summarizes the number of complete diurnal cycles restricted to this period, a total of 4,626.

2. Example analyses and sources of error

To illustrate the strategy of calculation, Ward and Armstrong (2006e) presented an example using August 2004 sonde data from Station WE. Here we further exemplify the procedure and illustrate some of the potential sources of error. We examine the record from a station also, like WE, representative of the Lower Klamath reach, viz. the station near Orleans, and also under relatively quiescent river-flow conditions. During mid-summer of 2005, this station was subject to moderate and diminishing streamflows with few external disturbances, and the pattern of both temperature and DO was a modest cyclic diurnal variation, see Figure 2. The amplitude of the

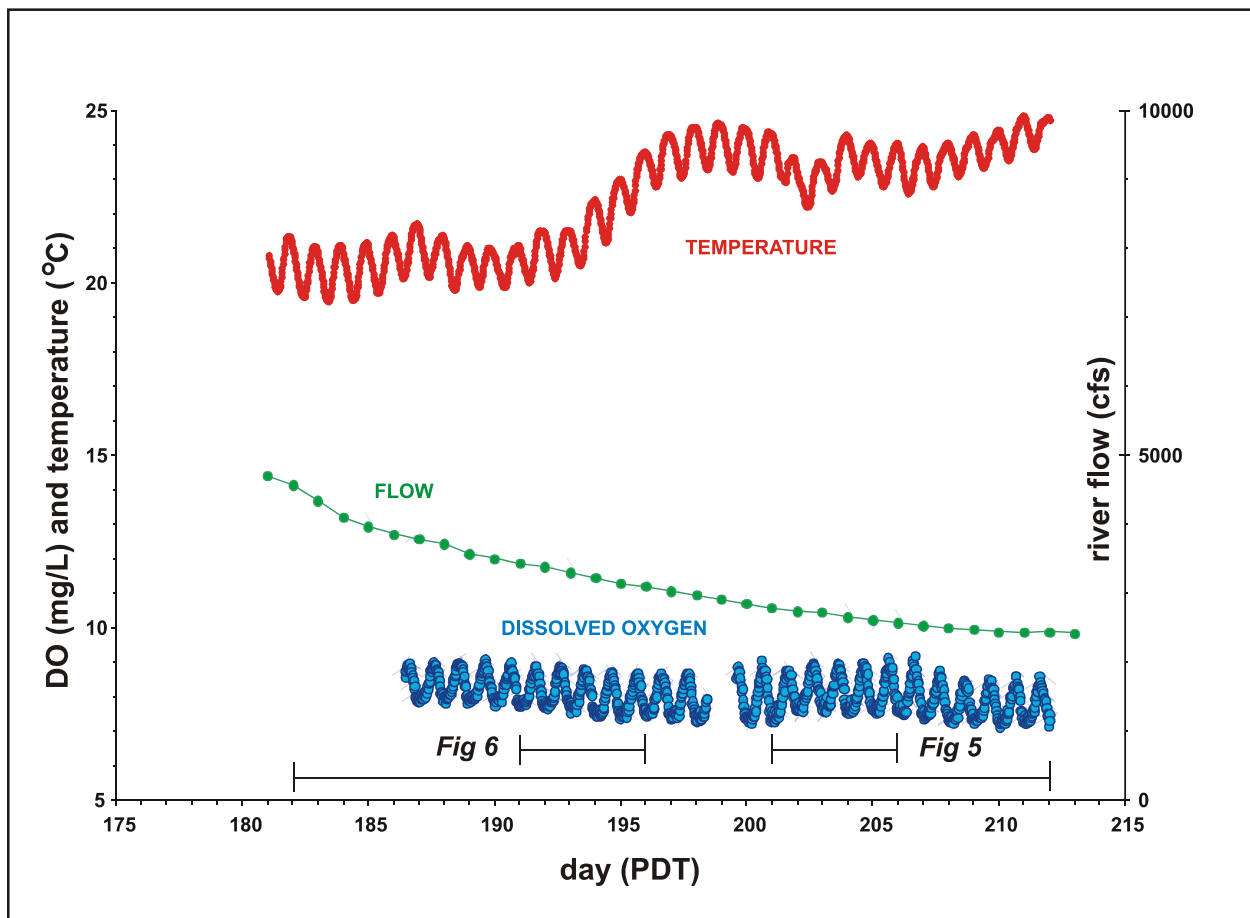


Figure 2 - Sonde records of DO and water temperature, with USGS gauged river flow, from Station OR in Klamath, July 2005

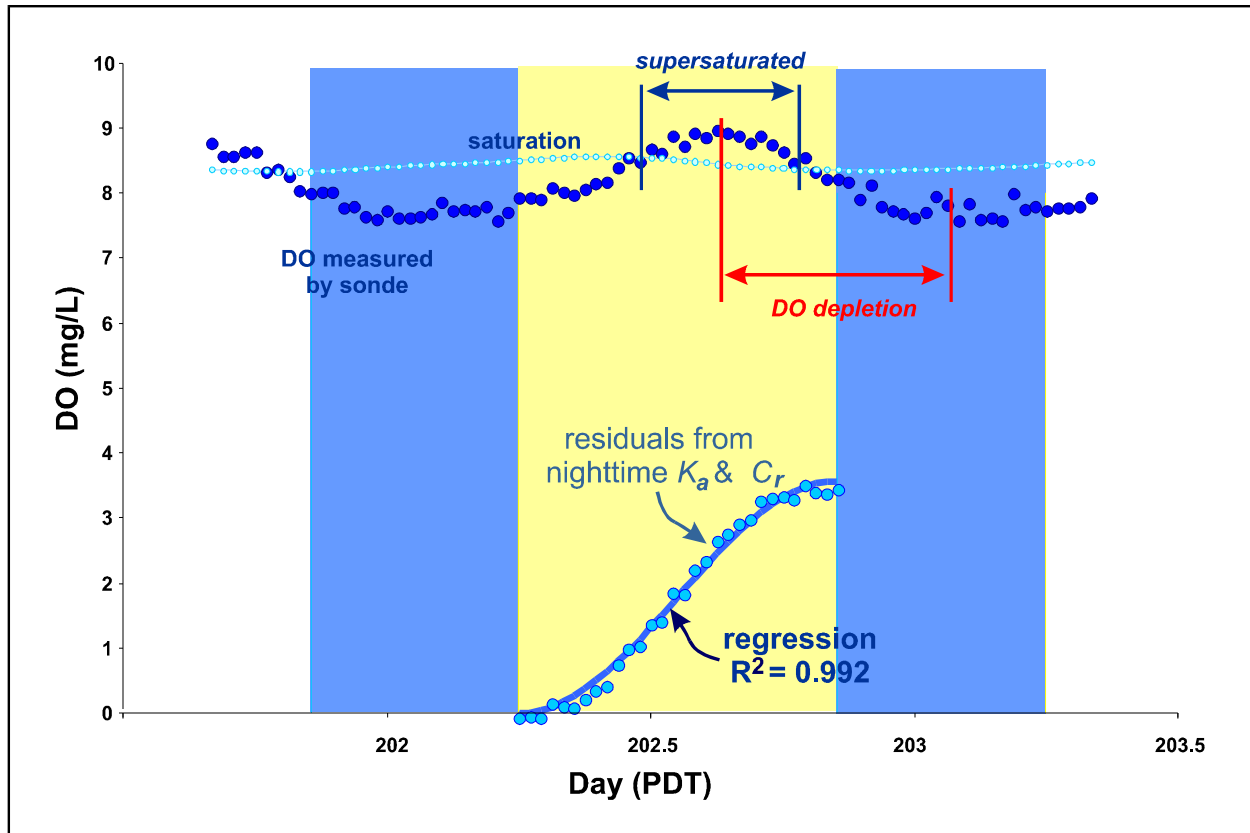


Figure 3 - Sonde records of DO and saturation calculated from water temperature, Station OR 22 July 2005, and least-squares fit to estimated photosynthesis, equation (3)

temperature variation of about 1.2°C is insufficient to account for the DO variation of about 1.1 mg/L (and, moreover, is out of phase), so it is clear that photosynthetic activity is at work. A single day (22 July) is isolated in Figure 3, in which the time traces are shown of the sonde measurements of DO and the computed values of saturation. There are two adjacent nighttime periods available for estimating the kinetic parameters K_a and C_r . Their calculation from the later set of nighttime data, i.e. the evening from sunset of 22 July (day 202) to sunrise on 23 July (day 203), is illustrated in Figure 4. (The values of K_a and C_r are at ambient temperature.) Unlike the example of WE (Ward and Armstrong, 2006e), these data are considerably noisier. The averages of the K_a and C_r values for the preceding and following nighttime periods are used

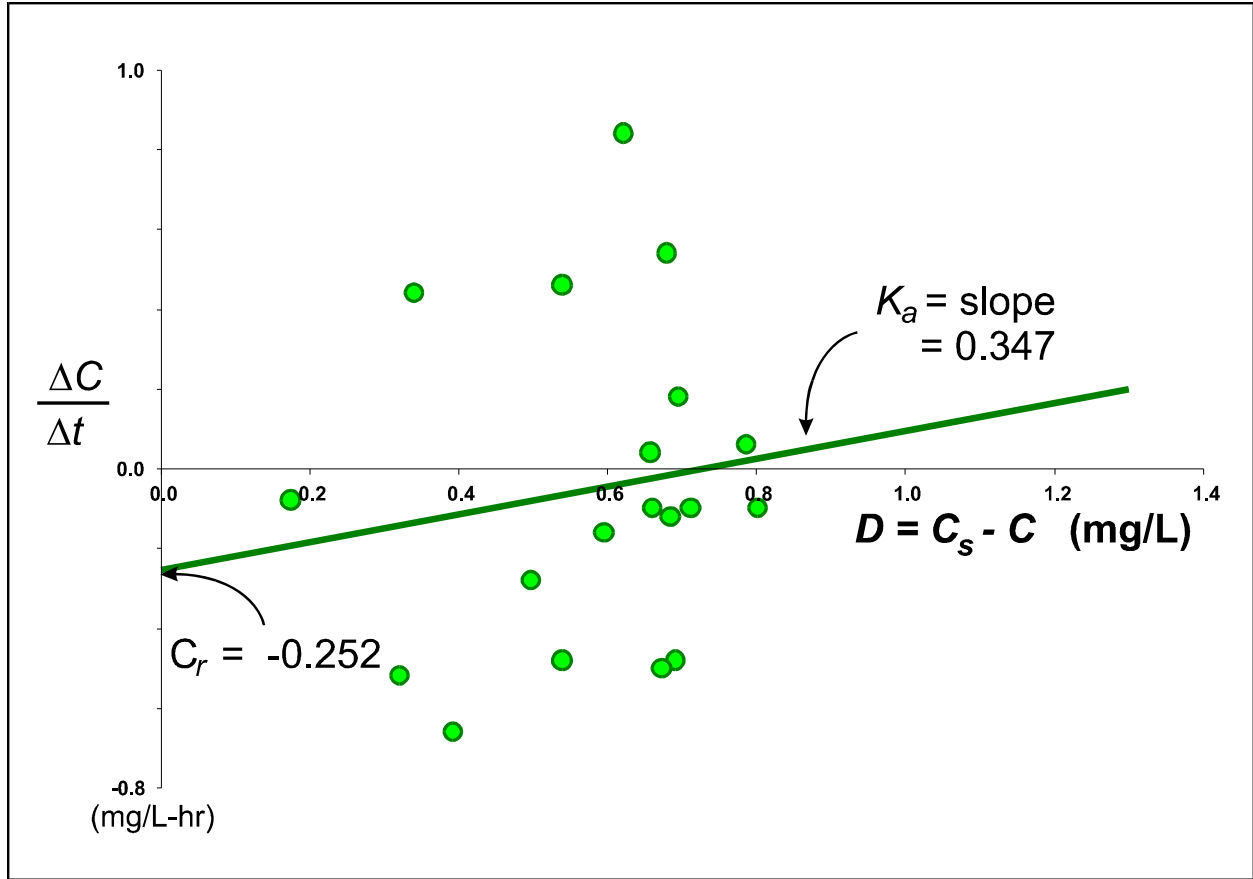


Figure 4 - Regression of dC/dt versus deficit, from nighttime sonde data, Station OR in Klamath, nighttime period 22-23 July 2005

to compute the incremental gross photosynthesis in Equation (3), whose time series and the associated least-squares regression of the mathematical form $\sin\{\pi(t - t_n)/t_d\} + 1$ are shown for 22 July in Figure 3.

Over the daylight period of 14.4 hrs, the net DO depletion resulting from the average value of C_r is about 3.2 mg/L. The cosine amplitude $S = 0.39$ mg/L/hr corresponds to a gross photosynthetic DO influx of about 3.6 mg/L. During the course of the day, DO is driven to supersaturation by late morning, see Fig. 3. Throughout this supersaturated interval both mechanical DO exchange with the atmosphere and respiration operate to remove DO from the water column, so that in early afternoon the concentration of DO begins to diminish.

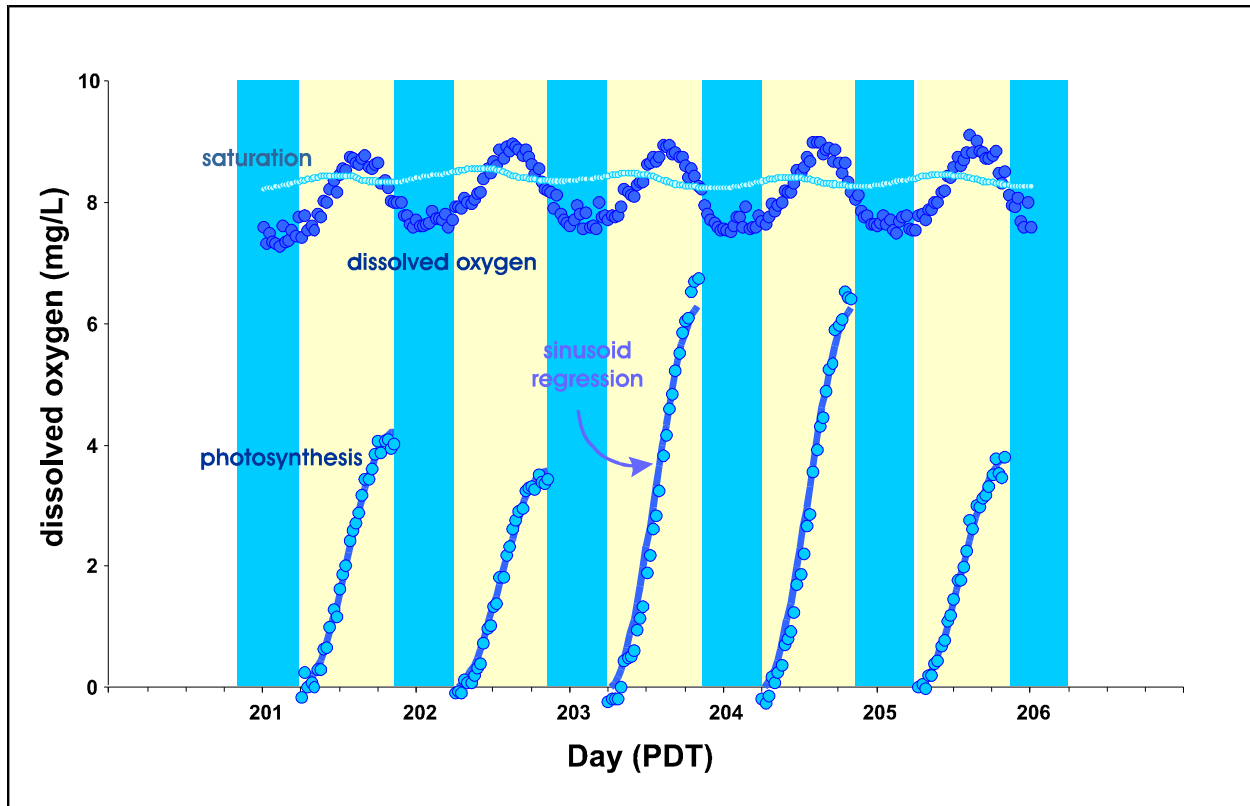


Figure 5 - Sonde records of DO and saturation, Station OR 21-25 July 2005, with least-squares fits to estimated photosynthesis, cf. Fig. 3

As can be seen in Fig. 3, the sinusoidal-type regression applied to the time series of incremental production, i.e. equation (3), is spectacularly successful in depicting the time variation, achieving an explained variance of over 99%. More discussion of this unconscionably good predictive performance is given below. For now, we observe that this high explained variance is a quantitative demonstration that the residual diurnal DO variation, i.e. the DO values after the effect of reaeration and community respiration are subtracted out, see equation (3), is closely modeled by a half-cycle sinusoid with inflection at solar noon. (In other words, the residual rate of change of DO is closely modeled by a half-cycle cosine centered on solar noon.)

A time series of a five-day sequence containing the diurnal period of Fig.3 is shown in Figure 5, and indicates equal success in fitting the time series of the incremental values computed from

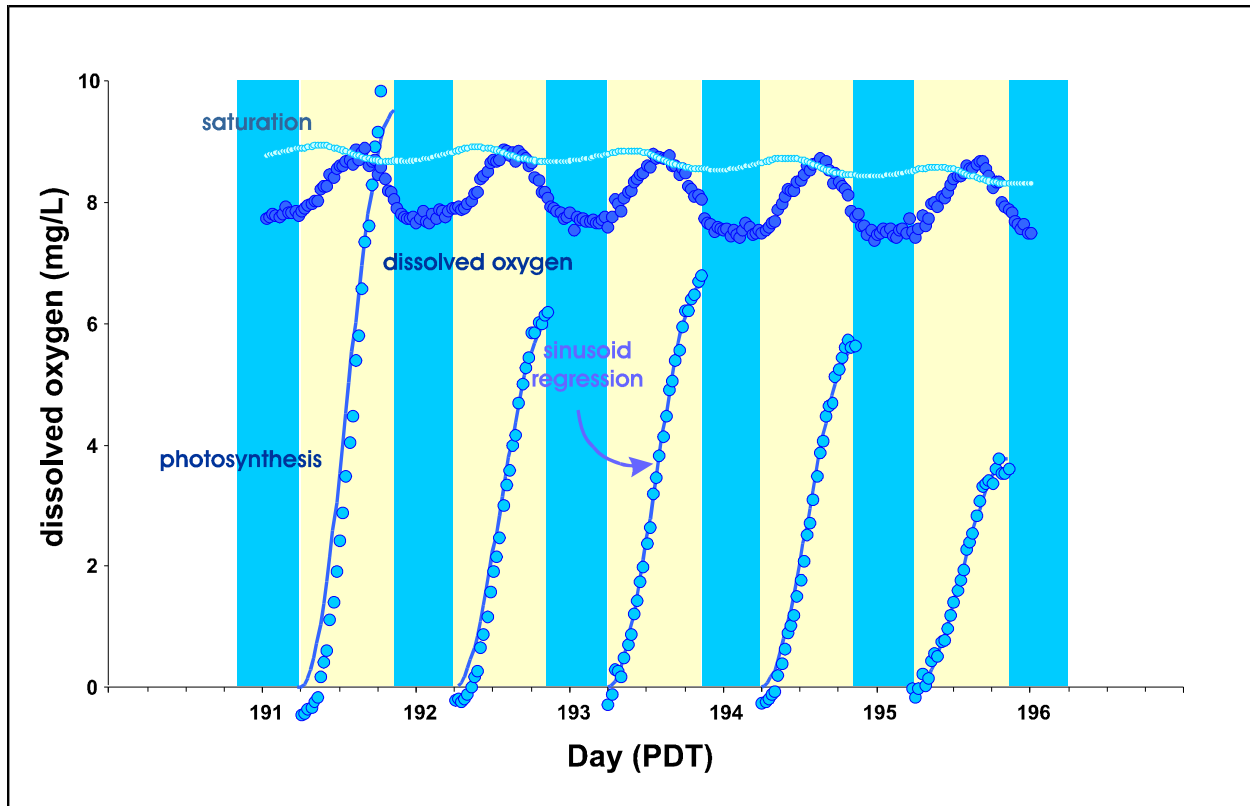
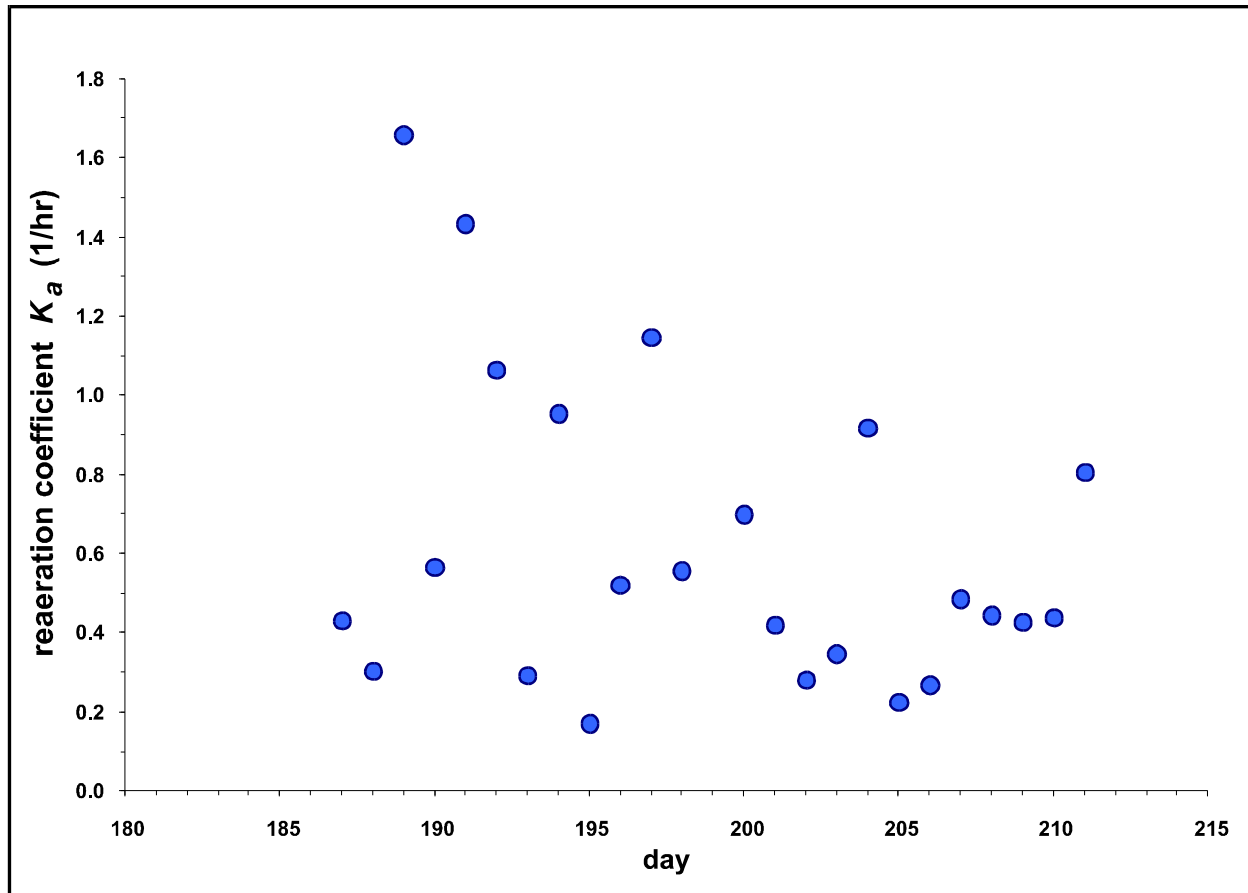


Figure 6 - Sonde records of DO and saturation, Station OR 11-15 July 2005, with least-squares fits to estimated photosynthesis, cf. Fig. 5

equation (3). A five-day sequence from earlier in the month is shown in Figure 6. Over the period depicted in Figs. 5 and 6, there is consistency in the diurnal variation of DO, superposed on a slow increase in supersaturation, especially evident in the later period of Fig 5. On day 191, DO becomes briefly supersaturated around noon, after which the daily duration of supersaturation gradually increases. This is consonant with the slight surfeit of gross production over respiration inferred from Figs. 3 and 4 above. However, the day-to-day consistency in the DO cycle does not obviously accord with the factor-of-two range of variation in the apparent amplitude of the residual diurnal cycle.



**Figure 7 - Reaeration coefficients, Station OR July 2005,
from linear regressions of nighttime DO change versus deficit, cf. Fig. 2**

Part of this excessive variation in the computed photosynthesis originates in the variance of the regression of dC/dt , cf. Fig. 4, selected as an example of relatively poor correlation. As is well known, differencing a time series, in this case the sonde record of DO to compute $\Delta C/\Delta t$, increases the variance, so the time series of $\Delta C/\Delta t$ is noisier than the time series of C (i.e., DO) from which it is derived. Indeed, the primary motivation for using equation (2), rather than (1), as the basis for fitting the daytime residual DO is to avoid the noise created by differencing the data. (Compare, for example, Fig. 4 of Ward and Armstrong, 2006e, which shows $\Delta C/\Delta t$ fitted to a cosine.) The daily values of reaeration K_a computed from the data of Fig. 2 are shown in Figure 7. While part of the day-to-day variation is real, some of it is introduced by the noise in

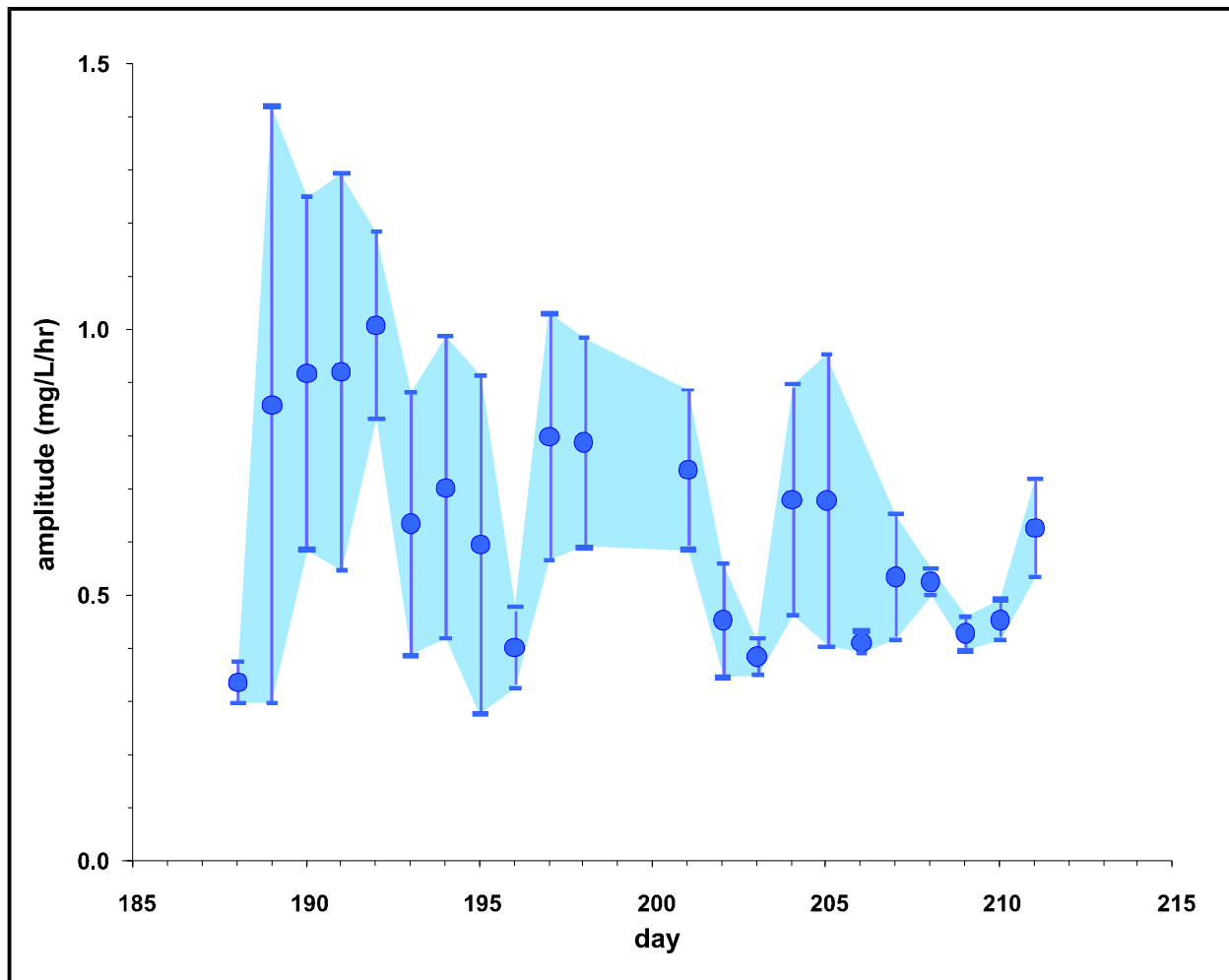


Figure 8 - Amplitude S of photosynthesis, Station OR July 2005

the $\Delta C/\Delta t$ time series. This can be compensated to some extent by the tactic of using the *average* of the nighttime values of K_a and C_r preceding and following a daylight time series to compute photosynthesis, as noted above (see Fig. 3). Moreover, the range of computed photosynthesis for a given daylight period using the values of K_a and C_r separately from the night before and night after provides a measure of the uncertainty arising from their variation. Figure 8 shows the time series of photosynthesis amplitude for July 2005, with the range based upon using each of the

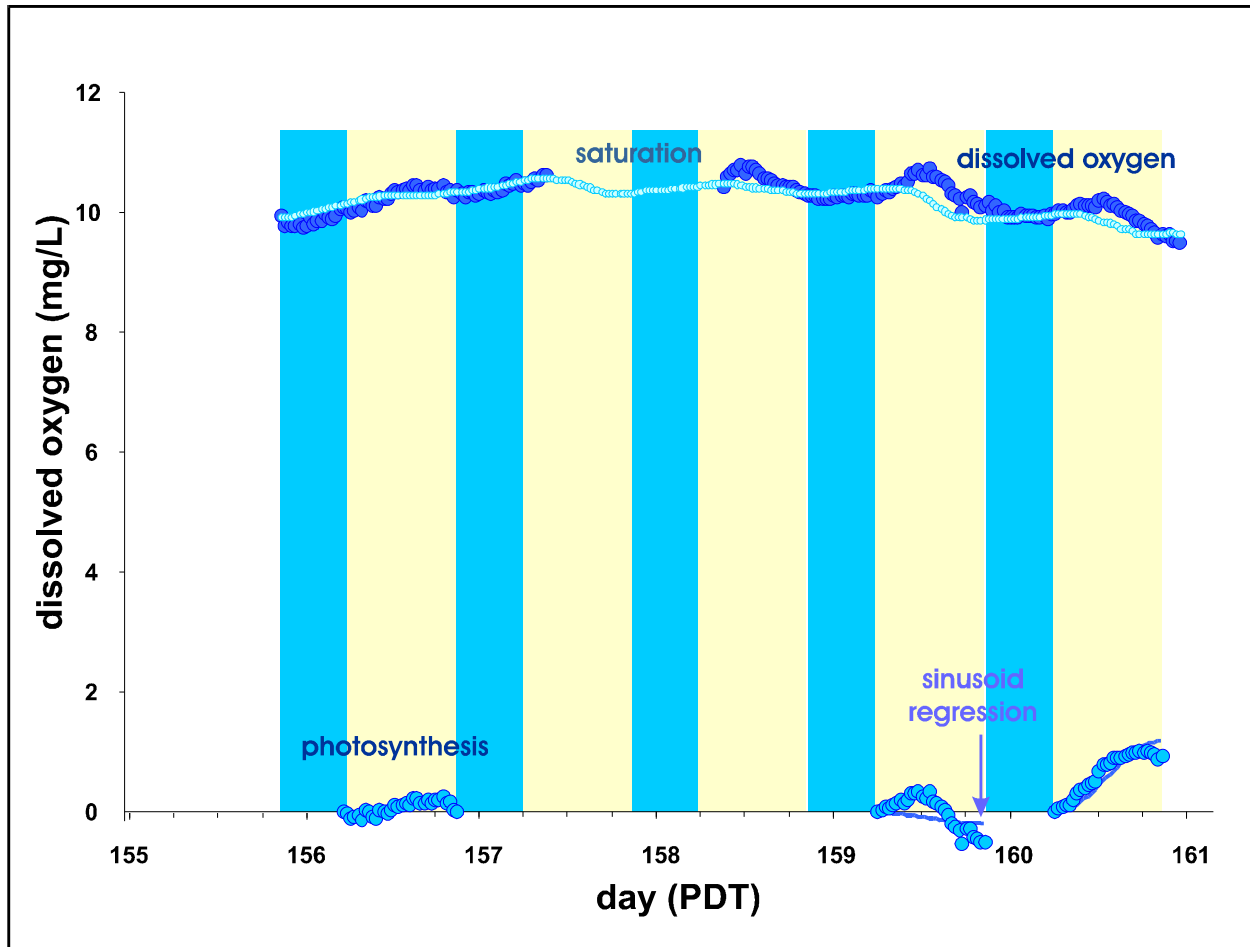


Figure 9 - Sonde records of DO and saturation, Station OR 6-10 June 2005, with least-squares fits to estimated photosynthesis, cf. Fig. 5

night periods before and after each daily value. (The daily gross photosynthesis in mg/L is obtained by multiplying these values by $2 t_d / \pi$, $t_d \approx 14.7$ hrs for OR in July.) Because K_a and C_r are anticorrelated, the computed photosynthesis proves to be less sensitive to their variance: for example, the coefficient of variation of reaeration in Fig. 7 is 64%, but that of the associated photosynthesis Fig. 8 is 30%.

A different computational problem is illustrated in the previous month at the same station, see Figure 9. Here the nighttime values of DO track very close to saturation. The corresponding

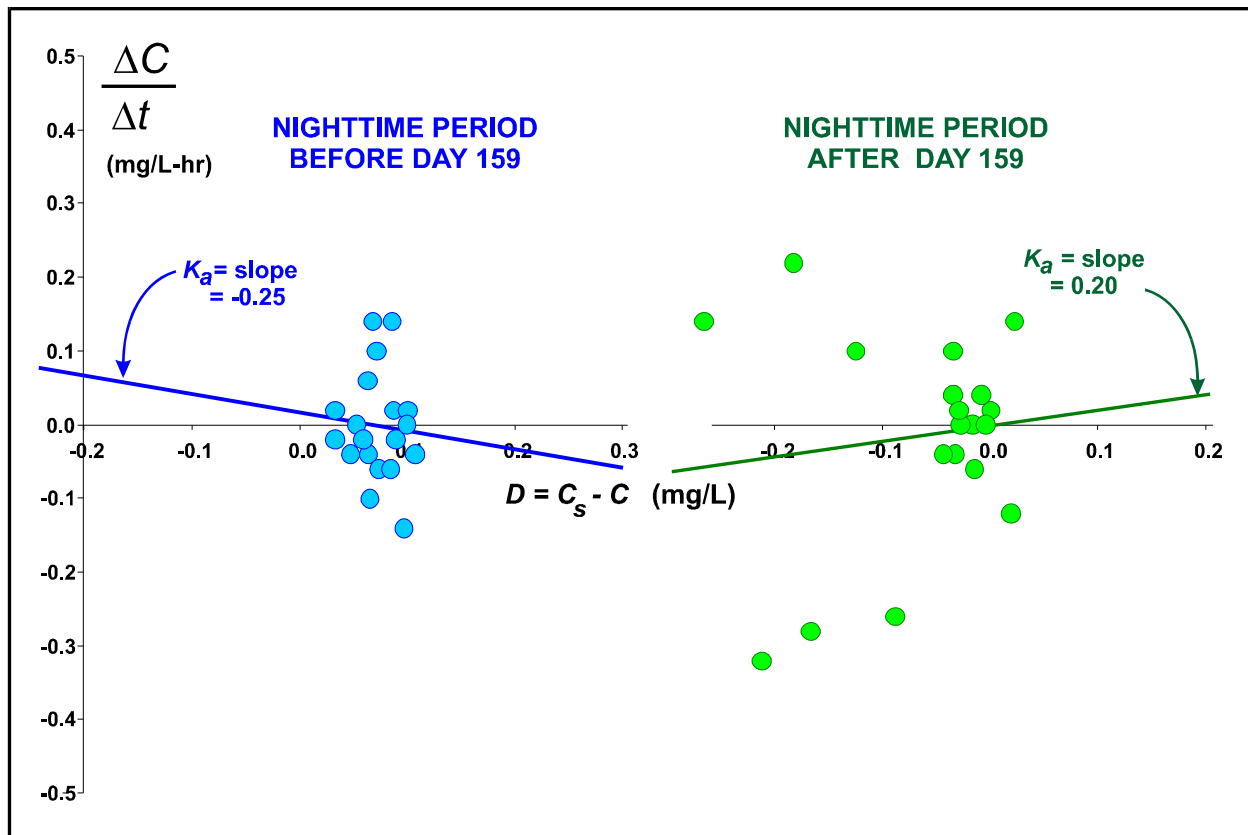


Figure 10 - Regression of dC/dt versus deficit, from nighttime sonde data, Station OR 2005, nighttime periods 8-9 June (left) and 9-10 June (right)

values of deficit are small, much less than 0.5 mg/L, so in a regression with deficit as the independent variable, its range of variation is too small to allow an accurate correlation. The noise introduced by differencing the DO measurements further corrupts the statistics, so that the regression line is meaningless, see Figure 10. The average K_a used in the daylight regression in Fig. 9 is spurious (and happens to be negative), producing an equally spurious (and negative) photosynthesis. Physically, when the DO tracks saturation as in the example of Fig. 9, nighttime respiration is zero, reaeration is shut off because the deficit is zero, and K_a cannot be determined by the regression method. When photosynthesis is substantial, and the resulting nighttime respiration produces a wider range of deficit values, the regression approach is valid. In Fig. 5, even though the diurnal-mean deficit is small, the intradiurnal range of variation is large enough

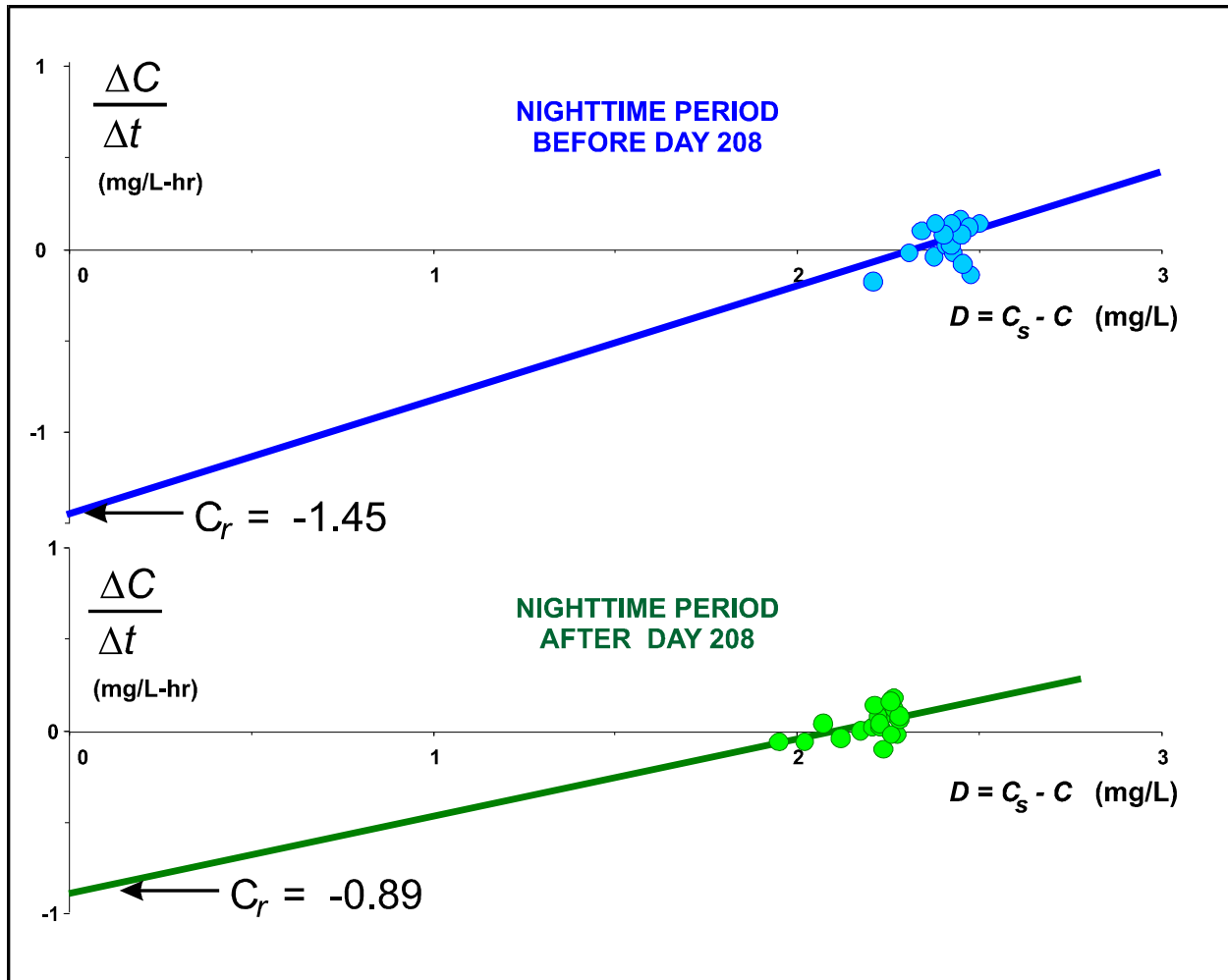


Figure 11 - Regression of dC/dt versus deficit, from nighttime sonde data, Station SH 2005, nighttime periods 27-28 July (above) and 28-29 July (below)

that valid regressions can be performed. In assessing the validity of the calculated photosynthesis, it is important to examine the degree of departure of DO from saturation over the diurnal period.

Even with large values of deficit, however, a different type of numerical problem can arise, illustrated in Figure 11. Despite the validity of the correlation, the resulting extrapolation from a deficit of more than 2 to the zero intercept in effect amplifies the variance in the slope of the regression line, the “lever-arm effect,” introducing in this case a 50% difference in the estimated

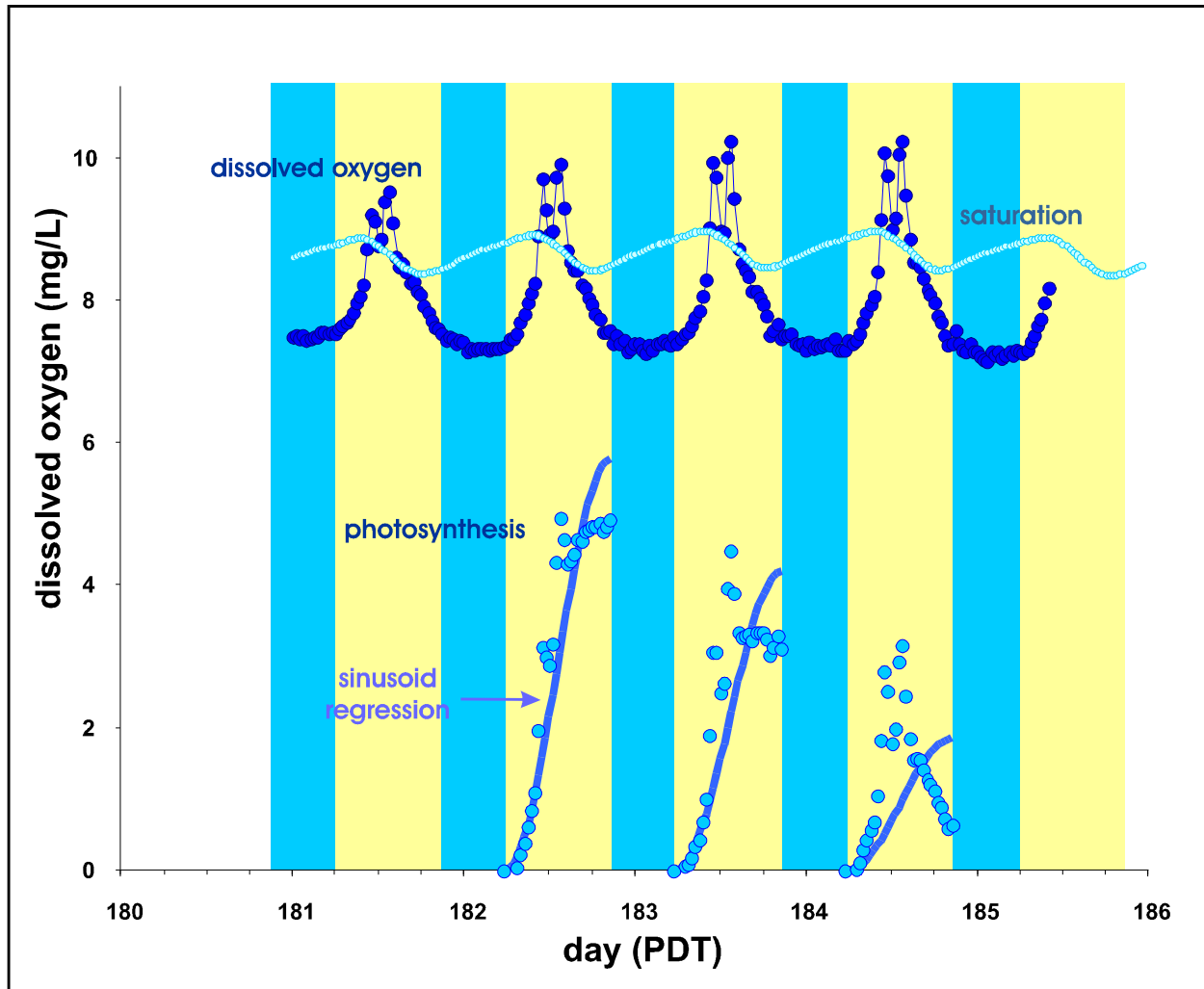


Figure 12 - Sonde records of DO and saturation, Station HC 1-5 July 2005, with least-squares fits to estimated photosynthesis, cf. Fig. 5

respiration C_r (cf. Fig. 4). Any data sets exhibiting systematic DO depression or supersaturation over the diurnal period can result in increased uncertainty in the community respiration, even when the reaeration rate K_a (the slope of the regression) is fairly well-determined.

Finally, there is one additional category of sources of error, whose presence may elude inference from the data, namely violation of any of the four assumptions listed in Section 1 above that underlie the mathematical analysis of the data. Short-term variation in either respiration or reaeration that leads to differences between the nighttime and daytime rates will corrupt the

analysis. Inhomogeneous oxygen distribution across the section can entail the sonde sensor encountering water with different oxygen values. At best, this will contribute to the noise in the DO data; at worst, this can produce systematic variation in the measured DO that will be misinterpreted as the result of kinetic processes. The assumption of negligible advection of DO (i.e., that $\partial C/\partial t \approx dC/dt$) may be violated by downstream transport of a longitudinal DO gradient: particularly during sudden runoff events, water of different oxygen content may be advected into the sonde vicinity, and the associated time change in DO misattributed to respiration or photosynthesis. Finally, any disruption of the relation between insolation and production, such as physical shading of the sonde, or rapid development of an algal bloom, may produce variation in the measured oxygen response that violates our underlying mathematical model of a cosinusoid insolation function. How is one to interpret DO variation such as exhibited in Fig. 12, in which the values above saturation undergo a sharp rate of increase then a systematic depression precisely at noon (Pacific daylight saving time)? Sonde malfunction? Or the operation of one of these processes that violate the assumptions of the model?

The foregoing focus on the various aberrations in the sonde data may give the impression that these data sets and the analysis methods are riddled with sources of error and are not to be trusted. In fact, the majority of the data is well-behaved and the sources of error enumerated above have a minimal impact upon the inferred values of reaeration, community respiration, and gross photosynthesis, as will be seen in the following section. Nonetheless, these sources of error do represent a trap for the unwary, which motivates a strategy of data processing to minimize the potential effects of such anomalies. Two strategies were implemented in the present analysis. First, the time-series analyzed data (at a daily timestep) were subjected to a running, centered 5-point average. As a simple low-pass filter (e.g., Hamming, 1973), this has the effect of smoothing out fluctuations, including both normal noise in the data and erratic variation introduced by the aberrancies exemplified above. Philosophically, it could be argued, this retains both valid and invalid data so that the average is corrupted: a report is not rendered more valid by including only a fraction of a sea serpent. Therefore a second approach is to completely screen out the data points that evidence possible corruption by one or several of the sources of error listed above. The screening protocol employed in the present analysis is indicated by the following Venn diagram (Fig. 13):

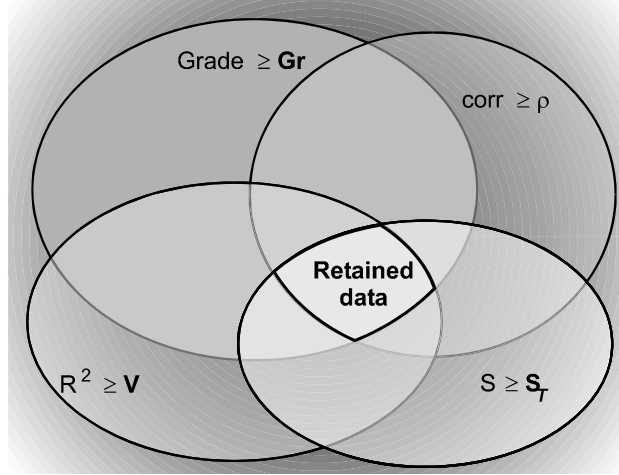


Figure 13 - Schematic of application of data screens (see text)

where

Grade \equiv grade assigned to deployment based upon data-set quality (e.g., Fig. 1)

\mathbf{Gr} \equiv screening threshold for grade (based upon $A = 4.0$, $F = 0.0$)

corr \equiv linear correlation of (nighttime) $\Delta C/\Delta t$ versus DO deficit

ρ \equiv threshold value of correlation

R^2 \equiv explained variance of sinusoid regression of DO residuals, eqn (3)

V \equiv threshold explained variance (between 0.0 and 1.0)

S \equiv amplitude of cosine model of photosynthesis $P(t)$ in eqns (1) & (2)

S_T \equiv threshold value of S

We emphasize that both the selection of screening parameters and the order that the screens are applied are matters of judgment. The specific threshold values employed are summarized in Table 2. This screening reduced the number of complete diurnal cycles for analysis by 36%

Table 2
Screening thresholds in order of application, cf. Fig. 13

<i>variable</i>	<i>designation in Fig. 13</i>	<i>threshold value</i>
Grade	\mathbf{Gr}	3.0
corr	ρ	0.2
R^2	V	0.4
S	S_T	0.0

relative to the number available after the correction process, and 38% for the June – September period, see Tables 3a and 3b (compared to Tables 1a and 1b, resp.). The two most brutal screens are the exclusion of data graded less than “B”, as this removes entire deployments in one fell swoop, and the requirement that the $\Delta C/\Delta t$ versus deficit correlation be at least 0.2 . With respect to the latter, we note that these excluded data sets are not necessarily suspect, but rather are simply not amenable to the analysis methodology pursued here. Without a reasonable correlation, there is no means of inferring values of K_a and C_r from the time variation of DO, hence no way to isolate the effects of reaeration and respiration on the DO budget from that of photosynthesis. With an alternative estimate of K_a and C_r , however, these data sets could be used as well for estimation of gross photosynthesis. Even with such brutal screening, the screened data represent a formidable base of measurements, with nearly a thousand separate diurnal cycles available for analysis, and for the period June – September, well over 800.

Table 3a
Number of records of complete diurnal cycle measured by sondes, after correction process,
screened by thresholds of Table 2, cf. Table 1b

<i>Station</i>	<i>2001</i>	<i>2002</i>	<i>2003</i>	<i>2004</i>	<i>2005</i>
IG	38	29	15	15	25
K1				131	121
SH	89	98	16	43	57
K2			47	46	84
SC	107	79		7	86
SV	120	107	41	41	101
HC	68	71	45	50	16
SA	98	61	3	32	49
OR	105	85	61	40	73
WE	85	69	111	52	106
TR	77	44	51	51	93
MF/TC/KBW	56	58	85	108	45
TG/KAT	51	98	12	70	89
Total	894	799	487	686	945

Table 3b
Number of records of complete diurnal cycle measured by sondes, after correction, June – September,
screened by thresholds of Table 2, cf. Table 1c

<i>Station</i>	<i>2001</i>	<i>2002</i>	<i>2003</i>	<i>2004</i>	<i>2005</i>
IG	31	23	15	13	25
K1				91	106
SH	74	67	5	43	57
K2			41	42	71
SC	86	65		7	73
SV	81	74	41	41	85
HC	49	58	40	46	9
SA	86	49	3	28	32
OR	74	70	51	40	54
WE	72	64	80	47	103
TR	63	29	38	45	90
MF/TC/KBW	38	46	71	93	42
TG/KAT	44	81	9	59	84
Total	698	626	394	595	831

3. Behavior of DO and its kinetics in the Klamath

Relative locations of the principal sonde stations are indicated on the stem diagram of Figure 14. The corrected data sets and their analyses are presented in the format of EXCEL[®] workbooks, to serve both as a data archive and a permanent record of the data reduction and analysis in which the sources of data, calculations, and tabular and graphical results are presented and linked. There are two sets of these workbooks. The first set contain the raw sonde data and associated information, such as deployment records, notes of conditions, data logged from handheld sensors at insertion and extraction, meteorological and hydrological observations, and station data. These workbooks have comprehensive development of the corrections, their motivation and application, and the assigned data grades, as well as the final sets of corrected data. Such a workbook was prepared for each sonde station and for each sampling year, a total of 59 such workbooks, each averaging about 30 MB in size. The second set of EXCEL[®] workbooks each starts with the corrected sonde time series from the first set, which are now subjected to the calculations outlined in Section 1 above, in which the diurnal series are separated into night and

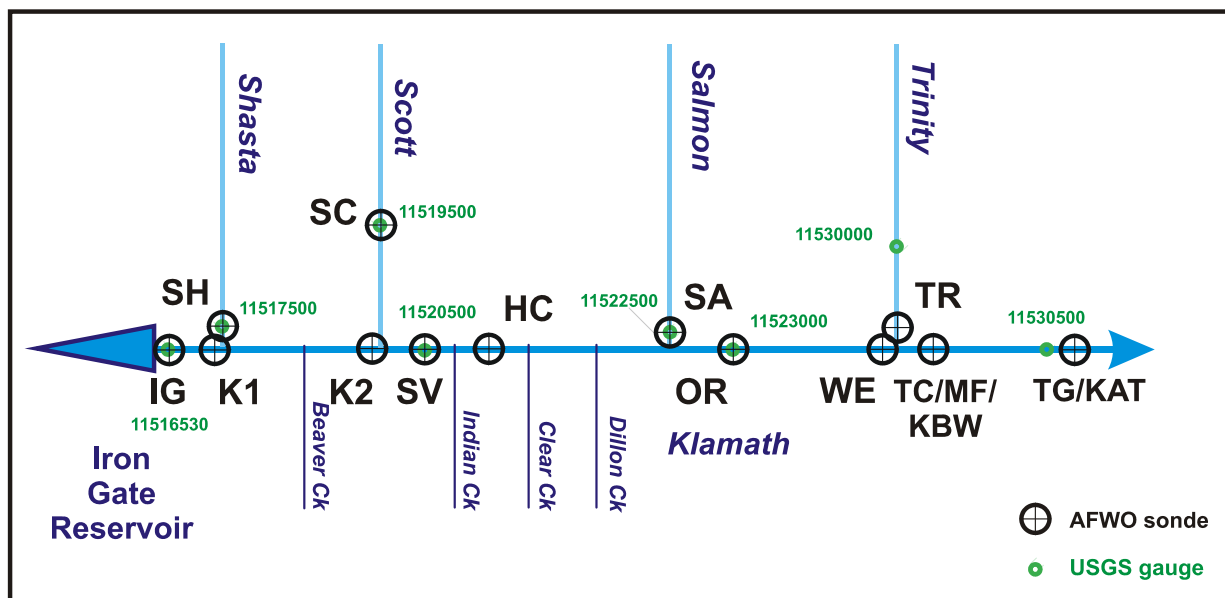


Figure 14 - Stem diagram of Klamath and major tributaries showing relative locations of sonde stations

day series, the former being used to estimate reaeration coefficients K_a and community respiration rates C_r , and the latter to separate the component of gross photosynthesis from the estimated respiration and reaeration. Again, there is one workbook for each station/year, of size about 30 MB.

These data sets can be analyzed in many ways. DO variations (and associated kinetics) during specific diurnal periods along with ancillary information on river flow, meteorology and insolation can be given detailed evaluation. Events, such as flow pulses or apparent organic load injections, can be identified in the record and tracked downstream over time, during which their effects on DO kinetics can be isolated. In this section, we undertake a larger scale view, to distill the information from these massive workbooks to exhibit the general behavior of the DO budget of the Klamath over the 2001-2005 period, i.e., to present a DO “climatology” of the river.

The upstream limit of the study reach, *viz.* the lower Klamath, is Iron Gate Reservoir, releases from which typically dominate the hydrology of the first 150 km (100 mis) below the dam during the low-flow summer season (Ward and Armstrong, 2006a). The 2005 DO record from the uppermost sonde station IG, located just downstream from Iron Gate, is shown in the upper panel of Figure 15. The individual (corrected) sonde measurements are indicated by the fine trace, upon which is superposed the running 24-hr mean. The variation of instantaneous DO about this running mean is a direct indication of photosynthetic activity. The concentration of DO saturation, computed from the sonde-measured water temperature, is the dark blue line. (The vertical lines on this figure denote the sonde deployment periods.) The river flow is essentially the release from Iron Gate, and during the summer this release is substantially constant. Two features of the DO variation are immediately evident: (1) the photosynthetic variation of DO is small; (2) there is a large DO deficit, which, though highly variable, generally increases toward the end of summer and early fall. These features prove to be characteristic of DO at this station for each year of the study period. The DO deficit of water exiting the reservoir is due to summer stratification of Iron Gate (with the associated decline in DO through the thermocline layer), so that lower DO water is entrained into the release, which is drawn from a layer of depth about 10 m (35 ft). The marked increase in deficit late in the season, typically the early fall, is the effect of the seasonal overturn of the reservoir.

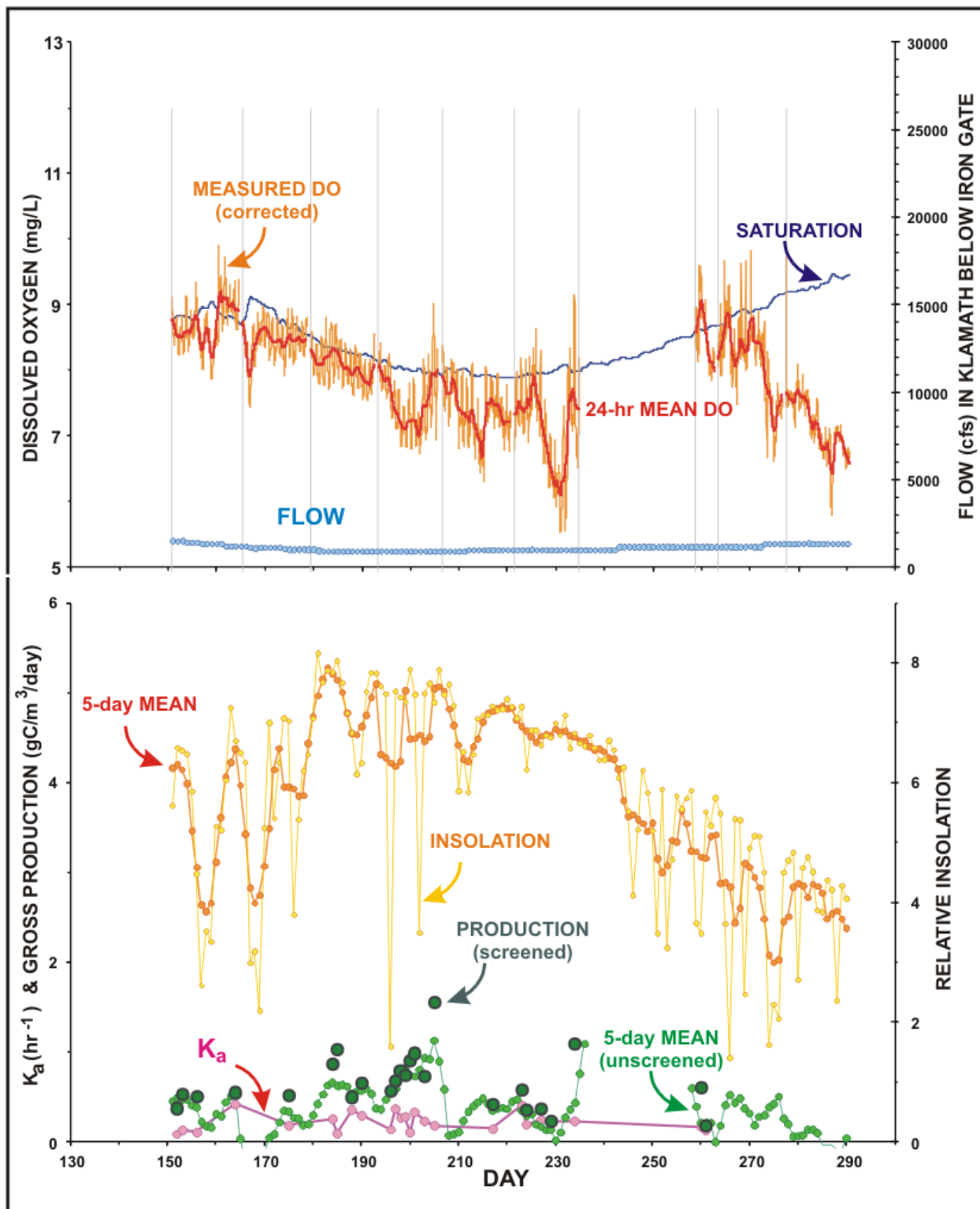


Figure 15 - Measured DO time series (corrected) at Station IG, 2005, with streamflow, relative insolation and computed kinetic variable (see text)

In the lower panel of Fig. 15 are displayed the corresponding time series of insolation (solar radiation received at the ground surface), reaeration coefficient, and gross daily production. Both the 5-day running mean and screened values of production are shown in the plot. (Screened data are not subjected to a running average because the screening too frequently interrupt the continuity of the time series.) Insolation data were obtained from records of the U.S. Geological Survey (unpublished data), from stations established according to NWCG (2005). The nearest radiation station (or an average of several) to each sonde station was used to estimate daily solar radiation over the data-collection period. Unfortunately, these data sets proved to be problematic: poorly calibrated, with sudden shifts in calibration, inconsistency across data files, and corruption by errant spikes. Armed with the expectation that daily clear-sky solar radiation should vary as the cosine of the local solar zenith, we were able to empirically adjust or expunge the anomalies to produce a time series of *relative* insolation (i.e., uncalibrated to the actual insolation at a sonde station). This suffices to address the correlation of primary production with insolation, which is its sole purpose in this analysis.

With distance down the river, runoff and tributary flows dilute the reservoir water and add organics and nutrients, so that the features of the Iron Gate station, reflecting the release from the reservoir, exemplified in Fig. 15, become transformed into those more typical of a flowing river. This is illustrated by the same data series at Station WE, at Weitchpec, shown in Figure 16. (Figures 15 and 16 have the same time and variable axes to facilitate their intercomparison.) Over the summer, the DO concentration generally tracks its solubility, first decreasing then increasing as temperature rises in early summer then declines in late summer. The daily range of variation about the mean, on the order of ± 1 mg/L (even before the effects of respiration are removed), evidences algal production, resulting in increasing supersaturation as the summer progresses. The photograph of Fig. 17 attests to presence of a dense algal population. Reaeration coefficient K_a is stable over the course of the summer, which is consistent with the stability of river flow and the generally quiescent meteorology of the summer, and indicates that there is little corruption of the analysis due to the potential sources of error summarized in the preceding section. The pattern of a modest increase in K_a in July (days 180-210) and decline in September (days 245-275) is consistent with its dependency upon water temperature. Most

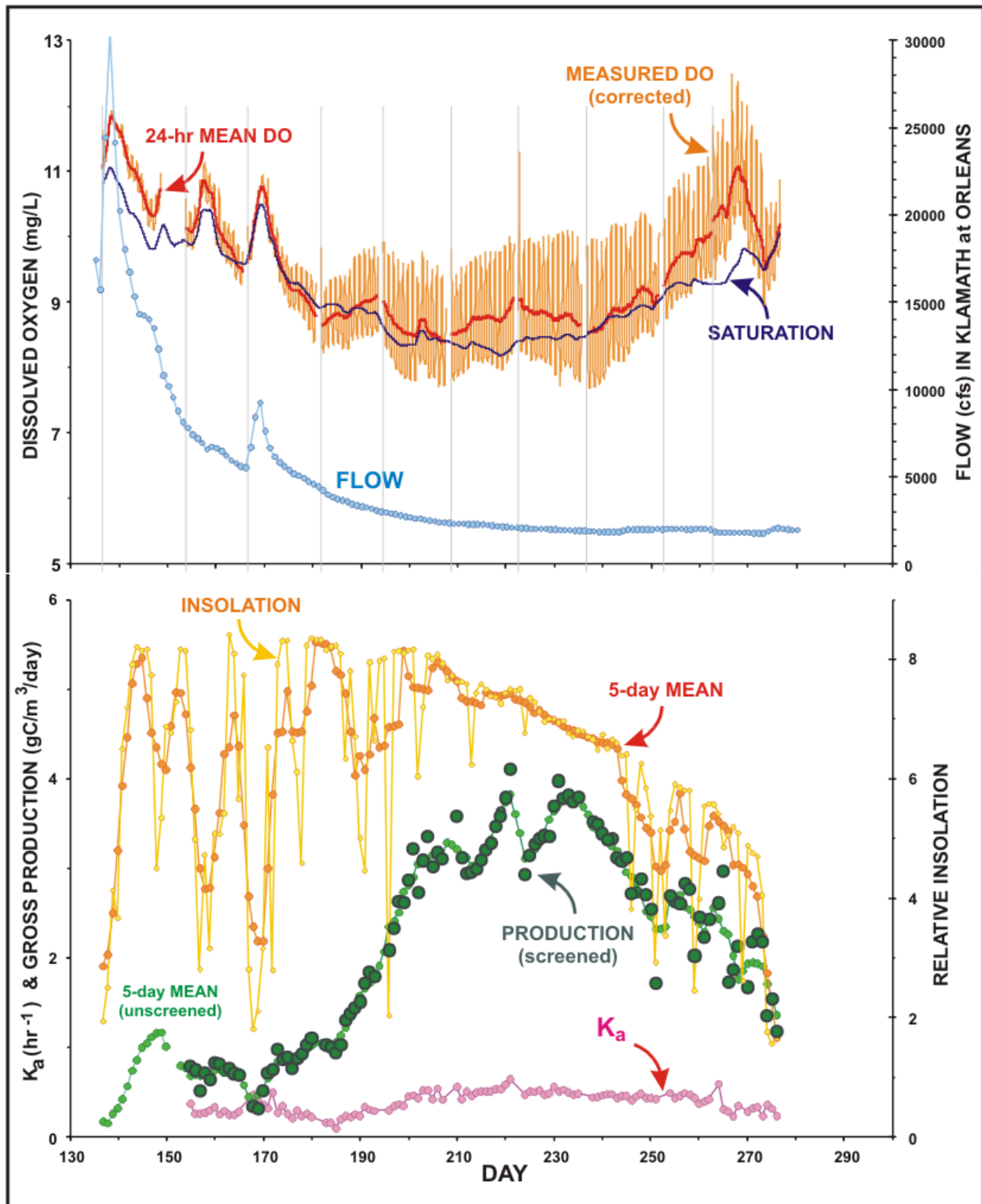


Figure 16 - Measured DO time series (corrected) at Station WE, 2005, with streamflow, relative insolation and computed kinetic variable (see text)



Figure 17 - Station WE, Klamath at Weitchpec, 8 September 2005
(*cf.* deployment break, Day 252, Fig. 16)

prominent, of course, is the substantial increase in estimated gross production during June and its maintenance through the remainder of the summer into early fall.

There are several low-insolation events in this record, which appear to be associated with drops in production, notably those on days 157, 168, 251 and 259. These are examples of events that would warrant detailed study. The event of 168-170 is of particular interest, being coincident with a major depression that became stationary off the Northern California coast for nearly a week, producing heavy cloud and rain, whence the associated surge in river flow. The reaeration

coefficient exhibits an associated rise despite the decrease in water temperature, suggesting a response to meteorology (probably wind and waves).

The reaeration coefficient is a key parameter in the oxygen budget of a watercourse. Generally, this coefficient is driven by the intensity of turbulence in the water column, so is expected to increase with the current speed, increase with surface wave intensity, and decrease with depth, perhaps nonlinearly. In a flowing stream, such as the Klamath, the current and water depth are considered to dominate other factors so long as the flow is sufficiently large. A number of formulae have been developed for its prediction, given physical parameters of the system. For flowing streams and rivers, one of the best-known and most widely applied formulae is the quasi-theoretical relation derived by O'Connor and Dobbins (1958):

$$K_a = 0.164 U^{1/2} / H^{3/2} \quad (4)$$

for K_a in hr^{-1} , U the current speed in m/s, and H the water depth in m, see also Chapra (1997).

At its gauging stations, the USGS has established rating relations giving U and H as functions of flow, as described in Armstrong and Ward (2008b). These were used in (4) to calculate the O'Connor-Dobbins (OD) reaeration coefficient at each of the sonde stations, based upon the daily streamflow, for comparison to the empirical values given by (3). The coefficient K_a increases with temperature according to a van't Hoff-Arrhenius relation

$$K_a(T) = K_a(20) \theta^{(T-20)} \quad (5)$$

for water temperature T in $^{\circ}\text{C}$. The OD equation (4) applies at $T = 20^{\circ}\text{C}$. Because our present interest is in the day-to-day variation in the oxygen budget, the values of K_a extracted from the $\Delta C/\Delta t$ versus deficit relation are reported at the *ambient* water temperature. Therefore, the corresponding value given by equation (5) is converted to ambient temperature for comparison to the empirical value of K_a , for which a value of $\theta = 1.024$ is employed. (The K_a values from the Churchill-Elmore-Buckingham, 1962, equation were also computed, but these proved to be very close to the OD values, so were not considered further.)

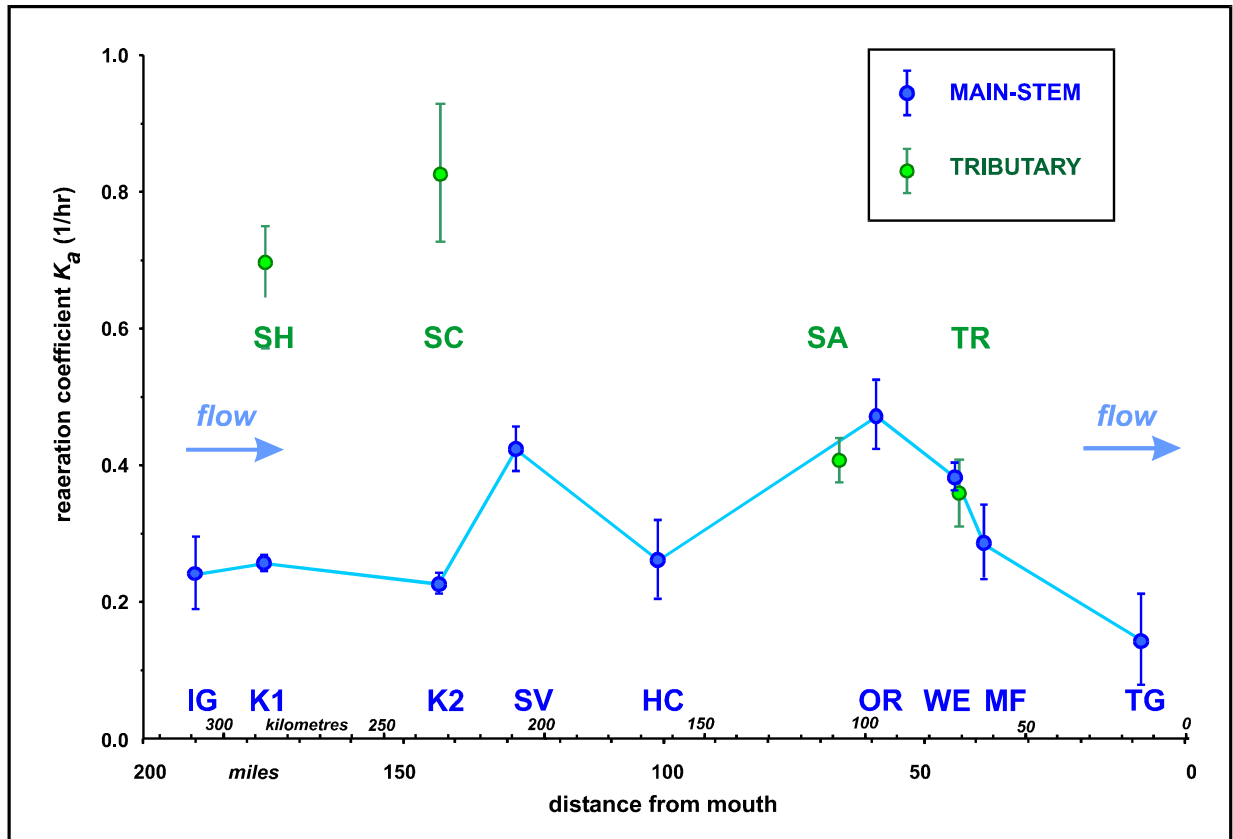


Figure 18 - Longitudinal variation of means of 2001-05 annual averages of K_a from sonde data (Table 4). Error bars are standard deviations of annual means about the 2001-05 average at each station.

In Table 4 are presented the average values of K_a determined both from the sonde data and by application of the O'Connor-Dobbins equation with the USGS values of U and H , averaged over the entire monitoring period of the sonde data, for each year of data collection and each sonde station, as well as the averaged station values over the 2001-2005 period. There is year-to-year consistency in the magnitude and distribution of the coefficients, as shown in the graph of 2001-05 means versus distance along the river in Figure 18. (There is, of course, additional day-to-day variation in K_a suppressed by the longer term average, *cf.* Figs. 15 and 16.) Generally there is an increase with distance downstream from Iron Gate to about Orleans, then a decline to the mouth of the river, the exception to this pattern being the depressed value at Happy Camp (HC). The

Table 4
Reaeration coefficient (K_a) from kinetic analysis and from O-Connor-Dobbins formula, all data

<i>Station</i>		<i>number</i>	<i>K_a</i>	<i>OD K_a</i>	<i>number</i>	<i>K_a</i>	<i>OD K_a</i>
<i>mainstem</i>	<i>tributary</i>	<i>of data</i>	<i>(1/hr)</i>	<i>(1/hr)</i>	<i>of data</i>	<i>(1/hr)</i>	<i>(1/hr)</i>
		2001			2002		
IG		38	0.18	0.12	29	0.32	0.13
K1		0			0		
	SH	89	0.69	0.41	98	0.73	0.37
K2		0			0		
	SC	107	0.83	2.17	79	0.86	1.15
SV		120	0.41	0.14	107	0.41	0.14
HC		68	0.22	0.14	71	0.30	0.16
	SA	98	0.35	0.30	61	0.48	0.26
OR		105	0.45	0.04	85	0.41	0.04
WE		85	0.36	0.04	69	0.39	0.04
	TR	77	0.41	0.14	44	0.37	0.14
MF/TC/KBW		56	0.31	0.07	58	0.31	0.07
TG/KAT		51	0.13	0.06	98	0.17	0.06
		2003			2004		
IG		15	0.31	0.13	15	0.23	0.14
K1		0			131	0.26	0.13
	SH	16	0.88	0.26	43	0.74	0.39
K2		47	0.22	0.15	46	0.25	0.19
	SC	0			7	0.84	0.92
SV		41	0.49	0.13	41	0.41	0.17
HC		45	0.19	0.15	50	0.35	0.17
	SA	0			32	0.41	0.25
OR		61	0.53	0.04	40	0.46	0.04
WE		111	0.37	0.03	52	0.41	0.04
	TR	51	0.33	0.11	51	0.37	0.13
MF/TC/KBW		85	0.28	0.06	108	0.23	0.06
TG/KAT		12	0.29	0.04	70	0.16	0.06
		2005			2001-05 average		
IG		25	0.23	0.13	122	0.24	0.13
K1		121	0.25	0.12	252	0.26	0.13
	SH	57	0.56	0.36	303	0.70	0.38
K2		84	0.22	0.16	177	0.23	0.16
	SC	86	0.79	1.04	279	0.83	1.50
SV		101	0.44	0.14	410	0.42	0.14
HC		16	0.24	0.14	250	0.26	0.16
	SA	49	0.43	0.23	240	0.41	0.27
OR		73	0.54	0.03	364	0.47	0.04
WE		106	0.39	0.03	423	0.38	0.04
	TR	93	0.33	0.11	316	0.36	0.12
MF/TC/KBW		45	0.39	0.06	352	0.29	0.06
TG/KAT		89	0.09	0.06	98	0.17	0.06

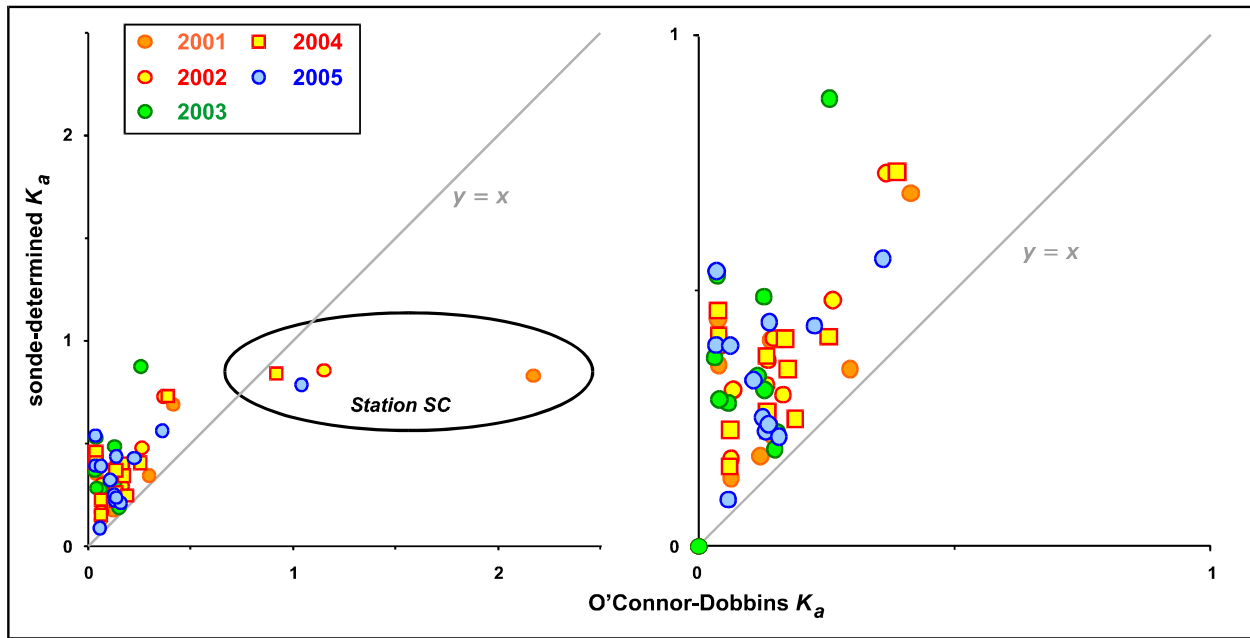


Figure 19 - Comparison of annual averages of K_a from sonde data and from O'Connor-Dobbins formula (4)

two upper tributaries, the Scott and Shasta, are systematically about a factor of three higher than the corresponding values on the main stem.

The K_a values that are indicated by the O'Connor-Dobbins equation prove to be much smaller than those determined from the sondes, by a factor of 2 – 10, see Figure 19. The exception to this statement is the station in the Scott, where the OD value was about 50% greater than that from the sonde, see the circled values in Fig. 19. The disagreement of the OD equation with the sonde-derived values may be a consequence of inaccuracy in the section-mean water depth and current, which have been extrapolated from the USGS section values, especially for the Scott where the mean depth is estimated to be about 0.3 m. But this discrepancy may also result from physical processes operating in the Klamath that are not reflective of the assumptions underlying the OD equation, e.g., the production of more intense turbulence due to extreme bed roughness deriving from the cobble-boulder river bed. Some insight might be obtained from examining the

Table 5
June – September averaged values of kinetic parameters from screened sonde data

<i>Station</i>		<i>flow</i>	<i>K_a</i>	<i>C_r</i>	<i>prod- uction</i>	<i>daily C_r</i>	<i>net ecoprod</i>	<i>relative auto- trophy</i>
<i>mainstem</i>	<i>tributary</i>	<i>(cfs)</i>	<i>(1/hr)</i>	<i>(ppm/hr)</i>	<i>(gC/m³)</i>	<i>(gC/m³)</i>	<i>(gC/m³)</i>	
2001								
IG		1021	0.21	-0.53	0.98	4.77	-3.79	0.21
K1								
	SH	20	0.60	-0.90	4.16	8.07	-3.92	0.52
K2								
	SC	6	0.80	-1.27	8.19	11.45	-3.26	0.72
SV		1047	0.38	-0.68	4.16	6.09	-1.94	0.68
HC		1050	0.23	-0.39	2.55	3.51	-0.96	0.73
	SA	92	0.32	-0.39	1.74	3.50	-1.76	0.50
OR		1210	0.35	-0.41	3.01	3.67	-0.67	0.82
WE		1210	0.41	-0.62	3.33	5.57	-2.25	0.60
	TR	722	0.39	-0.35	0.73	3.15	-2.42	0.23
MF/TC/KBW		1880	0.31	-0.49	2.03	4.42	-2.39	0.46
TG/KAT		2664	0.12	-0.29	1.54	2.61	-1.07	0.59
2002								
IG		666	0.40	-0.28	0.69	2.55	-1.86	0.27
K1								
	SH	24	0.66	-0.94	3.30	8.49	-5.19	0.39
K2								
	SC	16	0.89	-1.30	4.22	11.71	-7.49	0.36
SV		789	0.36	-0.66	4.39	5.92	-1.53	0.74
HC		792	0.34	-0.42	2.05	3.74	-1.69	0.55
	SA	169	0.47	-0.56	2.01	5.04	-3.03	0.40
OR		1277	0.28	-0.46	2.15	4.10	-1.96	0.52
WE		1264	0.40	-0.59	3.36	5.32	-1.95	0.63
	TR	710	0.31	-0.38	0.64	3.40	-2.76	0.19
MF/TC/KBW		2037	0.32	-0.41	2.18	3.66	-1.48	0.60
TG/KAT		2088	0.18	-0.38	1.56	3.46	-1.91	0.45
(continued)								

daily sonde values of K_a in more detail to see what dependencies on velocity and depth they follow.

Table 5 presents the June-September averaged values of the kinetic parameters derived from the sonde records. The data used in the averages are screened as described in Section 2, see Table 2

Table 5
(continued)

<i>Station</i>		<i>flow</i>	<i>K_a</i>	<i>C_r</i>	<i>prod- uction</i>	<i>daily C_r</i>	<i>net ecoprod</i>	<i>relative auto- trophy</i>
<i>mainstem</i>	<i>tributary</i>	<i>(cfs)</i>	<i>(1/hr)</i>	<i>(ppm/hr)</i>	<i>(gC/m³)</i>	<i>(gC/m³)</i>	<i>(gC/m³)</i>	
2003								
IG		995	0.22	-0.19	0.23	1.67	-1.44	0.14
K1								
	<i>SH</i>							
K2		1062	0.27	-0.28	2.07	2.50	-0.43	0.83
	<i>SC</i>							
SV								
HC		1235	0.18	-0.23	0.93	2.03	-1.11	0.46
	<i>SA</i>							
OR		2070	0.51	-0.48	2.45	4.29	-1.84	0.57
WE		2060	0.42	-0.37	1.98	3.31	-1.33	0.60
	<i>TR</i>	1029	0.39	-0.20	0.82	1.82	-0.99	0.45
MF/TC/KBW		3207	0.24	-0.23	1.57	2.08	-0.51	0.76
TG/KAT								
2004								
IG		830	0.19	-0.19	0.60	1.73	-1.13	0.35
K1		737	0.27	-0.46	2.61	4.11	-1.51	0.63
	<i>SH</i>	35	0.71	-0.83	2.58	7.51	-4.92	0.34
K2		646	0.24	-0.52	2.24	4.65	-2.41	0.48
	<i>SC</i>	13	0.75	-1.15	2.55	10.39	-7.83	0.25
SV		1031	0.43	-0.42	2.83	3.81	-0.98	0.74
HC		811	0.43	-0.78	3.85	7.04	-3.19	0.55
	<i>SA</i>	232	0.41	-0.49	1.58	4.39	-2.81	0.36
OR		1583	0.37	-0.52	2.73	4.66	-1.93	0.59
WE		1569	0.40	-0.67	2.33	6.07	-3.74	0.38
	<i>TR</i>	887	0.36	-0.35	0.73	3.19	-2.47	0.23
MF/TC/KBW		2533	0.19	-0.22	1.46	2.02	-0.56	0.72
TG/KAT		3289	0.19	-0.31	1.22	2.76	-1.53	0.44
(continued)								

and Fig. 13. The corresponding averaged daily flows (third column of Table 5) are only those daily flows for which the corresponding diurnal sonde data passed the screen (as these flows are employed in correlation analyses, presented in Section 4, below). The values of K_a differ

Table 5
(continued)

<i>Station</i>		<i>flow</i>	<i>K_a</i>	<i>C_r</i>	<i>prod- uction</i>	<i>daily C_r</i>	<i>net ecoprod</i>	<i>relative auto- trophy</i>
<i>mainstem</i>	<i>tributary</i>	<i>(cfs)</i>	<i>(1/hr)</i>	<i>(ppm/hr)</i>	<i>(gC/m³)</i>	<i>(gC/m³)</i>	<i>(gC/m³)</i>	
2005								
IG		1005	0.24	-0.26	0.51	2.35	-1.84	0.22
K1		999	0.24	-0.44	2.68	3.92	-1.24	0.68
	<i>SH</i>	37	0.48	-0.52	2.73	4.66	-1.93	0.58
K2		1035	0.23	-0.38	2.11	3.39	-1.28	0.62
	<i>SC</i>	21	0.80	-0.64	4.02	5.77	-1.75	0.70
SV		1103	0.42	-0.60	4.07	5.40	-1.33	0.75
HC		1110	0.32	-0.35	0.97	3.12	-2.16	0.31
	<i>SA</i>	248	0.57	-0.68	2.17	6.14	-3.97	0.35
OR		2044	0.41	-0.31	2.62	2.75	-0.13	0.95
WE		2166	0.51	-0.23	3.43	2.03	1.41	1.69
	<i>TR</i>	1150	0.38	-0.09	0.65	0.83	-0.18	0.78
MF/TC/KBW		3088	0.48	-0.31	2.08	2.75	-0.67	0.76
TG/KAT		3650	0.12	-0.11	0.98	0.99	-0.01	0.99
2001-2005 averages								
IG		903	0.25	-0.29	0.60	2.61	-2.01	0.24
K1		868	0.25	-0.45	2.64	4.01	-1.37	0.66
	<i>SH</i>	29	0.61	-0.80	3.19	7.18	-3.99	0.46
K2		914	0.25	-0.39	2.14	3.51	-1.37	0.64
	<i>SC</i>	14	0.81	-1.09	4.74	9.83	-5.08	0.50
SV		993	0.40	-0.59	3.86	5.31	-1.44	0.73
HC		1000	0.30	-0.43	2.07	3.89	-1.82	0.52
	<i>SA</i>	185	0.45	-0.53	1.88	4.77	-2.89	0.40
OR		1637	0.38	-0.43	2.59	3.90	-1.31	0.69
WE		1654	0.43	-0.50	2.89	4.46	-1.57	0.78
	<i>TR</i>	900	0.36	-0.28	0.71	2.48	-1.76	0.38
MF/TC/KBW		2549	0.31	-0.33	1.86	2.98	-1.12	0.66
TG/KAT		2923	0.15	-0.27	1.32	2.45	-1.13	0.62

somewhat from those of Table 4, because Table 4 values are averages over the entire screened data sets for each year, whereas Table 5 is restricted to the June-September period. Detailed monthly data are presented in the appendix.

Average community respiration C_r is represented in two forms in Table 5. First, it is given as the (average) regression intercept of equation (1) with $P = 0$, see Fig. 4, in units of ppm DO/hr (i.e., mg/L O₂/hr), positive for O₂ produced and negative for O₂ consumed (hence always negative in Table 5). Second, it is given as the daily cumulative respiration scaled to carbon liberated in units of gC/m³/d assuming mineralization of glucose (Ward and Armstrong, 2006e). Because this is carbon liberated, its sign is the reverse of the oxygen production rate of C_r (typically negative). “Production” in Table 5 means daily gross primary production as measured by the daytime O₂ liberation $\int_{t_r}^{t_s} P(t)dt$ in equation (1), expressed as carbon fixed in the glucose molecule (see Ward and Armstrong, 2006e). In the present context, we regard this simply as a units conversion from mg O₂/L to gC/m³ to facilitate comparison of the production data from the Klamath with literature values from other aquatic systems, and is consistent with the definitions outlined in, e.g., Odum (1956) and Williams (1993).

Two measures of ecosystem production are given in the last two columns of Table 5. “Net ecoprod”, for net ecosystem production or net community production, is the (signed) difference between daily influx of DO by gross production and consumption of DO by community respiration, both expressed in carbon units. “Relative autotrophy” is the ratio of gross primary production (“production” in Table 5) to daily community respiration (“daily C_r ” in Table 5) in consistent units. The two are of course equivalent, relative autotrophy $R = 1/(1-N/P)$ where N denotes net ecosystem production and P gross primary production, but one index may be preferable to another for purposes of comparison to other systems (e.g., Dobbs and Cole, 2007).

The data on production and respiration are displayed graphically in Figs. 20-24, as longitudinal profiles of the Klamath for each of the years 2001-05. To facilitate year-to-year comparison, the figures have the same axes, and the 2001-05 mean production (at each station) is plotted on every figure. (Respiration is represented as the rate of oxygen demand, rather than negative oxygen production, so the signs are reversed from those of Table 5.)

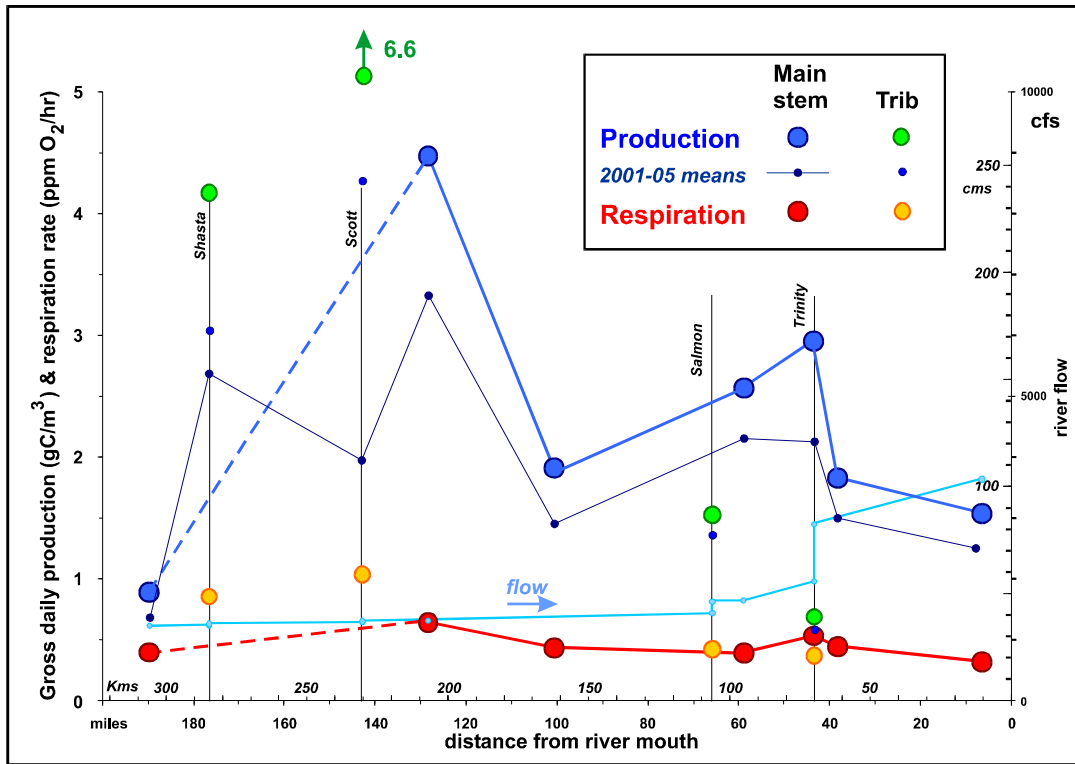


Figure 20 - Computed gross production (daily) and daily-mean community respiration rates, 2001

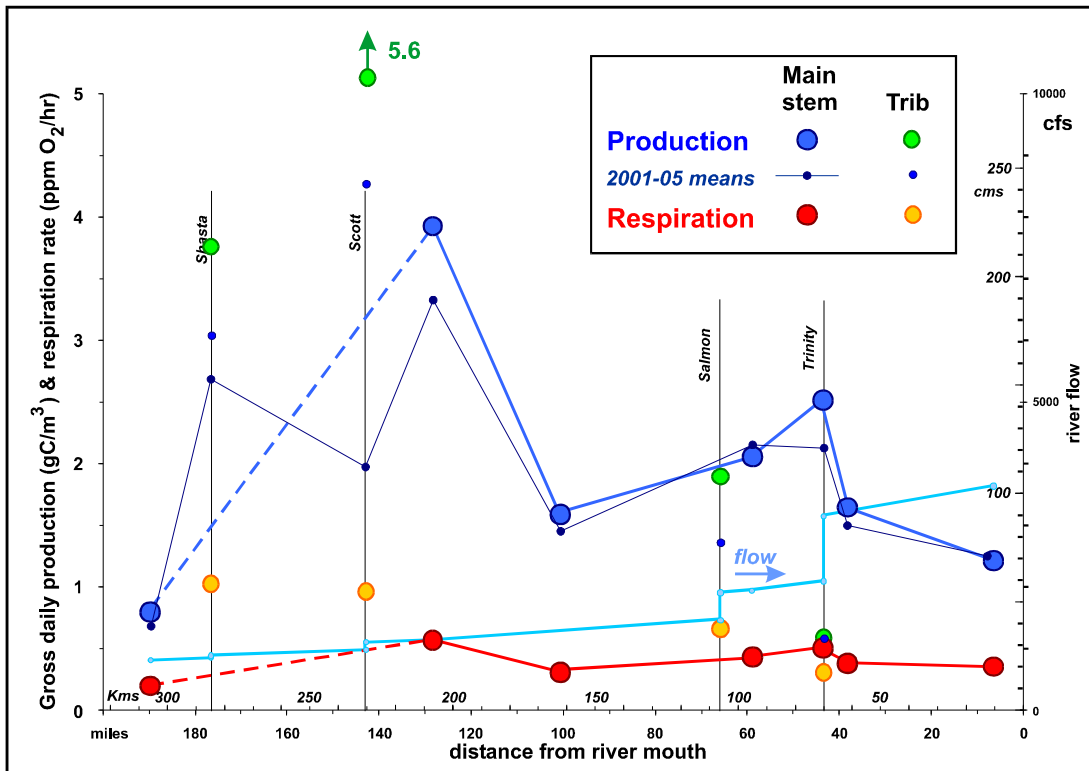


Figure 21 - Computed gross production (daily) and daily-mean community respiration rates, 2002

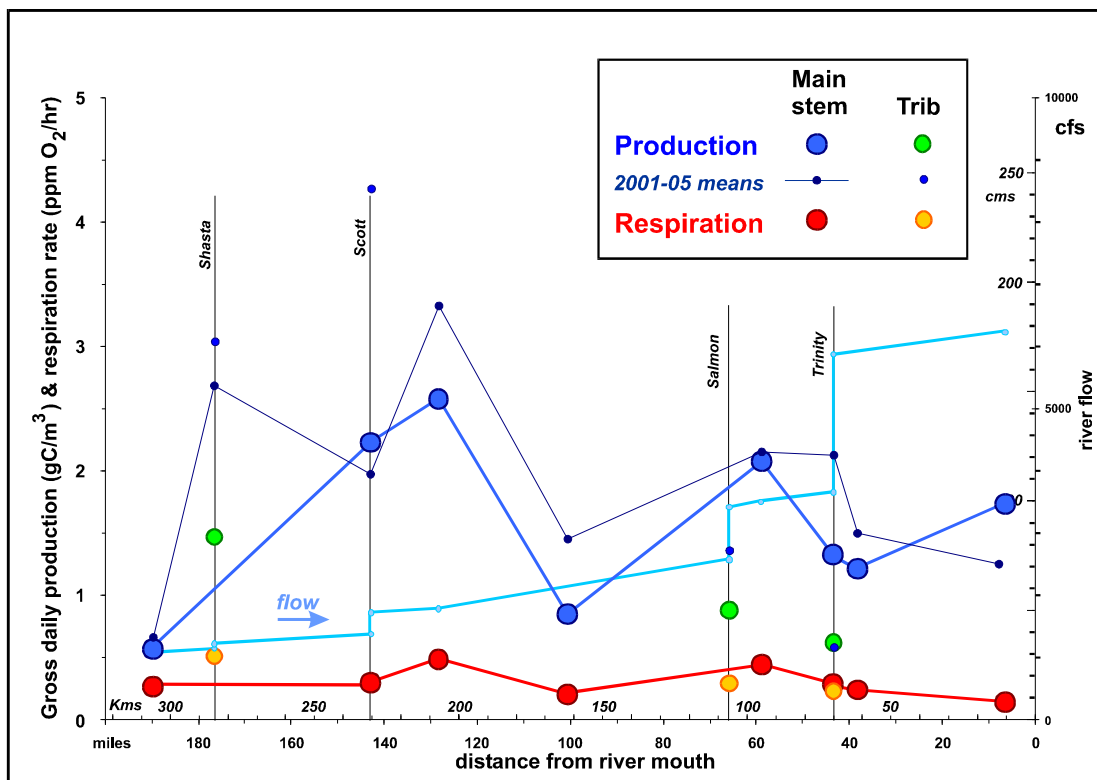


Figure 22 - Computed gross production (daily) and daily-mean community respiration rates, 2003

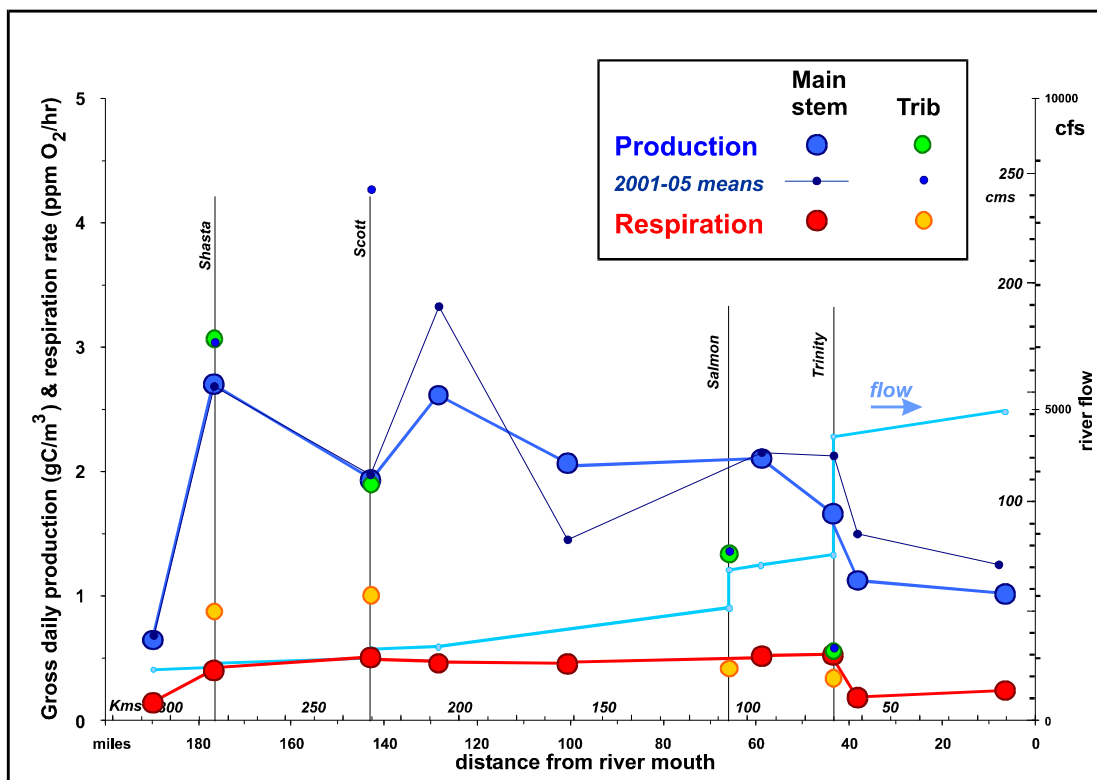


Figure 23 - Computed gross production (daily) and daily-mean community respiration rates, 2004

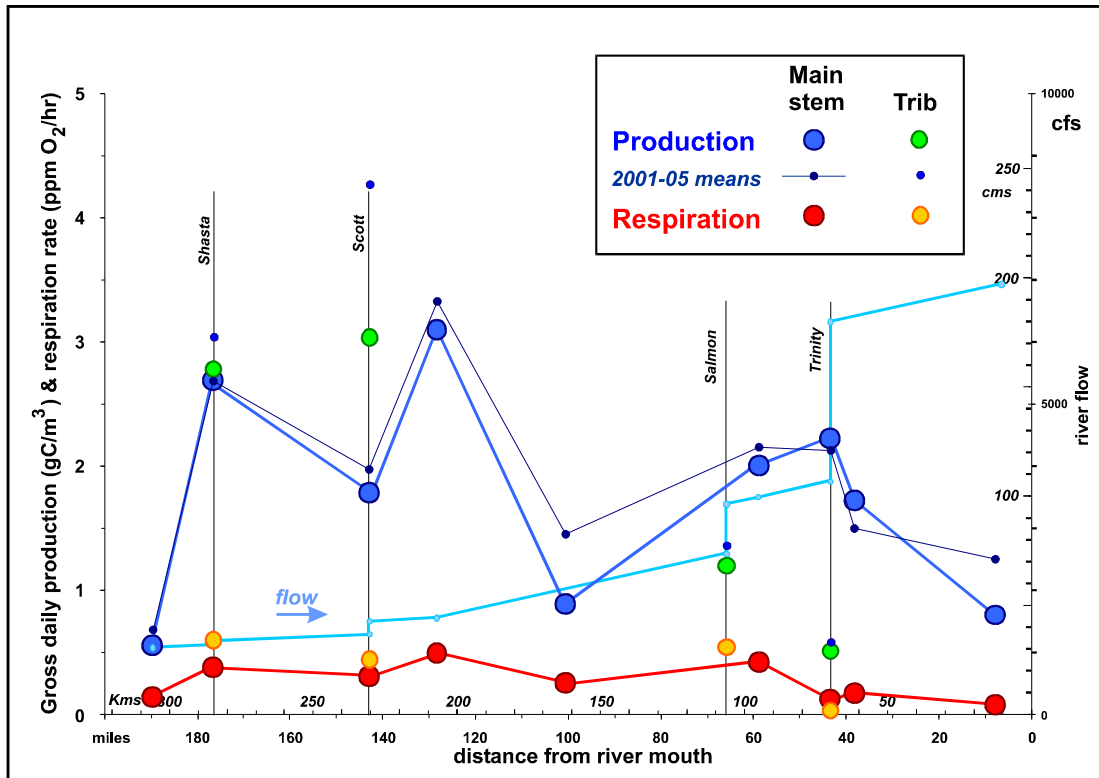


Figure 24 - Computed gross production (daily) and daily-mean community respiration rates, 2005

Several observations can be made about production and respiration in the Klamath:

- (1) The profile of respiration is remarkably consistent from year to year, being on the order of 0.4 mg O₂/L/hr, with a depressed value at IG (which is representative of the upper 10 m of the reservoir, since releases dominate the flow at this station), and with reduced values in the reach below the Trinity and around Happy Camp (HC).

- (2) Production is lowest at Iron Gate (IG), and increases with distance downstream, then declines in the reach from Orleans (OR) to the mouth, except for a depressed value at Happy Camp (HC). This general pattern is manifested in each of the study years. The highest values of production are exhibited in the low-flow years of 2001 and 2002, at both the mainstem and tributary stations.
- (3) In the Shasta and Scott are found the highest values of production encountered in the river system, typically a factor of 2 or 3 times the mainstem values, and respiration is typically about twice the mainstem value. In the Trinity, in contrast, both production and respiration are much lower than the mainstem values, with only slight year-to-year variation.

4. Interpretation: Associations and Correlations

In inferring possible causal controls on the kinetic behavior evaluated in the preceding section, we combine the kinetic data with information external to that extracted from the sondes, notably hydrography and water chemistry analyses. Most fundamental is the hydrological state of the river. The five years of study 2001-05 presented a range of flow conditions, as displayed in Figures 25-29. These figures show the observed daily flow at each of the four mainstem USGS gauges below Iron Gate (see the stem diagram of Fig. 14), for the period May - September. Though the chief focus of this analysis is on the summer period of June – September, May is included in these figures to display the magnitude of the spring runoff event. A split ordinate is used to better resolve the flows during the July – September low-flow season. On each of these

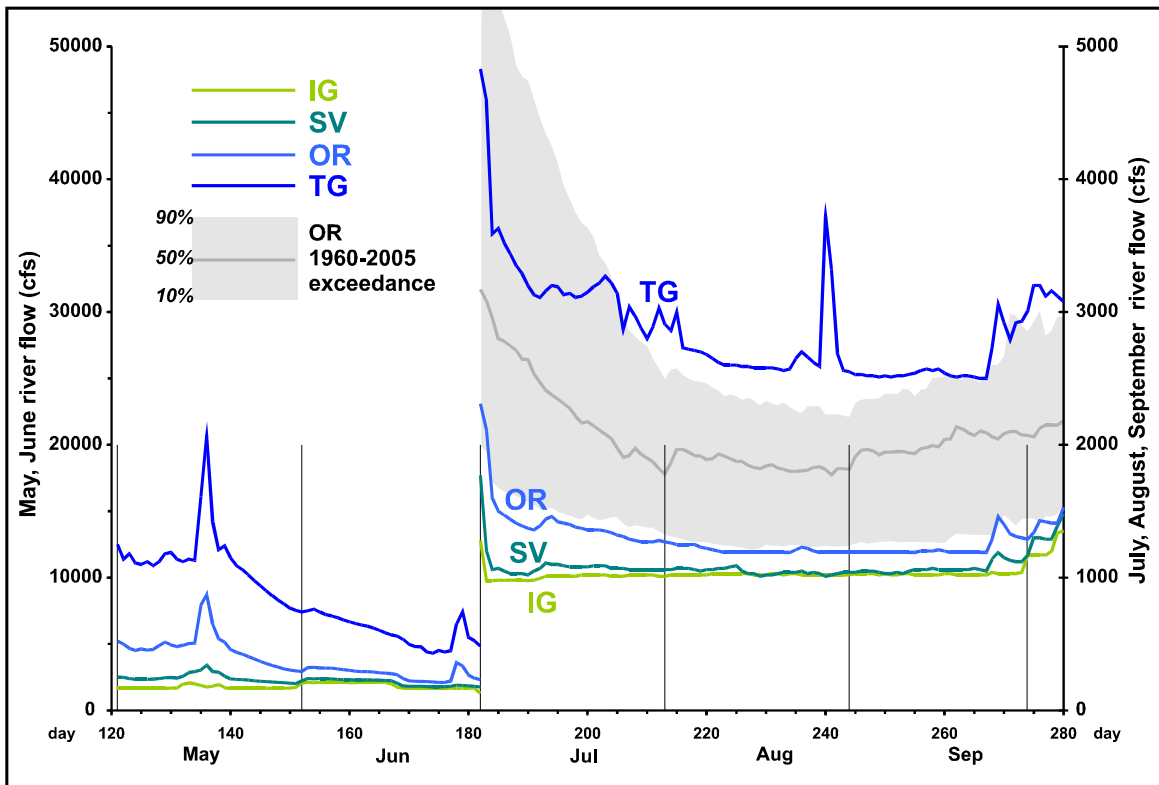


Figure 25 - Gauged flows in mainstem of Klamath, 2001 (cf. Fig. 14)

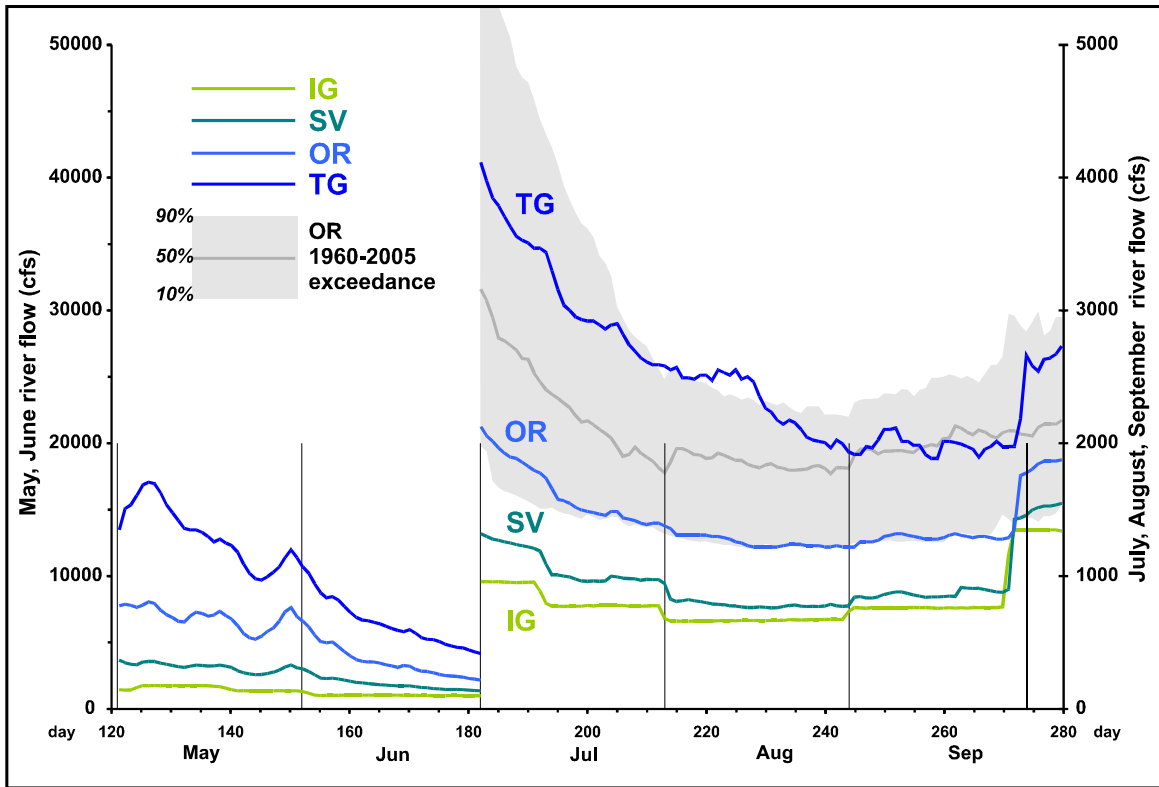


Figure 26 - Gauged flows in mainstem of Klamath, 2002

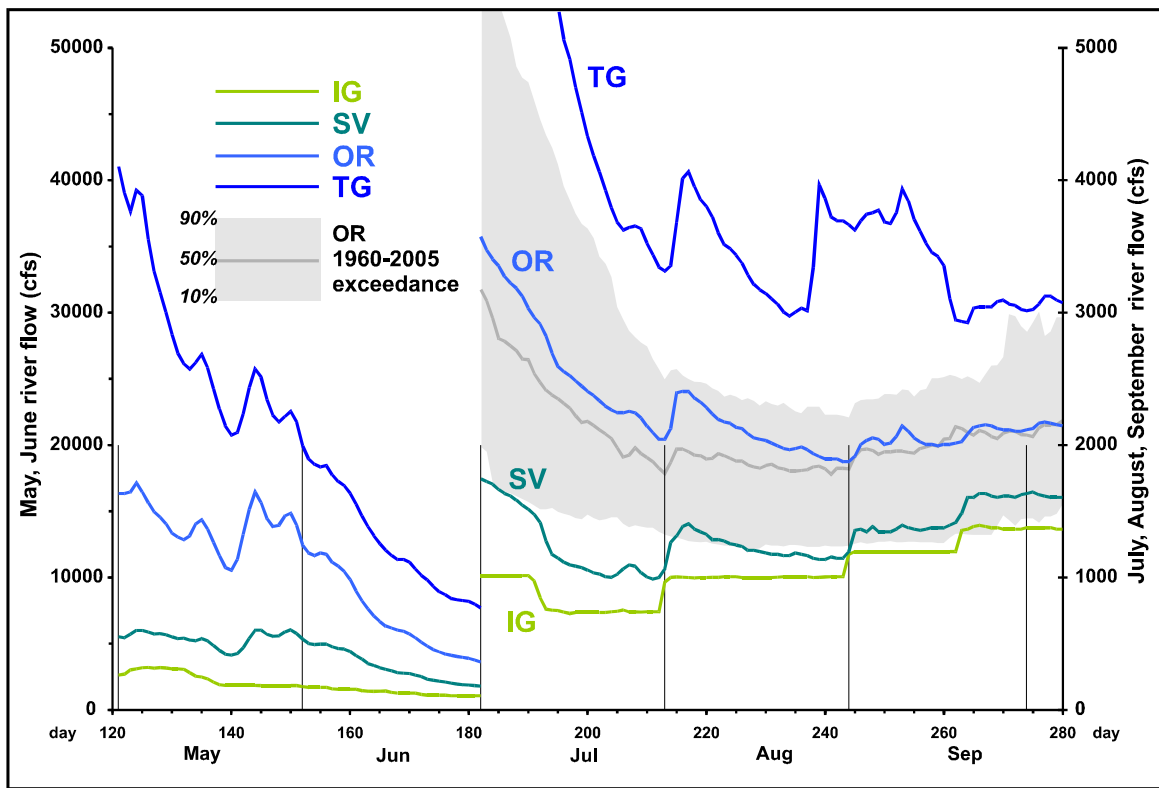


Figure 27 - Gauged flows in mainstem of Klamath, 2003

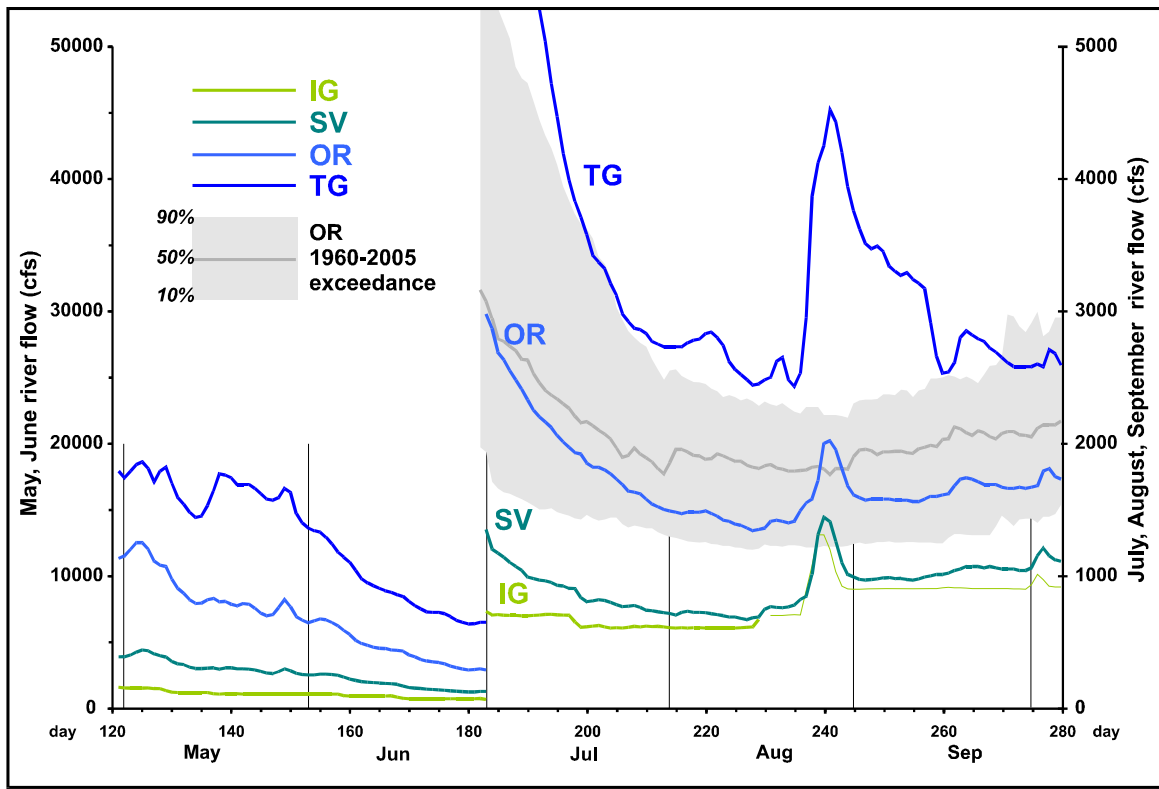


Figure 28 - Gauged flows in mainstem of Klamath, 2004

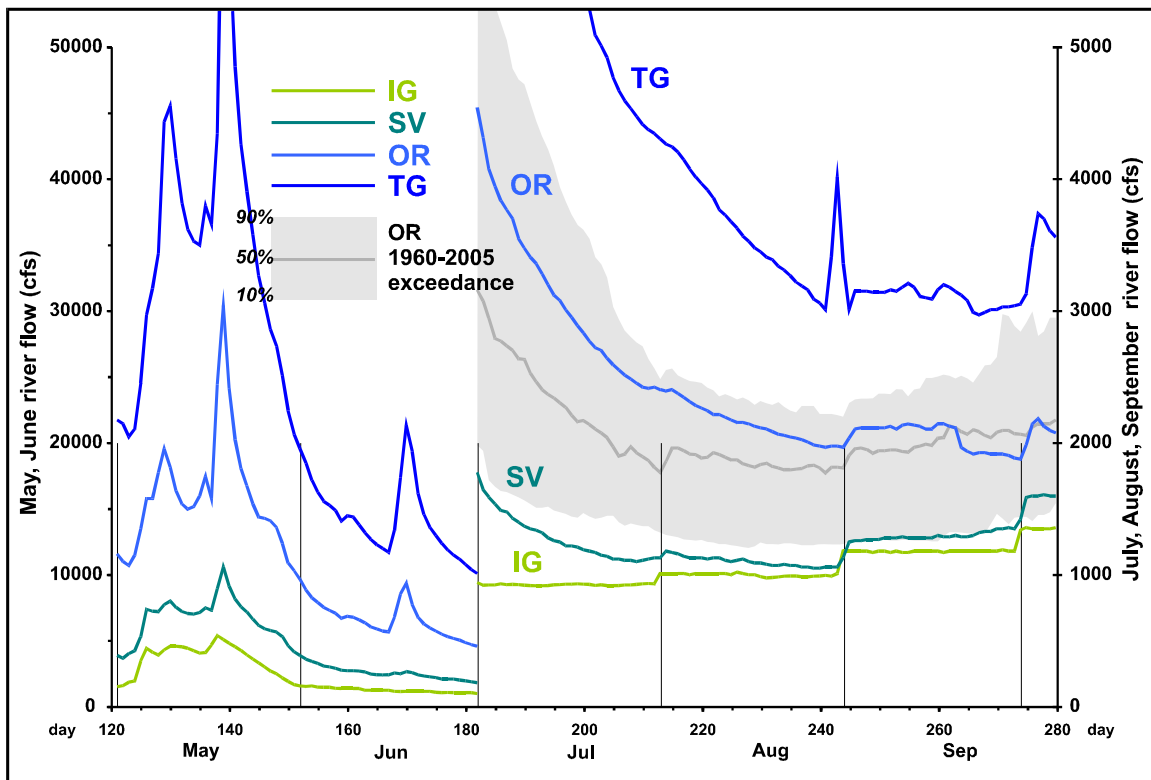


Figure 29 - Gauged flows in mainstem of Klamath, 2005

figures is shown the flows corresponding to daily exceedance values of 10%, 50% (median) and 90% for the low-flow season, to characterize the statistical variation of flows at Orleans (OR) over the 1960-2005 period (beginning with closure of Iron Gate dam). We see that flows at OR in both 2001 and 2002 were uncharacteristically low, generally exceeding only about 10% of the 1960-2005 flow data. Of course, it was in 2002 that the kill occurred below the Trinity confluence in the fall run of chinook salmon (Guillen, 2003). In year 2003 and 2004, flows were slightly above median and slightly below median, resp., but in both years the lower river (below the Trinity) experienced a major flow event in late August through early September. In 2004, this late-August event was manifested throughout the river below Iron Gate, but was most prominent in the coastal region, Fig. 28. The year 2005, Fig. 29, exhibited the highest flows of the study period, but declined to about median toward the end of the summer, with no major inflow events to disturb the more-or-less steady flows in the August-September period.

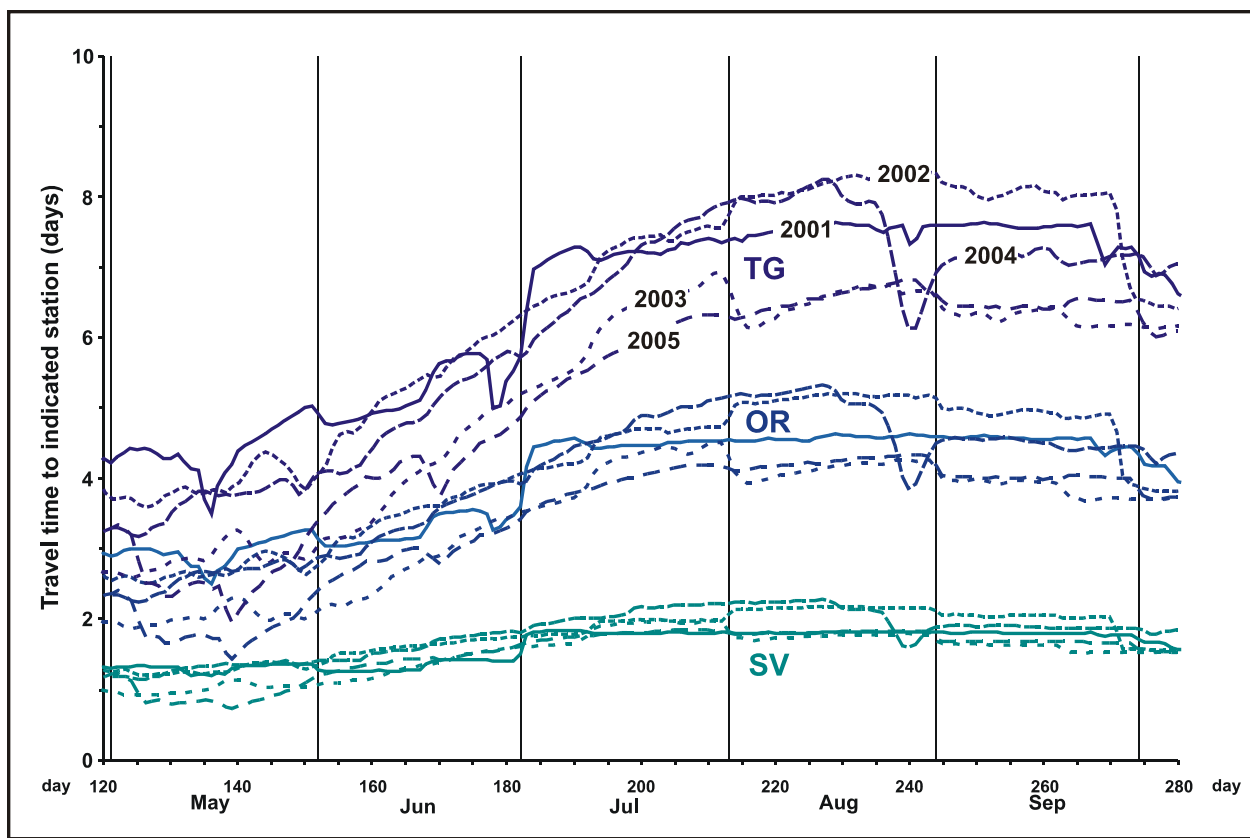


Figure 30 - Travel times from Iron Gate in mainstem of Klamath, 2001-05

These flows are summarized in a perhaps more cogent form in Figure 30 as travel times from IG to each of the three mainstem gauges, based upon the routine measurements of stream velocity performed by the USGS (Armstrong and Ward, 2008a). Two immediate inferences can be drawn that are crucial to interpretation of the sonde data. First, despite the wide range in flows through the May-September period and from year-to-year, the travel times are much more stable, especially during the low-flow period where they are about 2 days to SV (which agrees well with the RMA-2 model values presented by Deas and Orlob, 1999), 4-5 days to OR, and 6-8 to TG. This is because an increase in flow results primarily in a rise in water surface elevation (and associated increase in cross section), rather than an increase in current speed, consistent with hydraulic principles. Second, the entire reach of the Klamath from Iron Gate to the mouth is replaced by new water in about three days under the high spring runoff condition, and in about

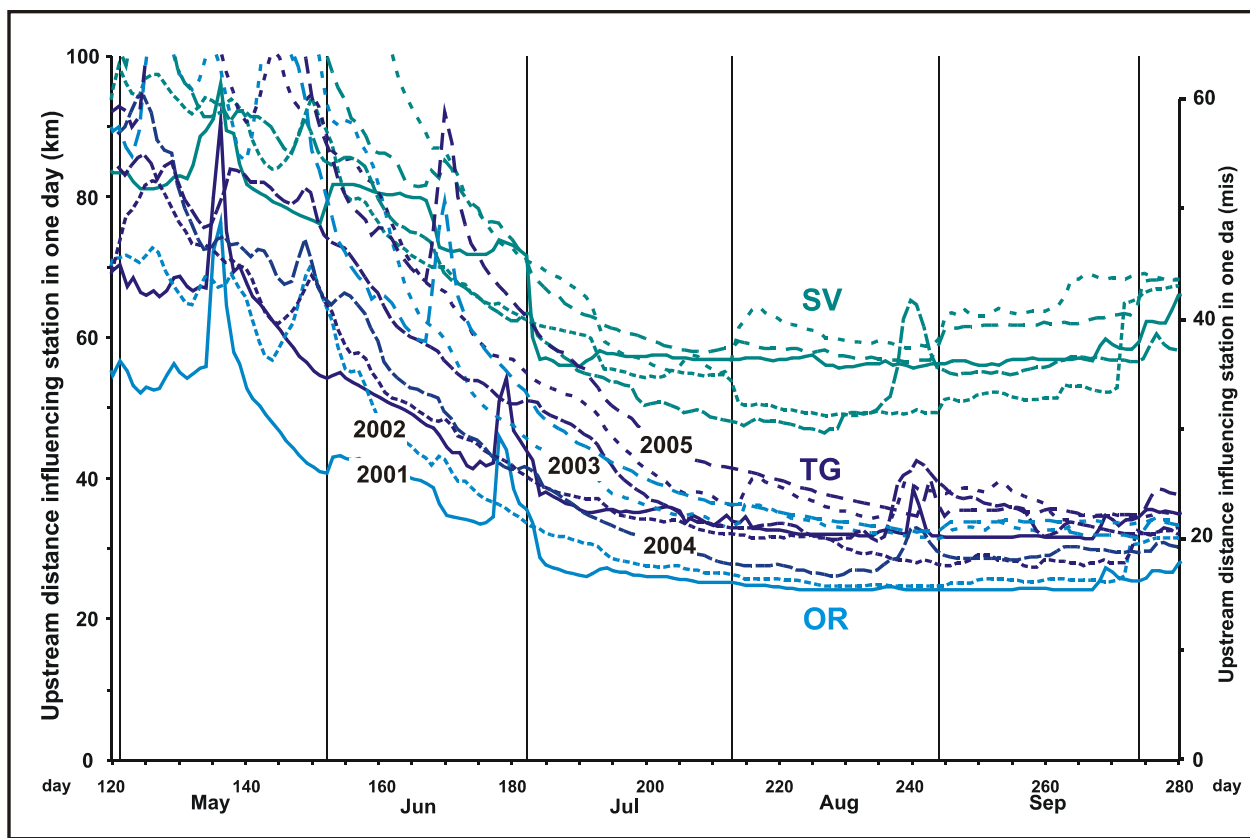


Figure 31 - One-day replacement distances in mainstem of Klamath, 2001-05

seven days under the summer low-flow condition. It is tempting to think of the kinetic information derived from the sondes, e.g. Table 5, as applying to a parcel of water at the sonde location, but in fact the water monitored by the sonde is continually replaced by streamflow, so the sonde data represents a volume of water traversing a considerable reach of the river. In a manner of speaking, the river's flow has the effect of “smearing” the kinetic behavior along a length of the river. Figure 31 displays how long this length is: this figure shows the length of reach that will be moved past the sonde position in a 24-hour period, the basic time unit for the kinetic analyses carried out here. Even at low flow, this is a distance of 20 miles in the reach below Orleans and 40 miles above Seiad Valley.

Figures 32 – 36 display longitudinal profiles of production and the associated relative autotrophy inferred from the sonde analyses, along with the nutrient concentrations (total organic and inorganic) determined in water samples of the AFWO program. To facilitate plotting on these

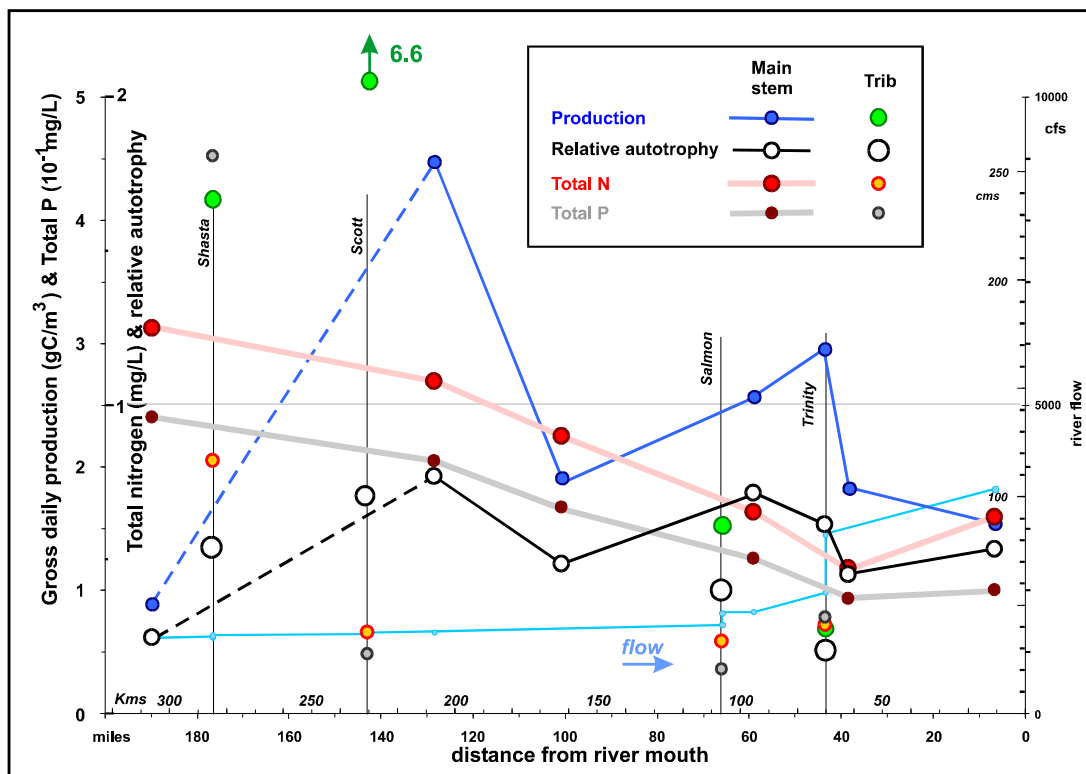


Figure 32 - Gross production, relative autotrophy, and water chemistry, Jun-Sep 2001 means in Klamath

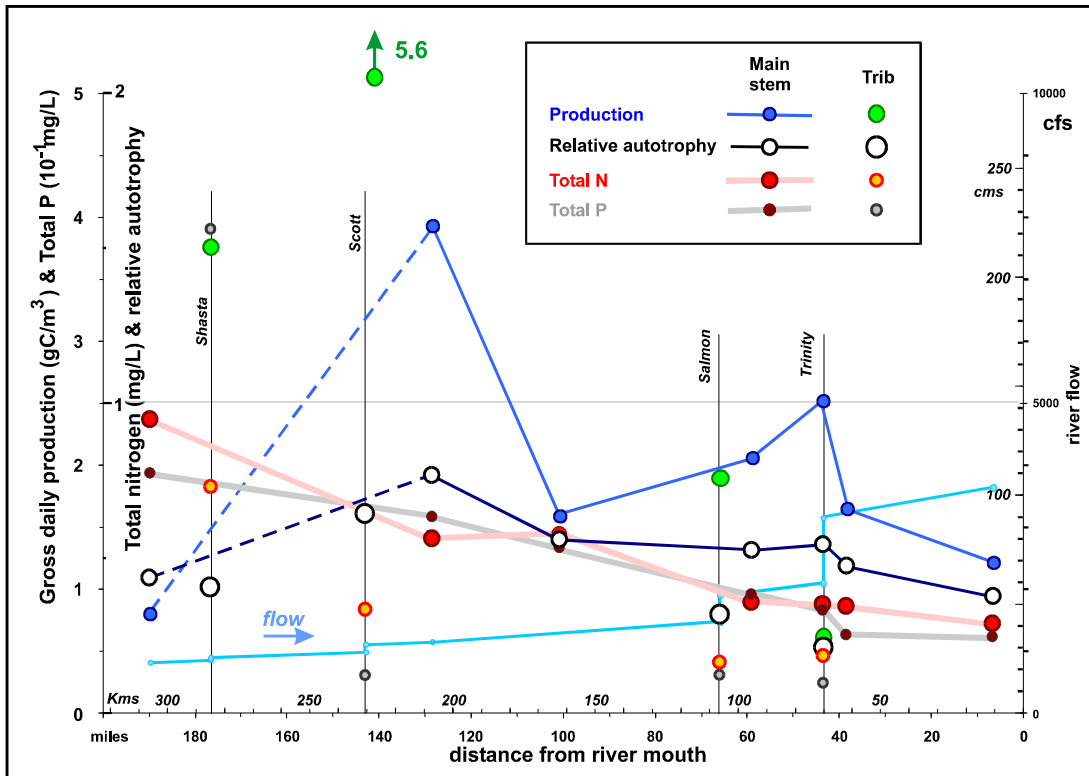


Figure 33 - Gross production, relative autotrophy, and water chemistry, Jun-Sep 2002 means in Klamath

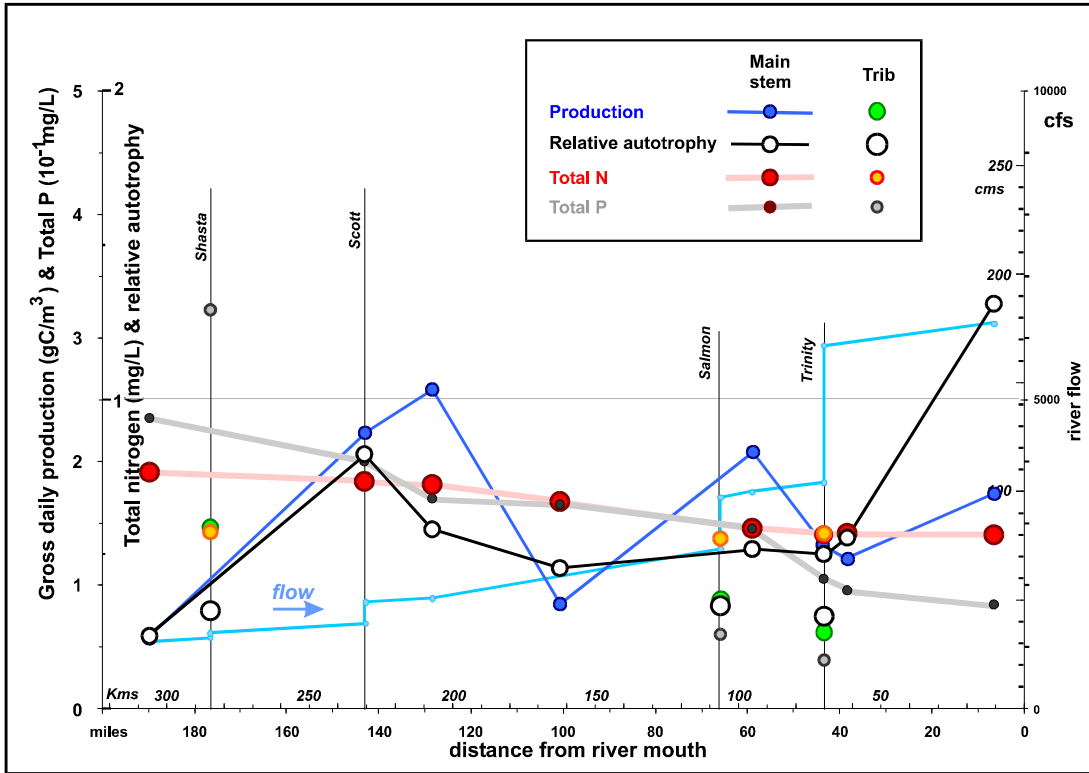


Figure 34 - Gross production, relative autotrophy, and water chemistry, Jun-Sep 2003 means in Klamath

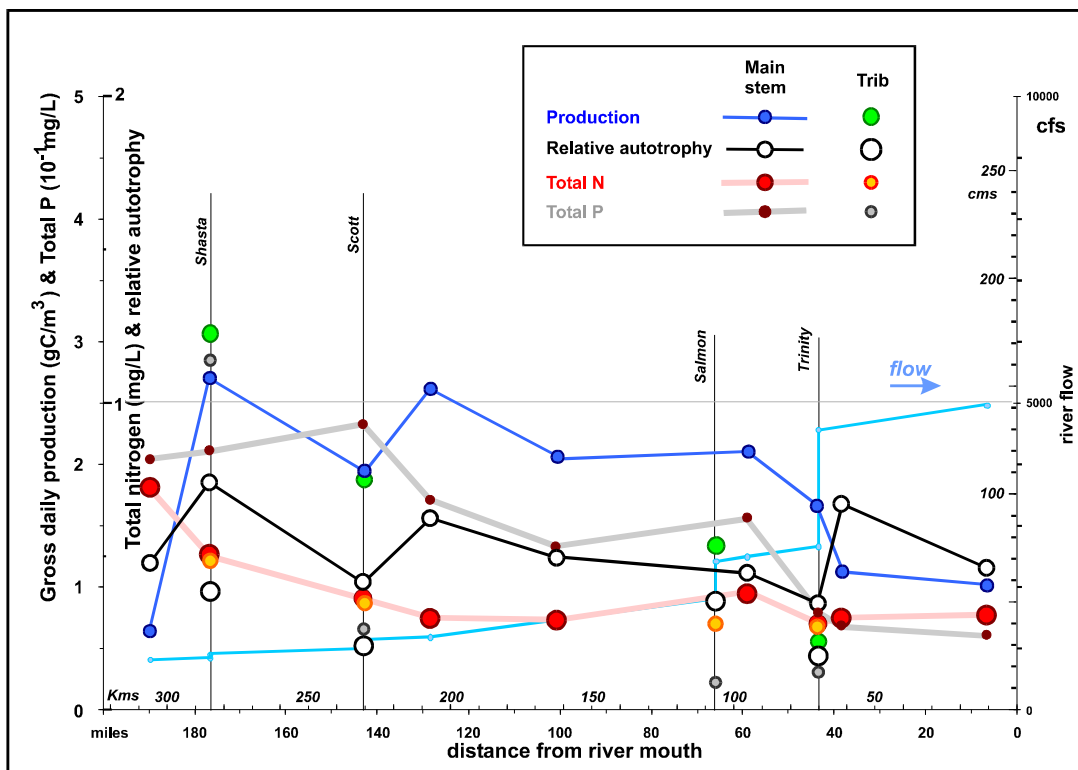


Figure 35 - Gross production, relative autotrophy, and water chemistry, Jun-Sep 2004 means in Klamath

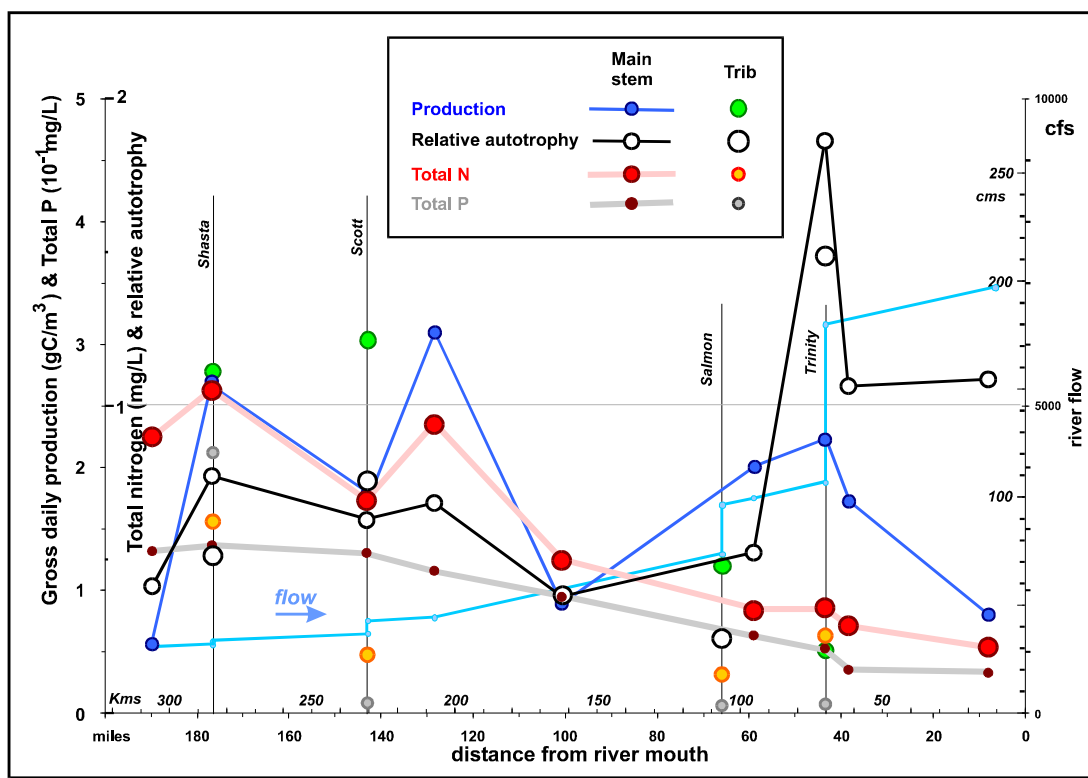


Figure 36 - Gross production, relative autotrophy, and water chemistry, Jun-Sep 2005 means in Klamath

multiple-axis graphs, the concentrations of phosphorus are scaled up by a factor of ten (i.e., represented in units of 0.1 mg/L), so that, e.g., a plotted value of 1 (such as the mainstem value downstream from the Trinity confluence in Fig. 32) represents a concentration of 0.1 mg/L. All data are averaged over the June – September period. These profiles are companions to Figs. 20-25, and should be considered together (no doubt with relief that all of these data are not plotted on single graphs).

Along the main stem, in every year, the average concentrations of nitrogen (N) and phosphorus (P) generally declined along the length of the river from Iron Gate to the mouth. This is consistent with the mass-budget analyses of Armstrong and Ward (2008b), which concluded that concentrations in the river are driven by the releases from Iron Gate, and are reduced downstream due to the combined effects of dilution by tributary inflows and decay, the former predominating. The very low values of production at IG reflect the released water from the reservoir and not a river-indigenous algal community. The rapid increase of production from IG to SV, however, is consistent with establishment of an algal community in the high concentrations of N and P. Typically, the highest value of gross primary production in the river occurs at SV. Below this, the behavior of primary production with distance down-stream is more complex, with a local minimum at HC, which often is also the mainstem minimum (save the value at Iron Gate), an increase to higher values between OR and the Trinity confluence, thence a decline to TG. The pattern of longitudinal profile of relative autotrophy is similarly complex. Above the Trinity confluence the river is heterotrophic, with a relative autotrophy of around 0.5. The highest values, around 0.7, are generally found in the reach from the Shasta to Seiad Valley, and decline from there to the vicinity of the Trinity confluence. Below the Trinity confluence, the relative autotrophy is highly variable, being low in the low-flow years 2001, 2002 and 2004, and quite high—in fact, autotrophic, in the higher-flow years of 2003 and 2005, though it is far from clear that river flow *per se* is the operative factor.

As noted above, gross primary production in the two upper tributaries, the Shasta and the Scott, is generally much higher than the mainstem value, and typically the highest to be found in the Klamath system. These tributaries are shallow and, under summer conditions, have limited flow with much slower current speeds than those of the mainstem river. Nutrient concentrations are

very different in the two tributaries. Nitrogen in the Shasta is on the same order as, but lower than the mainstem value, while in the Scott, it is lower yet, about half of that in the Shasta. There is even more disparity in phosphorus, being quite high in the Shasta, nearly twice the mainstem value, and low in the Scott. This disparity was most exaggerated during the low-flow years of 2001 and 2002. The fact that nitrogen and phosphorus are highest in the Shasta of all of the tributaries may be due to its point-source load. Community respiration in these two tributaries is higher than the mainstem values, and typically is the highest in the Klamath system. While both production and respiration are high, the relative autotrophy is about the same as the corresponding mainstem value, so these tributaries are net heterotrophic.

The Salmon regularly exhibits about the same level of respiration as the mainstem value, but nearly half the primary production, so the relative autotrophy is about half that of the mainstem. Nitrogen concentration is about half that of the mainstem (which has declined substantially from its level in the reach from Iron Gate to Seiad Valley). Phosphorus is even lower, typically much less than half the mainstem value.

The Trinity is the most curious of the tributaries. Nitrogen and phosphorus are lower in concentration than the mainstem, especially phosphorus. Both respiration and production are lower than the mainstem values: indeed, production in the Trinity is the lowest in the Klamath system. Consequently, the relative autotrophy in the Trinity is the lowest in the Klamath system (except for the reservoir-dominated IG station). The one exception is 2005 (Fig. 36), when the station was highly autotrophic, but this was a consequence of the extremely low value of community respiration. During the summer period depicted here, the Trinity represents more than a third of the total flow in the Klamath at TG, and likely exerts a strong influence on the quality of the Klamath downstream from the Trinity confluence.

Table 6 presents the (linear) correlation coefficients of gross primary production with several other chemical, kinetic and physical parameters that might be thought to influence, or be influenced by production. (In the appendix are given complete correlation arrays for monthly values of all variables, for every month for which there is data.) For each year, the correlation was computed between the monthly mean values of production and the monthly mean values of

Table 6
Correlations of screened data for June – September period
(boldface indicates absolute value greater than 50%)

<i>Station</i>		<i>Monthly mean production versus:</i>			<i>Daily mean production vs:</i>	
<i>mainstem</i>	<i>tributary</i>	<i>TN</i>	<i>TP</i>	<i>chl-a</i>	<i>C_r</i>	<i>insolation</i>
2001						
IG		-0.12	0.34	0.29	-0.02	0.04
K1						
	<i>SH</i>	0.91	0.50	0.00	-0.62	0.36
K2						
	<i>SC</i>	0.53	0.53	-0.50	-0.56	-0.19
SV		-0.43	-0.41	0.22	-0.75	0.49
HC		-0.28	0.14	0.37	-0.30	0.17
	<i>SA</i>	0.62	0.51	0.24	-0.01	-0.03
OR		-0.27	0.27	0.53	-0.20	0.09
WE					-0.35	-0.18
	<i>TR</i>	0.42	-0.56	-0.01	-0.70	0.13
MF/TC/KBW					0.11	0.11
TG/KAT					-0.42	0.36
2002						
IG		0.14	-0.49	-0.57	-0.25	0.11
K1						
	<i>SH</i>	-0.32	-0.21	-0.80	-0.56	-0.04
K2						
	<i>SC</i>				-0.20	0.35
SV		-0.02	-0.33	-0.30	-0.30	-0.20
HC		-0.29	-0.11	0.01	-0.71	-0.45
	<i>SA</i>	-0.12	-0.89	0.29	-0.10	0.48
OR					-0.46	0.43
WE		-0.16	-0.16	0.62	-0.49	-0.21
	<i>TR</i>	0.72	0.18	-0.17	-0.30	0.12
MF/TC/KBW		-0.21	-0.32	-0.50	0.23	-0.12
TG/KAT					-0.31	-0.52
(continued)						

chemical parameters, total nitrogen, total phosphorus and chlorophyll-a. The chemical analyses are performed on water samples generally taken at the same time as the servicing of the sonde, approximately a two-week interval, so the number of measurements upon which the monthly mean is based can range from one to three. The nondetects are represented in the mean values as

Table 6
(continued)

<i>Station</i>		<i>Monthly mean production versus:</i>			<i>Daily mean production vs:</i>	
<i>mainstem</i>	<i>tributary</i>	<i>TN</i>	<i>TP</i>	<i>chl-a</i>	<i>C_r</i>	<i>insolation</i>
2003						
IG					-0.31	-0.09
K1						
	<i>SH</i>				<i>0.14</i>	<i>-0.98</i>
K2					-0.68	0.63
	<i>SC</i>					
SV					-0.18	0.03
HC					-0.39	0.62
	<i>SA</i>				<i>-0.93</i>	<i>-0.92</i>
OR					0.02	-0.09
WE		-0.03	-0.08	0.82	-0.58	-0.09
	<i>TR</i>	<i>0.18</i>	<i>-0.88</i>	<i>0.76</i>	<i>-0.19</i>	<i>-0.57</i>
MF/TC/KBW		-0.95	-0.98	0.74	-0.50	-0.15
TG/KAT					-0.15	-0.97
2004						
IG					0.05	0.17
K1		0.69	-0.81	-0.73	-0.41	0.51
	<i>SH</i>				<i>-0.51</i>	<i>-0.10</i>
K2			0.22	0.76	0.22	0.52
	<i>SC</i>	<i>-0.54</i>	<i>0.45</i>	<i>1ⁿ</i>	<i>0.06</i>	<i>-0.63</i>
SV			-0.79	-0.53	-0.22	0.38
HC			-0.65	0.19	-0.85	0.38
	<i>SA</i>		<i>-1.00</i>	<i>-1ⁿ</i>	<i>-0.52</i>	<i>0.56</i>
OR		-0.29	0.97	<i>-1ⁿ</i>	-0.22	-0.02
WE			-0.10	-0.34	-0.42	0.19
	<i>TR</i>	<i>-0.92</i>	<i>0.05</i>	<i>0.13</i>	<i>-0.49</i>	<i>-0.17</i>
MF/TC/KBW			0.31	0.01	-0.58	0.00
TG/KAT		0.49	0.74	0.90	-0.12	-0.28

(continued)

ⁿ The correlation is numerically precise but is based upon only two data points.

one-half the method detection limit, as described in Armstrong and Ward (2008a). For each year and each station, therefore, there are four pairs of values for which the correlations are computed, so these will be noisy and uncertain. In contrast, the sonde data yield daily values of gross

Table 6
(continued)

<i>Station</i>		<i>Monthly mean production versus:</i>			<i>Daily mean production vs:</i>	
<i>mainstem</i>	<i>tributary</i>	<i>TN</i>	<i>TP</i>	<i>chl-a</i>	<i>C_r</i>	<i>insolation</i>
2005						
IG					-0.23	0.34
K1		-0.46	-0.40	0.17	-0.45	0.38
	<i>SH</i>	-0.40	-0.15	0.92	-0.45	-0.05
K2		-0.67	-0.13	0.69	-0.60	0.59
	<i>SC</i>	-0.05	-0.36	-0.88	-0.48	0.36
SV		0.88	0.84	0.94	-0.74	0.31
HC		1.00	0.98		0.52	-0.45
	<i>SA</i>	0.85	0.97	<i>1ⁿ</i>	-0.73	0.54
OR		0.49	0.57	0.56	-0.47	0.26
WE		0.80	0.67	0.92	-0.55	0.33
	<i>TR</i>	0.14	-0.95	-0.44	-0.61	0.31
MF/TC/KBW		0.92	0.24	0.89	-0.59	0.35
TG/KAT		0.08	0.64	0.85	-0.63	-0.07
2001-05 averages						
IG		0.01	-0.07	-0.14	-0.15	0.11
K1		0.11	-0.60	-0.28	-0.43	0.45
	<i>SH</i>	0.07	0.05	0.04	-0.40	-0.16
K2		-0.67	0.05	0.72	-0.35	0.58
	<i>SC</i>	-0.02	0.20	-0.69	-0.29	-0.03
SV		0.14	-0.17	0.08	-0.44	0.20
HC		0.14	0.09	0.19	-0.34	0.05
	<i>SA</i>	0.45	-0.10	0.27	-0.46	0.13
OR		-0.02	0.60	0.55	-0.27	0.14
WE		0.21	0.08	0.51	-0.48	0.01
	<i>TR</i>	0.11	-0.43	0.05	-0.46	-0.04
MF/TC/KBW		-0.08	-0.19	0.28	-0.26	0.04
TG/KAT		0.29	0.69	0.88	-0.33	-0.29

ⁿ The correlation is numerically precise but is based upon only two data points.

production and community respiration (C_r), and daily values of the physical parameter of relative insolation are also available, so the June-September correlations for these parameters were based upon far more numerous data (122 less the days lost to sonde maintenance, less the days rejected

in the Q/A process, less the days screened out for this analysis). The final set of data in Table 6 is the 2001-05 averages of the annual values of correlation for each station/parameter-pair.

Generally, the correlation of production on nutrients is weak and variable, ranging both positive and negative. This is not surprising, first because the causality can go either direction with opposite sign of the associated correlation, i.e., nutrients can stimulate production therefore initially be high when production is high, but as production increases nutrients are reduced due to assimilation, and second since the concentrations of N and P in the Klamath are generally high enough, exceeding five times the Michaelis constants, that they are unlikely to be limiting for production. The correlation of daily production versus daily community respiration is consistently negative but of generally modest magnitude, suggesting that while autotroph respiration is a major component of community respiration (so that the correlation is negative), the heterotrophic components of community respiration are sufficient large to erode this correlation.

The lack of substantial correlation of production with insolation is perhaps surprising, but is illustrative of the relation of correlation to time scale, and the attendant need to carefully interpret correlations over lengthy time periods. As demonstrated by the time plots of Fig. 16 (see the discussion in Section 3), there is a clear association of reduced production with insolation “events” arising from synoptic-scale disturbances over northern California. On the longer time scale represented by the June – September period, however, the correlated variation from these events is overbalanced by the anticorrelated seasonal decline in insolation and seasonal increase in the gross production (from the integrated effect of increasing water temperatures, stable river flows, and the establishment of a growing algal community in the river).

The most unexpected feature of the results of Table 6 is the unsystematic variation in correlation between primary production and the concentration of chlorophyll-a (chl-a), a nearly universal index to algal biomass. In the main stem, the averaged chlorophyll-a exhibits the same longitudinal decline as nutrients, while in the tributary stations the concentrations are all

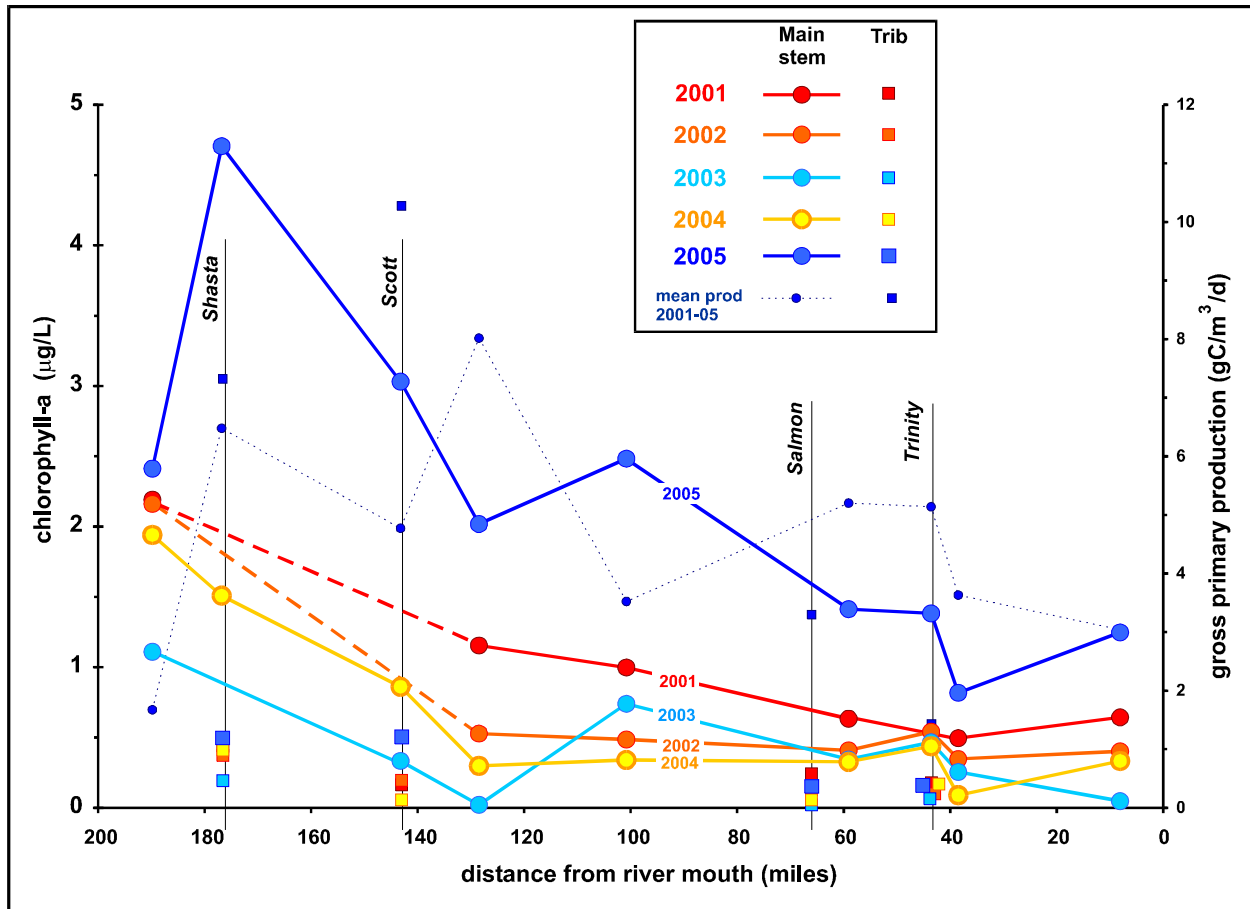


Figure 37 – Annual profiles of June-September mean chlorophyll-a in Klamath

systematically low, see Figure 37. While there is also a vague decline in mainstem production down the mainstem (see the 2001-05 averaged profile in Fig. 37, but compare the annual profiles in Figs. 32-36), chlorophyll-a does not track the month-to-month, year-to-year, and interstation variation of production, so the correlation between production and chl-a is similarly variable. The nature of the calculated primary production is that it measures the combined effect of all photosynthesizing organisms that affect the concentration of DO in the river, notably both phytoplankton and periphyton (benthic algae), while chl-a is measured in a water sample and is therefore limited to phytoplankton. The high variability in correlation between production and chl-a could therefore be diagnostic of a substantial benthic algae community. It should be also noted, however, that the 2002-04 phytoplankton enumeration data from the lower Klamath of Pacificorp (unpublished data available from the Pacificorp website: www.pacificorp.com/

Article/Article82803.html) do not appear to correlate with the accompanying chlorophyll-a determinations, so there may be an unresolved issue with the relation of water-sample chl-a to both phytoplankton biomass and production in the Klamath.

Some evidence of the relative importance of phytobenthos may be gleaned from the USGS studies in the Klamath reported by Flint et al. (2005). In this study, sediment oxygen demand (SOD) was measured by a bottom-mounted sealed opaque monitoring chamber (see Rounds and Doyle, 1997). Data were collected 12-14 August 2003 at six stations with 2-3 replicates per station in the Shasta River, 4-5 miles upstream from the sonde station SH. Unfortunately, no sonde data were collected after 8 July 2003, so a direct comparison with the USGS measurements is not possible. The total (dark) DO consumption in the USGS benthal chamber ranged 0.14 – 0.26 mg/L/hr, and averaged 0.19 mg/L/hr, of which 0.11 mg/L/hr was absorbed by sediments and 0.08 mg/L/hr in the overlying water (all values being corrected to ambient temperature), according to data from the blank chamber (Rounds, pers. comm., 2009), an identical apparatus from which sediment effects are excluded by an impermeable bottom.

The water depths at these stations ranged 0.4 – 0.9 m, so it is likely that light easily penetrated to the bottom hence that photosynthesis by phytoplankton took place through the water column and by phytobenthos on the river bed, to the extent that these organisms were present. (Extensive macrophytes were found at four of these stations, and were removed prior to installation of the chambers by cutting their stalks just above the river bed without disturbing the roots or sediment.) The chambers then incubated for a few hours during which the oxygen depletion was monitored. It would appear therefore that the total DO demand measured by these chambers corresponds to community respiration as determined in the present sonde analysis, including the respiration of microscopic autotrophs. The SOD and total DO demand data given above would indicate a partition of the oxygen demand (community respiration) into 60% benthal and 40% water-column (i.e., planktonic).

Because the AFWO sonde program included a station in the Shasta, *viz.* SH, we seek to compare the community respiration from the sonde to that from the benthal respirometer. The USGS value of 0.19 mg/L/hr is on the order of, but somewhat lower, than the values of C_r inferred for

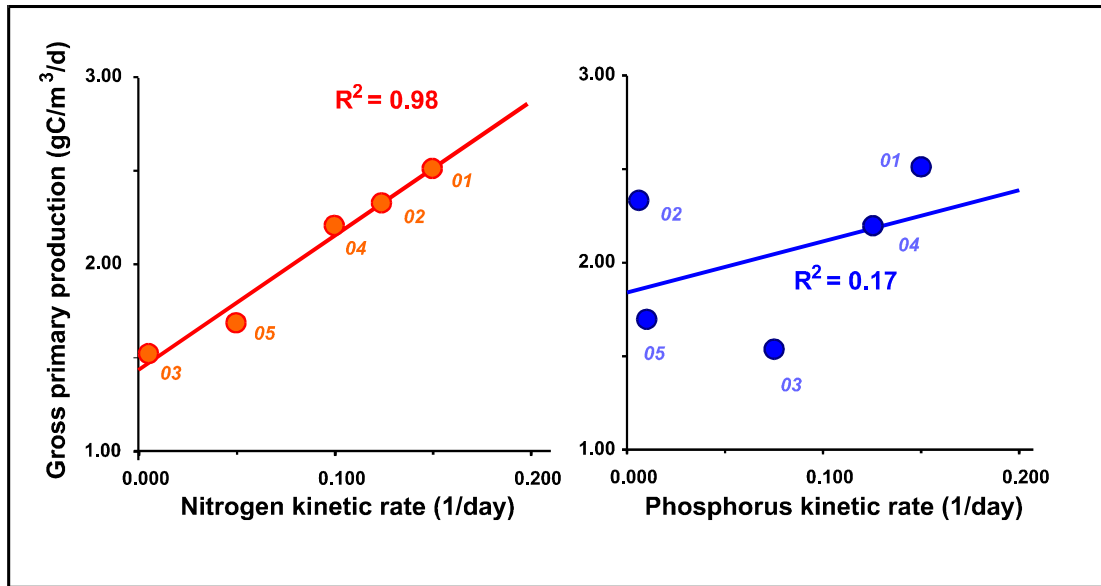


Figure 38 – Association of sonde-derived average main-stem production and decay rates from model fits to nutrient data (Armstrong and Ward, 2008b)

Station SH, about 0.49 mg/L/hr in July 2003 (Table A-5). This sonde value is, however, based upon only two data points that survived screening. The 1-8 July average of the unscreened 5-day sliding mean values is 0.21 mg/L/hr, in tolerable agreement with the USGS result. In other years, the (screened) SH value in August was on the order of 0.8 mg/L/hr, about four times the USGS value and typically the highest value of community respiration in the Klamath system. Probably the most significant property of these two types of measurement that limits their comparability, however, is that the USGS measurement applies to a limited reach of selected sediment characteristics over a time period of a few hours, while the sonde-derived value represents the daily respiration integrated over a 5-10 mile reach and over multiple days.

In the simple plug-flow mass-budget model of Armstrong and Ward (2008b), the variation of total N and total P along the Klamath mainstem was found to be well-explained by the high concentrations in the Iron Gate discharge, dilution by tributary inflows, and a modest decay rate, whose value was determined by the best fit to the profile of measurements for each year of the study period. Since one potential contributor to nutrient decay is biological activity, we inquire

whether there is some association of these modeled decay rates with the values of gross primary production extracted from the sonde data. Since the model decay rate is applied uniformly along the length of the river, to be comparable the production values were averaged over the mainstem stations. Further, this evaluation is limited to August production data, because August is typically the month of lowest and most stable river flow, as well as sufficiently late in the season that production values are generally highest. The results, shown in Figure 38, indicate that the sonde-derived production has a close association with the N decay rate (correlation 0.99), and a much weaker association with the P decay rate (correlation 0.41). Yielding to the temptation to overinterpret these results, we note (1) there is more uncertainty in the model-fitted total P decay rates because of the small concentrations, and (2) the decay of nitrogen concentration is due almost entirely to biological assimilation, while substantial inorganic phosphorus is lost to the additional process of adsorption to particulates and settling, which is entirely physical and unrelated to biology.

5. Concluding remarks

This report has focused on the application of the AFWO sonde data in quantifying the lotic community metabolism of the Klamath River below Iron Gate, notably primary production and related kinetic processes. The data from this evaluation were averaged to exhibit a water-quality “climate” of the river under summer “low-flow” conditions, especially as it is reflected in the behavior of dissolved oxygen. The evaluation of metabolism parameters by the method outlined in Section 1 is based upon the diurnal photocycle and the associated variation in dissolved oxygen, and therefore entails integration over a 24-hour period. This requires that over a considerable distance upstream from each sonde station the river must be longitudinally well-mixed and subjected to essentially the same rates of insolation, reaeration and respiration, in order for the assumptions underlying the analysis method to hold. Put another way, the results from the sonde analyses represent the DO kinetics substantially integrated in space (30 to 60 km, see Fig. 31) and time (at least 24 hours, several to many days if results are cumulated as longer-period averages, as done in Section 4).

In addition, these results are implicitly aggregated over major components of the river ecosystem. As noted earlier, the production ascribed to photosynthesis implicitly includes all plants in the watercourse that effect an influx of DO during daylight, including plankton, benthal algae (periphyton), and macrophytes (submerged aquatic vegetation). Community respiration includes algal respiration (both planktonic and benthic), bacterial stabilization of organics, respiration of zooplankton and higher heterotrophs in the water column, and oxygen demand by bacteria and benthal fauna in the sediments. It might be desirable in the future to isolate some of these components for more detailed study, which will require field measurements supplementary to the sonde program. The partition of oxygen demand into 60% benthal and 40% water-column in the USGS sediment oxygen demand data from the Shasta (Flint et al., 2005) offers some support for the hypothesis that a substantial benthic algae contribution may be made to gross primary production (thereby reducing the correlation between gross production inferred from the sonde data and water-column chlorophyll-a).

The picture of the Klamath community metabolism that emerges from the analyses of the sonde data is consistent in some respects with that of other large rivers, in being net heterotrophic but with a tendency for increasing relative autotrophy downstream toward the mouth (e.g., Dodds, 2006, Dodds and Cole, 2007). When the rates of respiration and production inferred from sonde data are converted to equivalent areal units (by multiplying times the prevailing depth under the ambient flow conditions), the rates are numerically consistent with literature values (e.g., Dodds, 2006, Garnier and Billen, 2007, McTammany et al., 2003 and citations therein) and indicate a mesotrophic system. We note, in passing, that volumetric rates, rather than areal, would appear to be more meaningful for the Klamath (e.g., Smith, 2007) and have been employed throughout this report.

The inferred metabolism parameters have been presented annually in the preceding sections, to exhibit their year-to-year variation, especially the extent to which river flow may be a controlling factor. When these results are further averaged over the 2001-05 study period, they appear more coherent in their behavior than exhibited in the individual years, see Figure 39. The most general features of the Klamath mainstem may be summarized as follows:

- (1) The release from Iron Gate dominates the chemistry of the river: nutrient concentrations, as measured by total nitrogen (N), total phosphorus (P) and total organic carbon (TOC), are maximal at IG, the station just below Iron Gate dam, and decline with distance downstream, primarily as a result of dilution by tributary inflow, secondarily due to kinetic decay.
- (2) Community production and respiration vary coherently down the mainstem to the mouth. This is suggestive that either production drives respiration, or that they are dominated by correlated controls (e.g., allochthonous inputs of nutrients and carbon).
- (3) In the reach immediately downstream from Iron Gate, production increases dramatically, indicative of the establishment of a riverine autotroph community. This level of production is generally maintained downstream through about river mile 130 (SV, the Seiad Valley station, and below the confluences of the Shasta and Scott). In

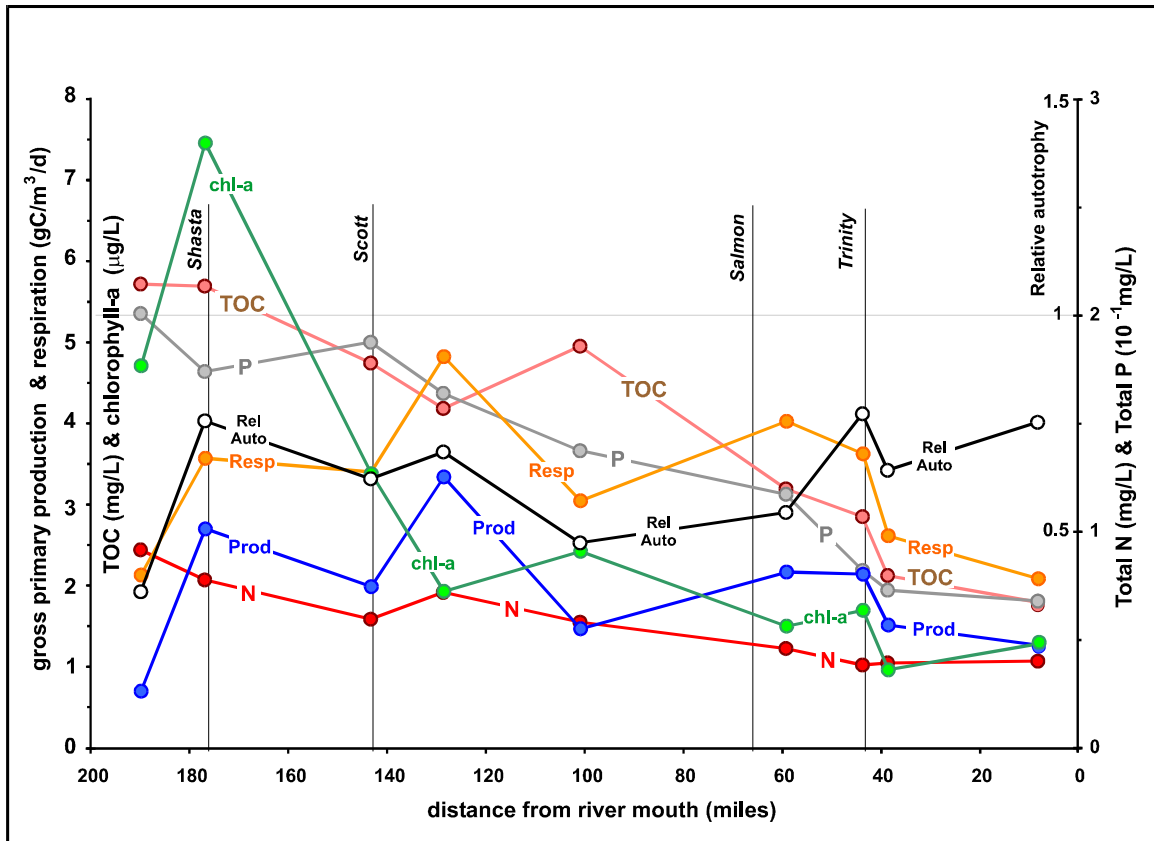


Figure 39 – Mainstem Klamath profiles of 2001-2005 average summer (June-September) metabolic parameters

the reach from SV to the Salmon confluence, production diminishes, whose cause remains elusive. This phenomenon is represented, unfortunately, by a single station, that at Happy Camp (HC), where production and respiration are consistently depressed in each year of the study. Production recovers below the Salmon confluence, but declines below the Trinity confluence, most likely due to dilution with waters of the Trinity.

- (4) Relative autotrophy and chlorophyll-a concentrations increase markedly in the reach immediately downstream from Iron Gate, supporting the interpretation of establishment of a vigorous community of autotrophs in the shallow, nutrient-rich waters. From the Shasta confluence to the Salmon confluence, relative autotrophy

generally declines to a value of about 0.5, then increases from below the Salmon to the mouth, in a few years exceeding unity. This increase in the lowermost reach is due primarily to a factor-of-two decline in respiration.

- (5) All of these parameters, *viz.* nutrients, chlorophyll, respiration and production, drop substantially with distance down the river below Iron Gate, this decline, with the sole exception of nitrogen, being almost entirely due to dilution with flow from the Trinity.
- (6) Not shown in the mainstem diagram of Fig. 39, production and respiration in the principal tributaries, *viz.* the Shasta, Scott, Salmon and Trinity, differ from each other and from the mainstem, and are consistent from year to year, suggesting very different kinetic processes and drivers in each tributary. Most exceptional is the Trinity, with surprisingly low values of production and respiration.

These results pose questions whose exploration was beyond the scope of the present effort. While these results indicate the Klamath to be net heterotrophic, the only major allochthonous source of carbon, *viz.* the discharge from Iron Gate, appears to be insufficient to fuel respiration in the lower Klamath. This suggests that secondary production may be responsible for the high respiration, which would imply a vigorous community of herbivores, either benthal or planktonic. (The five-day BOD's were almost uniformly below the detection limit of 2 mg/L.)

The lack of correlation between measured water-sample chlorophyll-a and daily primary production remains puzzling. This may be due to a major contribution to production by phytobenthos, which would not be included in a water-sample chlorophyll analysis, as suggested above. It may also be a simple manifestation of inadequate sampling: the heterogeneity of algae on short spatial and temporal scales may render a single grab sample taken at intervals of many days inadequate to measure the biomass of phytoplankton, particularly in comparison to the daily integrated values of production inferred from the sonde records. Certainly, however, the relative role of planktonic and benthal algae in the river system needs further study.

The estimations of reaeration coefficient from the nighttime DO time series are substantially higher, by a factor of 2 to 10, than the values given by the O'Connor-Dobbins equation. This result requires more detailed study, first to substantiate the sonde-derived coefficients, second to verify their functional dependence upon physical and hydraulic properties of the stream, and third to determine whether this disparity might extrapolate to other streams and rivers. Field measurements of reaeration are notoriously difficult to perform, consequently great reliance is placed upon the calculation of reaeration from relationships such as the O'Connor-Dobbins equation, particularly in the estimation of production from DO time series (e.g., Young and Huryn, 1998, Bott, 2007). Any limits to the applicability of these relations that might be indicated by the present data would be useful information in river metabolism investigations.

The data sets compiled by the Fish & Wildlife Service for the 2001-2005 period, particularly after being subjected to an exacting correction procedure, represent an invaluable resource for diagnosing the behavior of the Klamath River and its response to various external and internal factors. This report only scratches the surface of the analyses that can be supported by this rich data set. Two other parameters, pH and conductivity, have been processed using the same data-correction protocols, and are available for use in studies of the river. Moreover, the detailed response of DO, and the inferred metabolic parameters, to flow events, meteorology, and nutrient sources can be evaluated in much more detail on time scales of hours to a few days. There are sonde records in the AFWO data base from additional stations, and sondes have been deployed in the river by other researchers, whose correction following similar protocols and whose analysis with these methods outlined in this report should yield useful information.

References:

- Armstrong, N. and G. Ward. 2005. Review of the AFWO Klamath River Grab Sample Water Quality Database. Report to U.S. Fish & Wildlife Service, Arcata, CA.
- Armstrong, N. and G. Ward, 2008a: Nutrient Loading in the Lower Klamath River and Tributaries. Report to U.S. Fish & Wildlife Service, Arcata, CA.
- Armstrong, N. and G. Ward, 2008b: Coherence of Nutrient Loads and AFWO Klamath River Grab Sample Water Quality Database. Report to U.S. Fish & Wildlife Service, Arcata, CA.
- Bott, T.L., 2007: Primary productivity and community respiration. *In*: F. Hauer and G. Lamberti (eds), *Methods in stream ecology*, 2nd ed. Burlington, MA: Academic Press.
- Chapra, S.C., 1997: *Surface water-quality modeling*. Boston: WCB/McGraw-Hill.
- Churchill, M., H. Elmore and R. Buckingham, 1962: Prediction of stream reaeration rates. *J. San. Engr. Div. ASCE*, SA4.
- Deas, M., and G. Orlob, 1999: *Klamath River Modeling Project*. Rep. No. 99-04, Water Resources Modeling Group, Center for Environmental and Water Resources Engineering, University of California, Davis.
- Dodds, W., 2006: Eutrophication and trophic state in rivers and streams. *Limn. Oceanogr.* 51 (1 pt 2), pp 671-680.
- Dodds, W. and J. Cole, 2007: Expanding the concept of trophic state in aquatic ecosystems: It's not just the autotrophs. *Aquat. Sci.* 69, pp 427-439.
- Falkowski, P. and J. Raven, 1997: *Aquatic photosynthesis*. Malden, MA: Blackwell Science, Inc.
- Flint, L., A. Flint, D. Curry, S. Rounds and M. Doyle, 2005: *Water-Quality Data from 2002 to 2003 and Analysis of Data Gaps for Development of Total Maximum Daily Loads in the Lower Klamath River Basin, California*. Scientific Investigations Report 2004-5255, U.S. Geological Survey, Reston, VA.
- Garnier, J. and G. Billen, 2007: Production versus respiration in river systems: an indicator of an "ecological status." *Sci. Total Env.* 375, pp. 110-124.
- Guillen, G., 2003: *Klamath River fish die-off, September 2002: Report on estimate of mortality*. Rep. no. AFWO 01-03, U.S. Fish & Wildlife Service, Arcata, CA.
- Hamming, R., 1973: *Numerical methods for scientists and engineers*. New York: McGraw-Hill, Inc.

- Kirk, J.T.O., 1994: *Light and photosynthesis in aquatic ecosystems*, 2nd ed. Cambridge University Press.
- McTammany, M., J. Webster, E. Benfield, and M. Neatrout, 2003: Longitudinal patterns of metabolism in a southern Appalachian river. *J. N. Am. Benthol. Soc.* 22 (3), pp 359-370.
- National Wildfire Coordinating Group (NWCG), 2005: Weather Station Standards. Report PMS 426-3, National Fire Danger Rating System, Fire Weather Working Team, NWCG, Boise, ID. See: <http://www.fs.fed.us/raws/standards.shtml>
- O'Connor, D., and W. Dobbins, 1958: Mechanism of reaeration in natural streams. *Trans. ASCE* 123, pp. 641-684.
- Odum, H.T., 1956: Primary production in flowing waters. *Limnology & Oceanography* 1 (2), pp. 102-117.
- Rounds, S., and M. Doyle, 1997: *Sediment oxygen demand in the Tualatin River basin, Oregon, 1992-96*. Water-Resources Investigations Report 97-4103, U.S. Geological Survey, Reston, VA.
- Smith, V.A., 2007: Using primary productivity as an index of coastal eutrophication: the units of measurement matter. *J. Plankton Res.* 29 (1), pp. 1-6.
- Turner, R. and P. Zedonis, 2004a: *Arcata Fish and Wildlife Service's 2004 Multiprobe Maintenance and Deployment Protocol*. U.S. Fish & Wildlife Service, Arcata, CA.
- Turner, R. and P. Zedonis, 2004b: *Comparison of instruments used in water quality investigations of the Klamath River in 2003*. U.S. Fish & Wildlife Service, Arcata, CA.
- Young, R., and A. Huryn, 1998: Comment: Improvements to the diurnal upstream-downstream dissolved oxygen change technique for determining whole-stream metabolism in small streams. *Can. J. Fish. Aquat. Sci.* 55, pp 1784-1785.
- Wagner, R., R. Boulger, C. Oblinger, and B. Smith, 2006: *Guidelines and standard procedures for continuous water-quality monitors—Station operation, record computation, and data reporting*. Techniques and Methods 1–D3, U.S. Geological Survey, Reston, Virginia.
- Ward, G.H., 2003: Primary productivity in the Coastal Bend bays. Report to Texas General Land Office. Center for Research in Water Resources, University of Texas at Austin.
- Ward, G. and N. Armstrong, 2006a: Hydrological features of Lower Klamath River and tributaries. Report to U.S. Fish & Wildlife Service, Arcata, CA.
- Ward, G. and N. Armstrong, 2006b: Q/A Review of Klamath sonde data holdings. Report to U.S. Fish & Wildlife Service, Arcata, CA.

- Ward, G. and N. Armstrong, 2006c: Proposed correction procedure for Klamath sonde data holdings. Report to U.S. Fish & Wildlife Service, Arcata, CA.
- Ward, G. and N. Armstrong, 2006d: Correction procedure for sonde data. Report to U.S. Fish & Wildlife Service, Arcata, CA.
- Ward, G. and N. Armstrong, 2006e: Estimation of dissolved oxygen kinetic parameters from Klamath sonde data. Report to U.S. Fish & Wildlife Service, Arcata, CA.
- Ward, G. and N. Armstrong, 2006f: Formulas for saturation concentration for dissolved oxygen. Report to U.S. Fish & Wildlife Service, Arcata, CA.
- Watercourse Engineering, Inc., 2003: Klamath River Water Quality Synoptic Survey: August 2003. Tech. Memo. 6, WEI, Davis, CA.
- Weiss, R.F., 1970: The solubility of nitrogen, oxygen and argon in water and seawater. *Deep Sea Research* 17, pp 721-735.
- Williams, P.H., 1993: On the definition of plankton production terms. *International Council for the Exploration of the Sea Marine Science Symposium 197*, pp. 9-19.

APPENDIX

Detailed results and supporting data

Table A-1: Attributes of sonde station locations in Klamath and tributaries (depths at low stage)

<i>Sta ID</i>	<i>description</i>	<i>elevation (ft)</i>	<i>depth (ft)</i>	<i>substrate & channel</i>
Mainstem stations (Klamath River)				
IG	below Iron Gate	2178	3-8	cobble, edgewater macrophytes
K1	above Shasta	1860	3-8	cobble & boulder, edgewater macrophytes
K2	above Scott	1520	3-10	bedrock w/ pools
SV	Seiad Valley	1320	5-12	deep channel, bedrock w/ alluvial stretches
HC	Happy Camp	960	5-20	steep, incised channel, bedrock pools
OR	Orleans	400	5-20	ditto, some gravel point bars & riffles
WE	Weitchepec	240	5-20	increasing sediment & gravel point bars
MF/TC/KBW	above Tully Creek	280	5-20	ditto, but steeper w/ deeper canyon
TG/KAT	Terwer	8	5-20	increasing sediment & gravel point bars
Tributary stations (near mouths)				
SH	Shasta River near Yreka	2031	1-2	dominated by aquatic macrophytes
SC	Scott River near Fort Jones	1600	1-10	wide, cobble
SA	Salmon River at Sommes Bar	480	5-15	boulder & cobble
TR	Trinity River near mouth	240	5-15	bedrock

Table A-2: Longitudinal positions of sonde stations in Klamath and tributaries

	<i>mainstem (mis)</i>	<i>trib (mis)</i>	<i>mainstem (km)</i>	<i>trib (km)</i>	<i>nearest USGS gauging station</i>
Mainstem stations					
IG	189.8		305.5		co-located 11516530
K1	176.8		284.6		
K2	143.2		230.5		
SV	128.5		206.9		co-located 11520500
HC	100.8		162.3		
OR	59.1		95.1		co-located 11523000
WE	43.6		70.2		
MF/TC/KBW	38.5		62.0		
TG/KAT	6.7		10.8		near 11530500
Tributary stations					
SH	176.6	0.5	284.3	0.8	co-located 11517500
SC	143.0	1.5	230.2	2.4	co-located 11519500
SA	66.0	1.0	106.2	1.6	co-located 11522500
TR	43.5	0.5	70.0	0.8	downstream from 11530000

Table A-3: Monthly averaged values of kinetic parameters from screened sonde data, 2001

<i>Station</i>		<i>flow</i>	<i>K_a</i>	<i>C_r</i>	<i>prod- uction</i>	<i>insol- ation</i>	<i>daily C_r</i>	<i>net ecoprod</i>	<i>relative auto- troph</i>
<i>mainstem</i>	<i>tributary</i>	(<i>cfs</i>)	(<i>1/hr</i>)	(<i>ppm/hr</i>)	(<i>gC/m³</i>)		(<i>gC/m³</i>)	(<i>gC/m³</i>)	
June 2001									
IG		1843	0.17	-0.23	0.49	7.93	2.06	-1.56	0.24
	<i>SH</i>	25	0.67	-0.87	5.06	7.57	7.86	-2.80	0.64
	<i>SC</i>	48	1.03	-0.95	5.30	7.11	8.58	-3.28	0.62
SV		2135	0.40	-0.51	3.38	7.04	4.56	-1.18	0.74
HC		2011	0.16	-0.29	1.41	6.90	2.63	-1.22	0.54
	<i>SA</i>	371	0.47	-0.47	1.03	7.54	4.27	-3.24	0.24
OR		2793	0.57	-0.40	2.28	7.10	3.63	-1.35	0.63
WE		2712	0.26	-0.42	1.88	6.85	3.79	-1.90	0.50
	<i>TR</i>	1479	0.29	-0.36	0.57	6.68	3.27	-2.70	0.17
MF									
TG		5535	0.19	-0.40	1.47	7.99	3.59	-2.12	0.41
July 2001									
IG		1007	0.14	-0.36	1.31	7.47	3.27	-1.96	0.40
	<i>SH</i>	23	0.69	-1.11	4.40	7.33	9.95	-5.55	0.44
	<i>SC</i>	8	0.86	-0.91	5.84	7.84	8.18	-2.33	0.71
SV		1068	0.40	-0.86	6.26	7.80	7.73	-1.47	0.81
HC		1126	0.22	-0.32	1.96	7.89	2.90	-0.94	0.68
	<i>SA</i>	179	0.40	-0.41	1.72	7.78	3.65	-1.93	0.47
OR		1468	0.39	-0.40	2.35	7.77	3.57	-1.22	0.66
WE		1473	0.42	-0.63	3.03	7.35	5.64	-2.61	0.54
	<i>TR</i>	868	0.34	-0.32	0.78	7.70	2.85	-2.07	0.27
MF		2166	0.32	-0.49	1.65	7.05	4.40	-2.75	0.38
TG		3253	0.16	-0.34	1.64	7.39	3.10	-1.45	0.53
August 2001									
IG		1021	0.21	-0.53	0.98	7.03	4.77	-3.79	0.21
	<i>SH</i>	20	0.60	-0.90	4.16	6.62	8.07	-3.92	0.52
	<i>SC</i>	6	0.80	-1.27	8.19	6.91	11.45	-3.26	0.72
SV		1047	0.38	-0.68	4.16	6.92	6.09	-1.94	0.68
HC		1050	0.23	-0.39	2.55	7.02	3.51	-0.96	0.73
	<i>SA</i>	92	0.32	-0.39	1.74	6.92	3.50	-1.76	0.50
OR		1210	0.35	-0.41	3.01	6.92	3.67	-0.67	0.82
WE		1210	0.41	-0.62	3.33	6.38	5.57	-2.25	0.60
	<i>TR</i>	722	0.39	-0.35	0.73	6.49	3.15	-2.42	0.23
MF		1880	0.31	-0.49	2.03	6.53	4.42	-2.39	0.46
TG		2664	0.12	-0.29	1.54	6.19	2.61	-1.07	0.59
(continued)									

Table A-3 (continued)

<u>Station</u>		<i>flow</i>	K_a	C_r	<i>prod- uction</i>	<i>insol- ation</i>	<i>daily</i>	<i>net</i>	<i>relative</i>
<i>mainstem</i>	<i>tributary</i>						C_r	<i>ecoprod</i>	<i>auto-</i>
		(cfs)	(1/hr)	(ppm/hr)	(gC/m ³)		(gC/m ³)	(gC/m ³)	<i>trophy</i>
September 2001									
IG		1027	0.18	-0.49	0.79	5.35	4.43	-3.64	0.18
	SH	36	0.69	-0.57	3.08	5.43	5.09	-2.01	0.60
	SC	4	0.69	-1.03	7.02	5.62	9.29	-2.27	0.76
SV		1066	0.37	-0.54	4.10	5.68	4.89	-0.80	0.84
HC		1090	0.36	-0.76	1.75	5.02	6.80	-5.05	0.26
	SA	76	0.33	-0.44	1.64	5.62	3.96	-2.33	0.41
OR		1224	0.32	-0.39	2.65	5.71	3.52	-0.87	0.75
WE		1193	0.41	-0.48	3.59	5.46	4.31	-0.72	0.83
	TR	632	0.54	-0.47	0.71	5.19	4.27	-3.56	0.17
MF		1893	0.33	-0.38	1.82	5.13	3.39	-1.57	0.54
TG		2550	0.09	-0.26	1.53	5.06	2.30	-0.77	0.66

Table A-4: Monthly averaged values of kinetic parameters from screened sonde data, 2002

<u>Station</u>		<i>flow</i>	K_a	C_r	<i>prod- uction</i>	<i>insol- ation</i>	<i>daily</i>	<i>net</i>	<i>relative</i>
<i>mainstem</i>	<i>tributary</i>						C_r	<i>ecoprod</i>	<i>auto-</i>
		(cfs)	(1/hr)	(ppm/hr)	(gC/m ³)		(gC/m ³)	(gC/m ³)	<i>trophy</i>
June 2002									
IG		978	0.31	-0.10	0.79	6.46	0.86	-0.08	0.91
	SH	44	0.63	-1.24	6.19	6.66	11.17	-4.98	0.55
	SC	315	1.14	-0.75	3.51	7.65	6.75	-3.24	0.52
SV		1847	0.48	-0.52	3.31	7.41	4.70	-1.39	0.70
HC		1556	0.23	-0.20	0.79	7.47	1.82	-1.03	0.44
	SA	837	1.84	-1.13	2.35	7.10	10.14	-7.79	0.23
OR		2887	0.71	-0.44	1.94	7.46	3.96	-2.03	0.49
WE		2699	0.38	-0.52	1.57	7.04	4.69	-3.12	0.33
	TR	1310	0.22	-0.19	0.37	5.58	1.74	-1.37	0.21
MF		3588	0.35	-0.41	1.28	6.50	3.66	-2.38	0.35
TG		6275	0.21	-0.31	0.55	7.39	2.76	-2.21	0.20

(continued)

Table A-4 (continued)

<i>Station</i>		<i>flow</i>	<i>K_a</i>	<i>C_r</i>	<i>prod- uction</i>	<i>insol- ation</i>	<i>daily C_r</i>	<i>net ecoprod</i>	<i>relative auto- trophy</i>
<i>mainstem</i>	<i>tributary</i>	(<i>cfs</i>)	(<i>1/hr</i>)	(<i>ppm/hr</i>)	(<i>gC/m³</i>)		(<i>gC/m³</i>)	(<i>gC/m³</i>)	
July 2002									
IG		834	0.28	-0.17	0.92	7.97	1.49	-0.57	0.62
	<i>SH</i>	26	0.64	-1.12	2.65	7.83	10.11	-7.46	0.26
	<i>SC</i>	60	1.07	-1.00	10.44	7.30	8.97	1.47	1.16
SV		1219	0.38	-0.51	3.83	7.38	4.63	-0.80	0.83
HC		1025	0.28	-0.24	1.48	7.02	2.13	-0.65	0.70
	<i>SA</i>	312	0.43	-0.46	1.71	6.99	4.13	-2.42	0.41
OR		1634	0.47	-0.44	2.46	7.39	3.99	-1.52	0.62
WE		1649	0.42	-0.42	2.44	6.83	3.75	-1.31	0.65
	<i>TR</i>	822	0.35	-0.23	0.66	6.62	2.10	-1.43	0.32
MF		2602	0.32	-0.37	1.55	6.97	3.36	-1.81	0.46
TG		3155	0.18	-0.36	1.12	6.82	3.24	-2.13	0.34
August 2002									
IG		666	0.40	-0.28	0.69	6.98	2.55	-1.86	0.27
	<i>SH</i>	24	0.66	-0.94	3.30	6.58	8.49	-5.19	0.39
	<i>SC</i>	16	0.89	-1.30	4.22	6.67	11.71	-7.49	0.36
SV		789	0.36	-0.66	4.39	6.47	5.92	-1.53	0.74
HC		792	0.34	-0.42	2.05	6.11	3.74	-1.69	0.55
	<i>SA</i>	169	0.47	-0.56	2.01	6.18	5.04	-3.03	0.40
OR		1277	0.28	-0.46	2.15	6.02	4.10	-1.96	0.52
WE		1264	0.40	-0.59	3.36	5.63	5.32	-1.95	0.63
	<i>TR</i>	710	0.31	-0.38	0.64	5.30	3.40	-2.76	0.19
MF		2037	0.32	-0.41	2.18	5.92	3.66	-1.48	0.60
TG		2088	0.18	-0.38	1.56	5.77	3.46	-1.91	0.45
September 2002									
IG		759	0.40	-0.28	0.83	5.67	2.50	-1.67	0.33
	<i>SH</i>	29	0.69	-0.82	2.91	5.65	7.39	-4.49	0.39
	<i>SC</i>	12	0.65	-0.83	4.20	3.74	7.45	-3.25	0.56
SV		925	0.37	-0.59	4.18	3.67	5.27	-1.09	0.79
HC		892	0.37	-0.41	2.05	3.78	3.73	-1.67	0.55
	<i>SA</i>	125	0.43	-0.52	1.53	3.75	4.70	-3.17	0.33
OR		1292	0.28	-0.41	1.71	3.80	3.70	-1.99	0.46
WE		1285	0.39	-0.53	2.70	5.12	4.81	-2.10	0.56
	<i>TR</i>	619	0.42	-0.46	0.72	4.74	4.13	-3.41	0.17
MF		1931	0.29	-0.36	1.59	5.03	3.26	-1.67	0.49
TG		1994	0.16	-0.39	1.65	4.92	3.52	-1.87	0.47

Table A-5: Monthly averaged values of kinetic parameters from screened sonde data, 2003

<i>Station</i>		<i>flow</i>	<i>K_a</i>	<i>C_r</i>	<i>prod- uction</i>	<i>insol- ation</i>	<i>daily C_r</i>	<i>net ecoprod</i>	<i>relative auto- troph</i>
<i>mainstem</i>	<i>tributary</i>	<i>(cfs)</i>	<i>(1/hr)</i>	<i>(ppm/hr)</i>	<i>(gC/m³)</i>		<i>(gC/m³)</i>	<i>(gC/m³)</i>	<i>trophy</i>
June 2003									
IG	SH	1450	0.32	-0.01	0.57	8.01	0.09	0.49	6.46
		86	1.00	-0.55	1.65	7.64	4.92	-3.27	0.34
K2	SA								
SV		3213	0.51	-0.50	1.87	7.69	4.49	-2.62	0.42
HC	TR								
OR									
WE	TR	7067	0.35	-0.22	0.93	7.79	1.94	-1.01	0.48
		4380	0.31	-0.19	0.49	7.91	1.71	-1.22	0.29
MF/TC		9321	0.30	-0.21	0.67	7.80	1.91	-1.24	0.35
TG		16300	0.25	-0.15	1.74	7.82	1.33	0.41	1.31
July 2003									
IG	SH	794	0.34	-0.49	0.87	6.89	4.44	-3.56	0.20
		71	0.67	-0.49	1.30	8.28	4.39	-3.09	0.30
K2	SA	849	0.31	-0.41	3.24	7.03	3.70	-0.46	0.88
SV		1292	0.47	-0.49	3.28	8.01	4.40	-1.12	0.75
HC	TR	1165	0.24	-0.21	0.97	7.86	1.92	-0.95	0.51
		542	0.61	-0.30	0.89	8.14	2.67	-1.78	0.33
OR	TR	2413	0.61	-0.49	1.59	7.87	4.44	-2.85	0.36
WE		2641	0.39	-0.29	1.12	7.31	2.65	-1.53	0.42
MF/TC		1447	0.30	-0.23	0.49	7.32	2.03	-1.55	0.24
TG		4570	0.32	-0.28	1.46	7.39	2.52	-1.06	0.58
		794	0.34	-0.49	0.87	6.89	4.44	-3.56	0.20
August 2003									
IG	SH	995	0.22	-0.19	0.23	7.28	1.67	-1.44	0.14
K2	SA	1062	0.27	-0.28	2.07	6.64	2.50	-0.43	0.83
SV									
HC	TR	1235	0.18	-0.23	0.93	6.75	2.03	-1.11	0.46
OR	TR	2070	0.51	-0.48	2.45	6.64	4.29	-1.84	0.57
WE		2060	0.42	-0.37	1.98	6.42	3.31	-1.33	0.60
MF/TC		1029	0.39	-0.20	0.82	6.54	1.82	-0.99	0.45
TG		3207	0.24	-0.23	1.57	6.04	2.08	-0.51	0.76
(continued)									

Table A-5 (continued)

<u>Station</u>		<i>flow</i>	K_a	C_r	<i>prod- uction</i>	<i>insol- ation</i>	<i>daily</i> C_r	<i>net</i> <i>ecoprod</i>	<i>relative</i> <i>auto- troph</i>
<i>mainstem</i>	<i>tributary</i>	(<i>cfs</i>)	(<i>1/hr</i>)	(<i>ppm/hr</i>)	(<i>gC/m³</i>)		(<i>gC/m³</i>)	(<i>gC/m³</i>)	
September 2003									
IG	<i>SH</i>	1190	0.22	-0.40	0.64	6.21	3.62	-2.99	0.18
K2		1347	0.19	-0.21	1.39	5.62	1.93	-0.55	0.72
SV									
HC	<i>SA</i>	1474	0.17	-0.19	0.67	5.12	1.71	-1.03	0.39
OR		2068	0.51	-0.37	2.20	5.33	3.35	-1.15	0.66
WE		2044	0.33	-0.31	1.32	4.59	2.79	-1.47	0.47
	<i>TR</i>	727	0.37	-0.32	0.71	4.71	2.86	-2.15	0.25
MF/TC		3259	0.27	-0.26	1.20	4.34	2.34	-1.14	0.51
TG									

Table A-6: Monthly averaged values of kinetic parameters from *screened* sonde data, 2004

<u>Station</u>		<i>flow</i>	K_a	C_r	<i>prod- uction</i>	<i>insol- ation</i>	<i>daily</i> C_r	<i>net</i> <i>ecoprod</i>	<i>relative</i> <i>auto- troph</i>
<i>mainstem</i>	<i>tributary</i>	(<i>cfs</i>)	(<i>1/hr</i>)	(<i>ppm/hr</i>)	(<i>gC/m³</i>)		(<i>gC/m³</i>)	(<i>gC/m³</i>)	
June 2004									
IG	<i>SH</i>	944	0.22	-0.32	2.95	7.14	2.84	0.11	1.04
K1		64	0.95	-1.15	5.52	6.98	10.36	-4.84	0.53
K2									
SV	<i>SC</i>	266	0.91	-0.81	0.74	8.14	7.27	-6.54	0.10
HC									
OR	<i>SA</i>	3628	0.81	-0.68	1.66	8.13	6.15	-4.49	0.27
WE									
	<i>TR</i>	3065	0.38	-0.28	0.26	7.06	2.48	-2.22	0.11
TC		8917	0.29	-0.12	0.59	6.61	1.08	-0.48	0.55
TG		8068	0.09	-0.09	0.37	6.60	0.81	-0.44	0.45

(continued)

Table A-6 (continued)

<i>Station</i>		<i>flow</i>	<i>K_a</i>	<i>C_r</i>	<i>prod- uction</i>	<i>insol- ation</i>	<i>daily C_r</i>	<i>net ecoproduct</i>	<i>relative auto- troph</i>
<i>mainstem</i>	<i>tributary</i>	<i>(cfs)</i>	<i>(1/hr)</i>	<i>(ppm/hr)</i>	<i>(gC/m³)</i>		<i>(gC/m³)</i>	<i>(gC/m³)</i>	
July 2004									
IG		628	0.19	-0.11	0.63	6.50	0.98	-0.35	0.65
K1		637	0.30	-0.52	3.15	5.72	4.65	-1.51	0.68
	SH	40	0.60	-1.06	2.32	7.15	9.56	-7.24	0.24
K2		780	0.23	-0.54	2.01	8.25	4.84	-2.83	0.42
	SC	85	0.86	-1.06	2.41	4.90	9.58	-7.17	0.25
SV		1042	0.44	-0.50	2.66	7.99	4.54	-1.88	0.59
HC		962	0.50	-0.31	1.47	8.24	2.83	-1.37	0.52
	SA								
OR									
WE		2363	0.48	-0.32	1.24	8.04	2.89	-1.66	0.43
	TR	1313	0.48	-0.40	0.67	6.37	3.56	-2.89	0.19
TC		3890	0.29	-0.24	1.31	7.03	2.20	-0.89	0.59
TG		3269	0.22	-0.38	1.00	6.21	3.44	-2.44	0.29
August 2004									
IG		830	0.19	-0.19	0.60	5.84	1.73	-1.13	0.35
K1		737	0.27	-0.46	2.61	6.05	4.11	-1.51	0.63
	SH	35	0.71	-0.83	2.58	6.29	7.51	-4.92	0.34
K2		646	0.24	-0.52	2.24	6.61	4.65	-2.41	0.48
	SC	13	0.75	-1.15	2.55	7.10	10.39	-7.83	0.25
SV		1031	0.43	-0.42	2.83	5.72	3.81	-0.98	0.74
HC		811	0.43	-0.78	3.85	6.87	7.04	-3.19	0.55
	SA	232	0.41	-0.49	1.58	6.78	4.39	-2.81	0.36
OR		1583	0.37	-0.52	2.73	6.36	4.66	-1.93	0.59
WE		1569	0.40	-0.67	2.33	6.35	6.07	-3.74	0.38
	TR	887	0.36	-0.35	0.73	6.41	3.19	-2.47	0.23
TC		2533	0.19	-0.22	1.46	6.19	2.02	-0.56	0.72
TG		3289	0.19	-0.31	1.22	6.07	2.76	-1.53	0.44
September 2004									
IG		911	0.16	-0.15	0.72	5.41	1.37	-0.65	0.53
K1		913	0.27	-0.33	2.11	5.13	2.97	-0.86	0.71
	SH	44	0.60	-0.48	1.84	5.51	4.33	-2.49	0.42
K2		980	0.26	-0.49	1.56	4.96	4.43	-2.87	0.35
	SC								
SV		986	0.34	-0.47	2.36	5.99	4.20	-1.84	0.56
HC		1025	0.24	-0.29	0.88	5.68	2.62	-1.74	0.34
	SA	163	0.41	-0.36	1.12	4.93	3.20	-2.09	0.35
OR		1613	0.35	-0.37	1.93	5.62	3.33	-1.40	0.58
WE		1633	0.41	-0.60	1.44	5.02	5.43	-3.98	0.27
	TR	805	0.33	-0.36	0.53	4.30	3.21	-2.68	0.17
TC		2737	0.21	-0.16	1.16	5.03	1.43	-0.27	0.81
TG		3033	0.15	-0.20	1.51	5.05	1.84	-0.33	0.82

Table A-7: Monthly averaged values of kinetic parameters from screened sonde data, 2005

<i>Station</i>		<i>flow</i>	K_a	C_r	<i>prod-</i> <i>uction</i>	<i>insol-</i> <i>ation</i>	<i>daily</i> C_r	<i>net</i> <i>ecoprod</i>	<i>relative</i> <i>auto-</i> <i>trophy</i>
<i>mainstem</i>	<i>tributary</i>	(<i>cfs</i>)	(<i>1/hr</i>)	(<i>ppm/hr</i>)	(<i>gC/m³</i>)		(<i>gC/m³</i>)	(<i>gC/m³</i>)	
June 2005									
IG		1346	0.19	-0.08	0.50	6.27	0.75	-0.25	0.67
K1		1239	0.26	-0.43	3.09	5.38	3.85	-0.76	0.80
	SH	97	0.59	-0.55	2.31	5.56	4.98	-2.67	0.46
K2									
	SC	654	0.83	-0.19	2.66	5.67	1.70	0.96	1.57
SV		2590	0.42	-0.43	2.30	6.54	3.86	-1.56	0.60
HC									
	SA								
OR		6385	0.78	-0.26	0.82	7.30	2.34	-1.52	0.35
WE		6573	0.31	-0.06	0.76	5.62	0.53	0.22	1.42
	TR	5574	0.37	0.06	0.35	5.78	-0.57	0.92	-0.61
KBW									
KAT		15725	0.07	-0.02	0.26	5.20	0.20	0.06	1.29
July 2005									
IG		925	0.24	-0.24	0.84	6.93	2.13	-1.29	0.39
K1		925	0.23	-0.38	2.94	6.92	3.40	-0.46	0.86
	SH	35	0.55	-0.76	2.92	6.80	6.86	-3.94	0.43
K2		956	0.23	-0.36	1.88	7.49	3.20	-1.31	0.59
	SC	74	1.05	-0.46	3.27	7.22	4.12	-0.86	0.79
SV		1293	0.44	-0.46	2.92	7.73	4.14	-1.22	0.71
HC		1250	0.30	-0.28	0.74	8.09	2.51	-1.78	0.29
	SA	976	0.67	-0.54	0.51	7.22	4.86	-4.34	0.11
OR		2972	0.85	-0.75	2.48	7.31	6.77	-4.29	0.37
WE		3134	0.36	-0.19	2.26	7.24	1.74	0.53	1.30
	TR	2672	0.24	-0.03	0.54	7.24	0.24	0.30	2.28
KBW		4690	0.36	-0.19	1.50	7.33	1.68	-0.18	0.89
KAT		6570	0.09	-0.09	0.85	7.31	0.84	0.00	1.00
August 2005									
IG		1005	0.24	-0.26	0.51	6.83	2.35	-1.84	0.22
K1		999	0.24	-0.44	2.68	6.82	3.92	-1.24	0.68
	SH	37	0.48	-0.52	2.73	6.67	4.66	-1.93	0.58
K2		1035	0.23	-0.38	2.11	7.30	3.39	-1.28	0.62
	SC	21	0.80	-0.64	4.02	7.28	5.77	-1.75	0.70
SV		1103	0.42	-0.60	4.07	7.30	5.40	-1.33	0.75
HC		1110	0.32	-0.35	0.97	7.47	3.12	-2.16	0.31
	SA	248	0.57	-0.68	2.17	7.11	6.14	-3.97	0.35
OR		2044	0.41	-0.31	2.62	7.11	2.75	-0.13	0.95
WE		2166	0.51	-0.23	3.43	6.99	2.03	1.41	1.69
	TR	1150	0.38	-0.09	0.65	7.01	0.83	-0.18	0.78
KBW		3088	0.48	-0.31	2.08	6.96	2.75	-0.67	0.76
KAT		3650	0.12	-0.11	0.98	6.99	0.99	-0.01	0.99

(continued)

Table A-7 (continued)

<i>Station</i>		<i>flow</i>	<i>K_a</i>	<i>C_r</i>	<i>prod- uction</i>	<i>insol- ation</i>	<i>daily C_r</i>	<i>net ecoprod</i>	<i>relative auto- troph</i>
<i>mainstem</i>	<i>tributary</i>	<i>(cfs)</i>	<i>(1/hr)</i>	<i>(ppm/hr)</i>	<i>(gC/m³)</i>		<i>(gC/m³)</i>	<i>(gC/m³)</i>	
September 2005									
IG		1175	0.15	-0.02	0.39	4.50	0.21	0.19	1.91
K1		1179	0.27	-0.31	2.07	4.75	2.81	-0.74	0.74
	<i>SH</i>	51	0.63	-0.58	3.18	5.05	5.25	-2.07	0.61
K2		1244	0.20	-0.22	1.38	5.33	1.98	-0.59	0.70
	<i>SC</i>	16	0.66	-0.50	2.22	5.33	4.51	-2.29	0.49
SV		1285	0.44	-0.53	3.11	5.41	4.76	-1.64	0.65
HC		1293	0.26	-0.16	0.99	4.33	1.45	-0.46	0.68
	<i>SA</i>	193	0.39	-0.43	0.92	5.37	3.85	-2.93	0.24
OR		2052	0.42	-0.39	2.12	5.46	3.55	-1.43	0.60
WE		2048	0.41	-0.05	2.45	5.10	0.49	1.97	5.04
	<i>TR</i>	846	0.31	-0.10	0.52	5.11	0.89	-0.37	0.58
KBW		2868	0.38	-0.05	1.61	4.86	0.45	1.16	3.55
KAT		3119	0.08	-0.11	1.15	5.19	0.95	0.20	1.21

Table A-8: Correlation arrays of monthly means, all months, screened data, 2001

	C_r	<i>Production</i>	<i>insolation</i>	<i>flow</i>	<i>TN</i>	<i>TP</i>	<i>chl-a</i>
IG							
K _a	0.260	-0.027	0.359	-0.023	0.063	0.796	0.871
c _R		-0.112	0.831	0.595	-0.970	-0.414	-0.273
Production			0.268	-0.781	-0.120	0.341	0.287
insolation				0.328	-0.734	-0.054	0.107
flow					-0.462	-0.641	-0.483
TN						0.563	0.453
TP							0.975
SH							
K _a	0.329	-0.577	-0.888	0.986	-0.494	-0.711	0.314
c _R		-0.714	-0.600	0.365	-0.937	-0.509	0.447
Production			0.855	-0.623	0.913	0.502	-0.004
insolation				-0.931	0.778	0.597	-0.359
flow					-0.558	-0.638	0.410
TN						0.608	-0.262
TP							-0.069
SC							
K _a	-0.227	-0.618	0.728	0.644	-0.948	0.317	0.108
c _R		-0.288	-0.454	-0.354	-0.128	-0.680	0.447
Production			-0.154	-0.783	0.533	0.525	-0.499
insolation				0.332	-0.725	0.660	-0.618
flow					-0.856	-0.070	0.487
TN						-0.129	-0.024
TP							-0.576
SV							
K _a	0.065	-0.234	-0.239	0.194	0.262	-0.012	0.184
c _R		-0.851	-0.884	0.205	0.414	0.275	-0.498
Production			0.691	-0.532	-0.434	-0.406	0.219
insolation				0.140	-0.770	-0.448	0.152
flow					-0.516	-0.478	-0.373
TN						0.780	-0.041
TP							0.334
HC							
K _a	-0.914	0.079	-0.650	-0.601	0.550	0.529	0.005
c _R		-0.107	0.468	0.321	-0.357	-0.427	0.166
Production			0.467	-0.555	-0.282	0.137	0.367
insolation				0.297	-0.824	-0.613	-0.069
flow					-0.401	-0.520	-0.558
TN						0.882	0.608
TP							0.743
SA							
K _a	-0.802	-0.194	0.791	0.938	-0.795	-0.378	-0.459
c _R		0.022	-0.640	-0.684	0.749	0.421	-0.155
Production			0.404	-0.509	0.616	0.506	0.238
insolation				0.574	-0.369	0.132	-0.356
flow					-0.912	-0.422	-0.501
TN						0.423	0.142
TP							0.088
(continued)							

Table A-8: Correlation arrays, 2001 (continued)

	C_r	<i>Production</i>	<i>insolation</i>	<i>flow</i>	<i>TN</i>	<i>TP</i>	<i>chl-a</i>
OR							
K_a	-0.853	-0.565	0.391	0.996	-0.449	-0.638	-0.367
c_R		0.433	-0.326	-0.847	-0.523	-0.425	-0.474
Production			0.338	-0.530	-0.270	0.274	0.532
insolation				0.411	-0.935	-0.596	0.000
flow					-0.481	-0.663	-0.447
TN						0.827	0.249
TP							0.692
WE							
K_a	-0.846	0.859	-0.016	-0.906			
c_R		-0.841	-0.424	0.617			
Production			0.385	-0.624			
insolation				0.409			
flow							
TN							
TP							
TR							
K_a	-0.844	0.285	-0.500	-0.742	0.703	-0.691	-0.076
c_R		0.082	0.457	0.289	-0.239	0.201	0.125
Production			0.541	-0.424	0.423	-0.560	-0.011
insolation				0.521	-0.513	0.377	0.002
flow					-0.984	0.978	-0.080
TN						-0.987	-0.080
TP							0.040
MF							
K_a							
c_R							
Production							
insolation							
flow							
TN						0.783	0.649
TP							0.494
TG							
K_a							
c_R							
Production							
insolation							
flow							
TN						0.773	0.997
TP							0.793

Table A-9: Correlation arrays of monthly means, all months, screened data, 2002

	C_r	<i>Production</i>	<i>insolation</i>	<i>flow</i>	<i>TN</i>	<i>TP</i>	<i>chl-a</i>
IG							
K _a	0.243	-0.014	0.353	-0.531	0.230	-0.181	0.318
c _R		0.104	0.664	-0.050	-0.442	-0.903	-0.573
Production			0.375	-0.781	0.144	-0.488	-0.575
insolation				-0.520	0.313	-0.680	-0.102
flow					-0.414	0.357	-0.198
TN						0.458	0.377
TP							0.200
SH							
K _a	0.172	0.597	-0.740	0.959	-0.489	-0.365	0.034
c _R		-0.284	-0.424	0.050	-0.316	-0.191	0.209
Production			-0.614	0.768	-0.321	-0.210	-0.801
insolation				-0.715	0.852	0.618	0.594
flow					-0.509	-0.509	-0.877
TN						0.869	0.350
TP							-0.061
SC							
K _a							
c _R							
Production							
insolation							
flow							
TN						-0.363	0.339
TP							0.109
SV							
K _a	0.039	-0.554	-0.021	0.316	-0.431	-0.163	-0.018
c _R		-0.607	0.350	0.921	-0.739	-0.632	-0.870
Production			0.189	-0.805	-0.019	-0.334	-0.303
insolation				0.246	-0.846	-0.890	-0.471
flow					-0.730	-0.490	-0.390
TN						0.946	0.662
TP							0.702
HC							
K _a	-0.915	0.955	0.035	-0.829	-0.538	-0.361	-0.239
c _R		-0.946	0.236	0.852	0.382	0.050	-0.021
Production			-0.135	-0.954	-0.293	-0.107	0.006
insolation				0.212	-0.590	-0.858	-0.908
flow					0.024	-0.095	-0.199
TN						0.864	0.863
TP							0.974
SA							
K _a	-0.963	0.735	0.525	0.968	0.065	-0.666	0.723
c _R		-0.868	-0.611	-0.932	0.085	0.806	-0.548
Production			0.847	0.766	-0.115	-0.893	0.294
insolation				0.678	0.360	-0.807	0.444
flow					0.271	-0.748	0.805
TN						-0.056	0.700
TP							-0.326
(continued)							

Table A-9: Correlation arrays, 2002 (continued)

	<i>C_r</i>	<i>Production</i>	<i>insolation</i>	<i>flow</i>	<i>TN</i>	<i>TP</i>	<i>chl-a</i>
OR							
K _a							
c _R							
Production							
insolation							
flow							
TN						0.890	0.734
TP							0.859
WE							
K _a	-0.820	0.701	0.818	-0.226	0.308	-0.720	-0.095
c _R		-0.732	-0.690	0.161	-0.078	0.607	-0.107
Production			0.228	-0.756	-0.158	-0.161	0.618
insolation				0.374	0.325	-0.965	-0.504
flow					0.090	-0.465	-0.726
TN						-0.101	-0.730
TP							0.428
TR							
K _a	-0.513	0.274	-0.481	-0.122	0.455	0.660	-0.334
c _R		-0.232	0.433	0.453	-0.784	-0.274	0.518
Production			-0.118	-0.765	0.722	0.177	-0.168
insolation				0.410	0.286	-0.804	0.831
flow					-0.325	-0.456	0.543
TN						0.113	0.110
TP							-0.466
MF							
K _a	-0.864	0.222	0.812	0.817	0.335	-0.976	-0.910
c _R		-0.656	-0.799	-0.436	-0.103	0.868	0.901
Production			0.464	-0.379	-0.212	-0.323	-0.500
insolation				0.510	0.632	-0.908	-0.777
flow					0.474	-0.736	-0.554
TN						-0.428	-0.085
TP							0.928
TG							
K _a							
c _R							
Production							
insolation							
flow							
TN						0.365	-0.272
TP							0.766

Table A-10: Correlation arrays of monthly means, all months, screened data, 2003

	<i>C_r</i>	<i>Production</i>	<i>insolation</i>	<i>flow</i>	<i>TN</i>	<i>TP</i>	<i>chl-a</i>
IG							
<i>c_R</i>							
Production							
insolation							
flow					0.086	-0.756	0.659
TN							0.734
TP							-0.243
SH							
<i>K_a</i>	-0.650	0.189	-0.382	0.345			
<i>c_R</i>		0.610	0.896	-0.916			
Production			0.817	-0.855			
insolation				-0.990			
flow							
TN						0.186	-0.214
TP							-0.711
K2							
<i>K_a</i>	-0.950	0.958	0.945	-0.993			
<i>c_R</i>		-0.999	-0.870	0.960			
Production			0.867	-0.961			
insolation				-0.968			
flow							
TN							
TP							
SV							
<i>K_a</i>							
<i>c_R</i>							
Production							
insolation							
flow							
TN							
TP							
HC							
<i>K_a</i>	0.136	0.673	0.740	-0.636			
<i>c_R</i>		-0.134	0.427	-0.443			
Production			0.836	-0.826			
insolation				-0.990			
flow							
TN							
TP							
SA							
<i>K_a</i>							
<i>c_R</i>							
Production							
insolation							
flow							
TN							
TP							

(continued)

Table A-10: Correlation arrays, 2003 (continued)

	<i>C_r</i>	<i>Production</i>	<i>insolation</i>	<i>flow</i>	<i>TN</i>	<i>TP</i>	<i>chl-a</i>
OR							
K _a							
c _R							
Production							
insolation							
flow							
TN							
TP							
WE							
K _a	0.013	-0.081	0.348	0.568	-0.653	-0.599	0.183
c _R		-0.879	-0.426	0.732	-0.142	-0.172	-0.792
Production			0.154	-0.752	-0.026	-0.079	0.821
insolation				-0.020	-0.915	-0.885	-0.807
flow					-0.387	-0.488	-0.666
TN						0.972	0.531
TP							0.439
TR							
K _a	-0.812	0.993	-0.342	-0.878	0.328	-0.797	0.654
c _R		-0.821	0.431	0.909	-0.980	-0.491	0.661
Production			-0.284	-0.902	0.180	-0.879	0.762
insolation				0.425	-0.957	-0.019	0.226
flow					-0.816	0.296	-0.092
TN						0.310	-0.500
TP							-0.978
MF							
K _a	0.073	-0.541	0.435	0.465	-0.200	0.300	-0.748
c _R		-0.764	-0.355	0.745	-0.119	-0.586	0.920
Production			-0.005	-0.882	-0.954	-0.980	0.737
insolation				-0.032	-0.897	-0.569	0.065
flow					-0.471	0.017	-0.529
TN						0.874	-0.500
TP							-0.857
TG							
K _a							
c _R							
Production							
insolation							
flow							
TN						0.990	1.000
TP							0.990

Table A-11: Correlation arrays of monthly means, all months, screened data, 2004

	<i>C_r</i>	<i>Production</i>	<i>insolation</i>	<i>flow</i>	<i>TN</i>	<i>TP</i>	<i>chl-a</i>
IG							
K _a							
c _R							
Production							
insolation							
flow							
TN						-0.195	-0.487
TP							0.807
K1							
K _a	-0.566	0.100	-0.217	-0.775	0.794	0.450	-0.890
c _R		-0.833	-0.669	0.876	-0.935	-0.106	0.551
Production			0.911	-0.629	0.689	-0.806	-0.726
insolation				-0.350	-0.163	-0.825	0.095
flow					-0.941	-0.114	0.588
TN						-0.165	-0.797
TP							0.894
SH							
K _a					0.772	-0.816	0.942
c _R							
Production							
insolation							
flow							
TN						-0.905	-0.779
TP							0.089
K2							
K _a	-0.817	-0.712	-0.839	0.828		0.560	-0.038
c _R		0.395	0.372	-0.607		0.560	-0.038
Production			0.755	-0.970		0.225	0.757
insolation				-0.744		-0.589	0.003
flow						-0.298	-0.804
TN							
TP							0.807
SC							
K _a	0.861	-0.754	0.059	0.875	0.959	-0.924	
c _R		-0.984	0.559	1.000	0.681	-0.601	
Production			-0.700	-0.978	-0.538	0.447	
insolation				0.535	-0.226	0.326	
flow					0.702	-0.624	
TN						-0.994	-0.500
TP							0.427
SV							
K _a	0.007	0.917	0.436	0.989		-0.968	-0.824
c _R		0.406	-0.897	-0.139		0.245	0.561
Production			0.040	0.848		-0.786	-0.528
insolation				0.562		-0.649	-0.869
flow						-0.994	-0.897
TN						-0.669	
TP							0.940
(continued)							

Table A-11: Correlation arrays, 2004 (continued)

	C_r	<i>Production</i>	<i>insolation</i>	<i>flow</i>	<i>TN</i>	<i>TP</i>	<i>chl-a</i>
HC							
K _a	-0.356	0.555	0.944	-0.680		-0.962	-0.813
c _R		-0.963	-0.165	0.801		0.535	-0.327
Production			0.413	-0.928		-0.651	0.187
insolation				-0.649		-0.846	-0.944
flow						0.726	-0.085
TN						-0.558	
TP							0.623
SA							
K _a	-0.706	0.239	0.527	0.625			
c _R		-0.856	-0.974	-0.994			
Production			0.951	0.908			
insolation				0.993			
flow							
TN						-0.569	
TP							0.666
OR							
K _a	-0.894	-0.673	0.966	0.999	-0.515	-0.834	
c _R		0.269	-0.980	-0.876	0.845	0.499	
Production			-0.457	-0.701	-0.288	0.969	
insolation				0.955	-0.720	-0.662	
flow					-0.481	-0.855	
TN						0.223	0.987
TP							0.315
WE							
K _a	0.384	-0.240	0.898	0.906		-0.621	-0.410
c _R		-0.842	0.153	0.735		-0.547	-0.325
Production			0.160	-0.524		-0.096	-0.337
insolation				0.751		-0.940	-0.828
flow						-0.644	-0.436
TN						-0.480	
TP							0.969
TR							
K _a	-0.035	-0.013	0.579	0.275	-0.031	-0.695	-0.840
c _R		-0.906	0.630	0.804	0.928	-0.177	0.943
Production			-0.450	-0.875	-0.918	0.055	0.133
insolation				0.716	0.570	-0.970	-0.127
flow					0.978	-0.549	-0.861
TN						-0.414	
TP							0.312
TC							
K _a	-0.012	-0.236	0.759	0.721		-0.465	-0.987
c _R		-0.876	-0.371	0.571		0.034	0.681
Production			0.286	-0.691		0.308	0.010
insolation				0.482		-0.835	-0.815
flow						-0.607	-0.990
TN							
TP							0.382
(continued)							

Table A-11: Correlation arrays, 2004 (continued)

	C_r	<i>Production</i>	<i>insolation</i>	<i>flow</i>	<i>TN</i>	<i>TP</i>	<i>chl-a</i>
TG							
K_a	-0.982	0.407	0.243	-0.617	-0.326	-0.080	-0.856
c_R		-0.405	-0.149	0.660	0.420	0.177	0.906
Production			-0.641	-0.924	0.491	0.742	0.899
insolation				0.590	-0.846	-0.966	-0.994
flow					-0.165	-0.445	-0.997
TN						0.944	
TP							0.986

Table A-12: Correlation arrays of monthly means, all months, screened data, 2005

	C_r	<i>Production</i>	<i>insolation</i>	<i>flow</i>	<i>TN</i>	<i>TP</i>	<i>chl-a</i>
IG							
K_a					-0.138	-0.206	-0.799
c_R							
Production							
insolation							
flow							
TN						0.901	0.148
TP							0.408
K1							
K_a	0.470	-0.777	-0.995	0.958	-0.135	0.025	-0.495
c_R		-0.609	-0.500	0.220	0.447	0.231	-0.472
Production			0.791	-0.626	-0.464	-0.395	0.169
insolation				-0.951	0.070	0.033	0.555
flow					-0.307	-0.156	-0.502
TN						0.250	0.053
TP							0.717
SH							
K_a	-0.096	0.212	-0.870	0.496	-0.734	-0.816	-0.090
c_R		-0.360	-0.399	0.384	0.746	-0.469	-0.584
Production			-0.098	-0.732	-0.396	-0.147	0.915
insolation				-0.577	0.310	0.992	0.299
flow					-0.062	-0.511	-0.904
TN						0.539	-0.076
TP							0.289
K2							
K_a	-0.839	0.850	0.833	-0.813	-0.860	-0.559	0.354
c_R		-0.986	-0.992	0.974	0.741	0.213	-0.584
Production			0.958	-0.924	-0.667	-0.130	0.690
insolation				-0.995	-0.800	-0.298	0.483
flow					0.834	0.356	-0.397
TN						0.871	0.220
TP							0.621

(continued)

Table A-12: Correlation arrays, 2005 (continued)

	C_r	<i>Production</i>	<i>insolation</i>	<i>flow</i>	<i>TN</i>	<i>TP</i>	<i>chl-a</i>
SC							
K _a	0.195	0.444	0.558	0.095	0.661	-0.099	-0.171
c _R		-0.424	0.040	0.926	0.862	0.676	0.858
Production			0.680	-0.246	-0.049	-0.362	-0.881
insolation				-0.025	0.355	-0.501	-0.486
flow					0.769	0.840	0.886
TN						0.464	0.617
TP							0.951
SV							
K _a	0.460	-0.525	-0.864	-0.120	0.322	0.327	-0.325
c _R		-0.970	-0.388	0.663	-0.776	-0.926	-0.949
Production			0.558	-0.695	0.885	0.845	0.939
insolation				-0.111	0.373	-0.285	0.139
flow					-0.968	-0.812	-0.563
TN						0.752	0.671
TP							0.762
HC							
K _a	-0.949	0.428	0.926	-0.972	-0.365	-0.162	
c _R		-0.331	-0.941	0.929	0.220	0.011	
Production			0.068	-0.614		0.979	
insolation				-0.829	-0.680	-0.511	
flow					-0.228	-0.427	
TN						0.929	
TP							
SA							
K _a	-0.767	0.188	0.904	0.801	0.492	0.188	
c _R		-0.772	-0.874	-0.232	-0.992	-0.898	
Production			0.419	-0.437	0.845	0.972	
insolation				0.571	0.717	0.456	
flow					-0.135	-0.444	
TN						0.802	
TP							0.945
OR							
K _a	-0.482	-0.381	0.490	0.668	-0.995	-0.952	-0.989
c _R		-0.491	0.005	0.322	0.445	0.248	0.423
Production			-0.015	-0.868	0.487	0.570	0.562
insolation				0.485	-0.614	-0.757	-0.999
flow					-0.710	-0.814	-0.667
TN						0.963	0.999
TP							0.983
WE							
K _a	-0.560	0.944	0.450	-0.560	0.945	0.686	0.963
c _R		-0.651	-0.409	0.418	-0.302	0.072	-0.411
Production			0.515	-0.677	0.804	0.671	0.924
insolation				0.217	0.001	-0.340	0.123
flow					-0.684	-0.803	-0.865
TN						0.801	0.957
TP							0.854
(continued)							

Table A-12: Correlation arrays, 2005 (continued)

	C_r	<i>Production</i>	<i>insolation</i>	<i>flow</i>	<i>TN</i>	<i>TP</i>	<i>chl-a</i>
TR							
K_a	0.951	-0.732	-0.229	0.958	-0.837	0.334	0.089
c_R		-0.824	-0.222	1.000	0.154	0.919	-0.087
Production			0.635	-0.820	0.140	-0.946	-0.442
insolation				-0.231	0.682	-0.387	-0.982
flow					0.084	0.939	-0.067
TN						-0.226	-0.589
TP							0.245
KBW							
K_a	-0.796	0.970	0.719	-0.043	0.884	0.158	0.847
c_R		-0.697	-0.679	-0.287	-0.404	0.488	-0.335
Production			0.816	0.069	0.919	0.237	0.887
insolation				0.632	-0.205	-0.905	-0.277
flow					-0.845	-0.936	-0.882
TN						0.666	0.940
TP							0.753
KAT							
K_a	-0.593	0.476	0.745	-0.226	-0.709	-0.023	0.689
c_R		-0.944	-0.233	0.739	0.164	-0.466	-0.848
Production			0.206	-0.844	0.084	0.645	0.852
insolation				0.136	-0.909	-0.504	0.209
flow					0.043	-0.577	-0.884
TN						0.719	0.015
TP							0.705